CANADIAN LIGHT SOURCE INC.

# RESEARCH REPORT 2020

www.lightsource.ca

Canadian Light Source | Centre canadien de rayonnement synchrotron

THE BRIGHTEST LIGHT IN CANADA™

# ACKNOWLEDGEMENTS


## FUNDING PARTNERS

The Canadian Light Source thanks all of our funding partners for their commitment to the advancement of science and innovation.

### OPERATING

### CAPITAL


## USER INSTITUTIONS

Agriculture and Agri-Food Canada (AAFC)
Canadian Museum of Nature
Center for High Pressure Science & Technology Advanced Research (HPSTAR)
Chinese Academy of Agricultural Science
CSIR- Central Glass and Ceramic Research Institute
Dalhousie University
Donostia International Physics Center
Drexel University
École Polytechnique de Montréal
Environment and Climate Change Canada, Aquatic Ecosystem Protection Research Division
Environment Climate Change Canada
Federal University of Minas Gerais (UFMG)
Fudan University
Global Institute for Food Security
Institut National de la Recherche Scientifique (INRS)
Institute for Energy, Environment and Sustainable Communities
Institute of Applied Ecology
Institute of Environmental and Sustainable Development in Agriculture
Instituto de Investigaciones en Tecnología Química (INTEQUI, UNSL-CONICET)
James Madison University
Lanzhou University
Lawrence Berkeley National Laboratory
Leibniz Institute for Solid State Physics and Materials Research Dresden (IFW Dresden)
Massachusetts Eye and Ear
Massachusetts Institute of Technology
Max Planck Institute for Chemical Physics of Solids
Max Planck Institute for Solid State Research
McGill University
McMaster University
MicroBeam Advancement, Inc.
National Research Council of Canada
Natural Resources Canada
Palustris Environmental
Queen's University
Royal Saskatchewan Museum
Saskatchewan Cancer Agency
Saskatchewan Food Industry
Development Centre Inc.
Saskatchewan Polytechnic
Savannah River National Laboratory
ShanghaiTech University
Soochow University, Functional Nano & Soft Material Laboratory
Southwest Petroleum University
Texas A and M University
The Hospital for Sick Children
Trinity College, Dublin
Trinity University
UChicago Argonne LLC
United States Department of Agriculture, Forest Service
University of Alberta
University of Bayreuth
University of Bristol
University of British Columbia
University of Calgary
University of California, Davis
University of California, Irvine
University of California, San Diego
University of California, Santa Barbara
University of Cambridge
University of Colorado Boulder
University of Guelph
University of Helsinki
University of Illinois at Urbana–Champaign
University of Liverpool
University of Manitoba
University of Minnesota
University of Nevada, Las Vegas
University of New Brunswick
University of North Dakota
University of Ottawa
University of Oulu
University of Quebec, Abitibi-Temiscamingue
University of Regina
University of Rostock
University of Saskatchewan
University of Texas at Austin
University of Texas, Arlington
University of Toronto
University of Victoria
University of Waterloo
University of Western Ontario
University of Wyoming
Virginia Polytechnic and State University
Yale University

## TABLE OF CONTENTS




Canadian Light Source
Research Report 2020
Editor: Victoria Martinez



**www.lightsource.ca**


**Cover:** SARS-CoV-2 RBD in complex with Fab 15033 DOI: 10.2210/pdb7KLG/pdb

# SCIENCE DIRECTOR'S MESSAGE

**2020 was a challenging year for all of us.**

When the pandemic was declared, the CLS had just entered a maintenance shutdown to install important new beamline upgrades, and operations immediately moved into a warm standby mode, ready to be restarted when able to do so safely. The great majority of staff started working from home while a minimum staff complement kept the facility in a state of readiness. In May, maintenance work was restarted, taking all possible precautions to ensure staff safety, and over the year, onsite staff gradually increased to a maximum of 125.

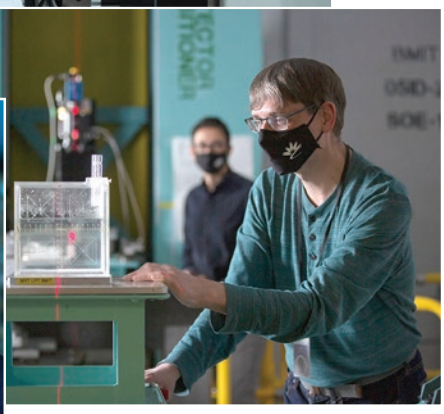

Gianluigi Botton

The CLS opened a special call for proposals focused on COVID-19, helping Canadian researchers understand the components of the SARS-CoV-2 virus structure, and to develop therapeutics, diagnostics and personal protective equipment (page 18 of this report). In July, the CLS resumed experiments, working on both COVID-19 research and previously scheduled research. This return to activity was our contribution to the global fight against the pandemic, shining light when it was most needed so that we could better know the enemy.

We ran a successful cycle, with beamline staff carrying out work more than 110 general user proposals through the mail-in program. Multiple beamlines started operating using No-Machine™ software, whereby CLS staff loaded samples on the beamlines and external users operated instruments remotely. CLS staff showed remarkable resilience throughout this difficult year, and in spite of all the challenges, we were able to operate all beamlines, even off-line equipment.

Major upgrades moved forward, including installing the CMCF beamline insertion device and its optical components, moving the IBM endstation from the IDEAS beamline to its permanent home on the BXDS beamline, and upgrading all the air-conditioning systems on BXDS and BioXAS.

In the fall, we held a very successful virtual Annual Users' Meeting as well as several workshops for users from Canada and around the world. Workshop topics included powder X-ray diffraction, mid-IR spectroscopy, far-IR applications, XAS, and macromolecular crystallography —combined, these events attracted almost 950 registrants, demonstrating high user engagement. I am grateful to all CLS staff and external lecturers who contributed to the success of these events.

The Education team continued to engage high school students and went global by holding virtual workshops for teachers with participants from around the world (page 24 in this report). As a consequence of this international excursion, the Education group will formally implement the Students on the Beamline and Teachers' Workshop program for Lightsources for Africa, Asia, Middle East and the Pacific (LAAMP), an international project of the International Science Council in partnership with the International Union of Crystallography and the International Union of Pure and Applied Physics. What a way to showcase the CLS around the world.

The CLS continues to build capacity for a high-performance computing cluster to support the massive data sets produced by advanced techniques and better detectors. This infrastructure will help users process data and shorten the time of publications.

The development of a strategy and vision for a new generation light source facility for Canada has made good process over the last few months. A concept design report has been prepared and is undergoing review by the CLS Board of Directors, the Users' Executive Committee, the Science Advisory Committee and the Machine Advisory Committee. With feedback from these important stakeholders the concept will be revised and will move to the next stage of development, including a complete design and detailed construction budget.

As evidenced by the scientific highlights in this report, while 2020 was a difficult year, all CLS staff raised to meet the challenges. Given how much we accomplished, I can only imagine what 2021 will bring.

**Gianluigi Botton**
Science Director

# HEALTH

Throughout this report, the following symbols will be used to indicate the techniques of highlighted research.

IMAGING SPECTROSCOPY DIFFRACTION

## Chemical gradients in human enamel crystallites

DeRocher, Karen A.; Smeets, Paul J. M.; Goodge, Berit H. et al. (2020). Chemical gradients in human enamel crystallites. *Nature* 583(7814), 66-71. DOI: 10.1038/s41586-020-2433-3

### SGM

Dental enamel is a principal component of teeth, and has evolved to bear large chewing forces, resist mechanical fatigue and withstand wear over decades. Functional impairment and loss of dental enamel, caused by developmental defects or tooth decay (caries), affect health and quality of life, with associated costs to society. Although the past decade has seen progress in our understanding of enamel formation (amelogenesis) and the functional properties of mature enamel, attempts to repair lesions in this material or to synthesize it in vitro have had limited success. This is partly due to the highly hierarchical structure of enamel and additional complexities arising from chemical gradients. Here we show, using atomic-scale quantitative imaging and correlative spectroscopies, that the nanoscale crystallites of hydroxylapatite ($Ca_5(PO_4)_3(OH)$), which are the fundamental building blocks of enamel, comprise two nanometric layers enriched in magnesium flanking a core rich in sodium, fluoride and carbonate ions; this sandwich core is surrounded by a shell with lower concentration of substitutional defects. A mechanical model based on density functional theory calculations and X-ray diffraction data predicts that residual stresses arise because of the chemical gradients, in agreement with preferential dissolution of the crystallite core in acidic media. Furthermore, stresses may affect the mechanical resilience of enamel. The two additional layers of hierarchy suggest a possible new model for biological control over crystal growth during amelogenesis, and hint at implications for the preservation of biomarkers during tooth development.

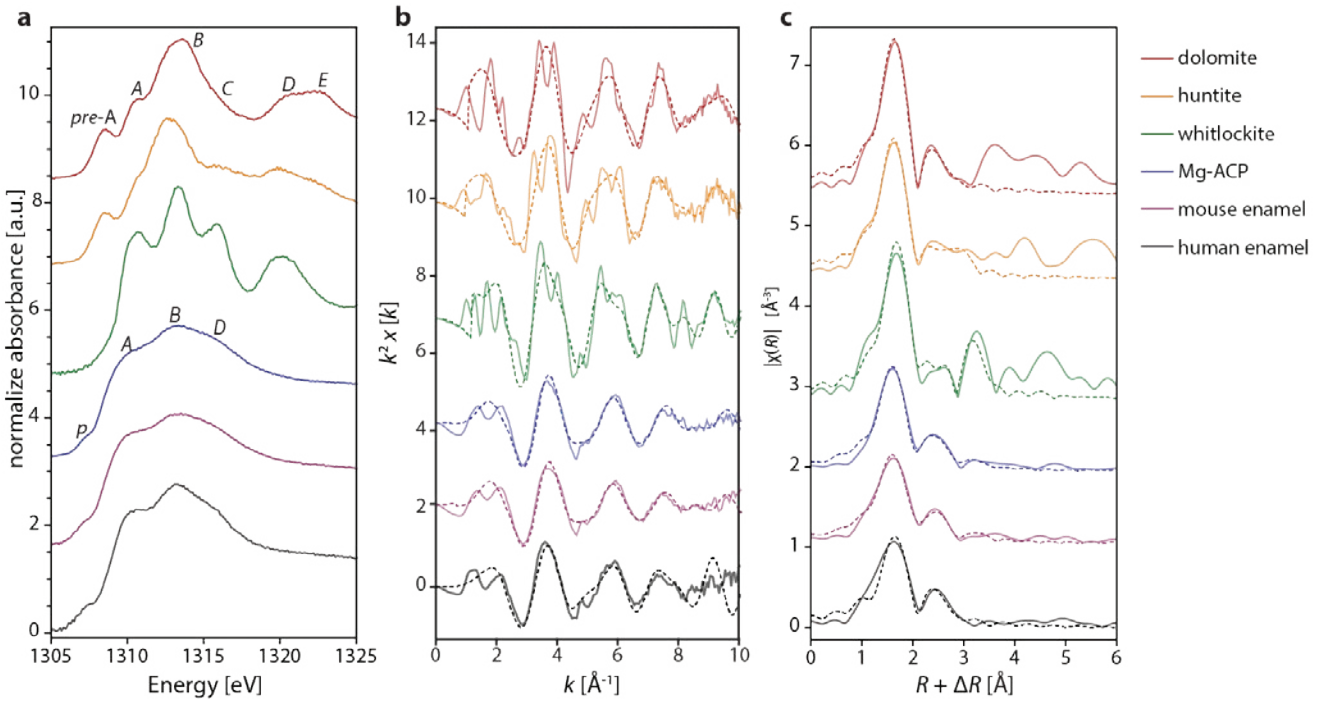


**Comparison of Mg K-edge X-ray absorption spectra of dental enamel from different species and reference compounds. Mg ACP, mouse enamel, and reference mineral spectra from Gordon et at. Science 2015. Human enamel spectra from M.J. Cohen Master's Thesis, Northwestern University (Evanston, IL) 2014 a) Mg K-edge XANES. b) Mg K-edge EXAFS (k2-weighted). c) Mg K-edge EXAFS (real space).**

Corresponding author:
Dr. Derk Joester

# A substrate binding model for the KEOPS tRNA modifying complex

Beenstock, Jonah; Ona, Samara Mishelle; Porat, Jennifer et al. (2020).
A substrate binding model for the KEOPS tRNA modifying complex.
*Nature Communications* 11(1).
DOI: 10.1038/s41467-020-19990-5. [PDB: 7kju]

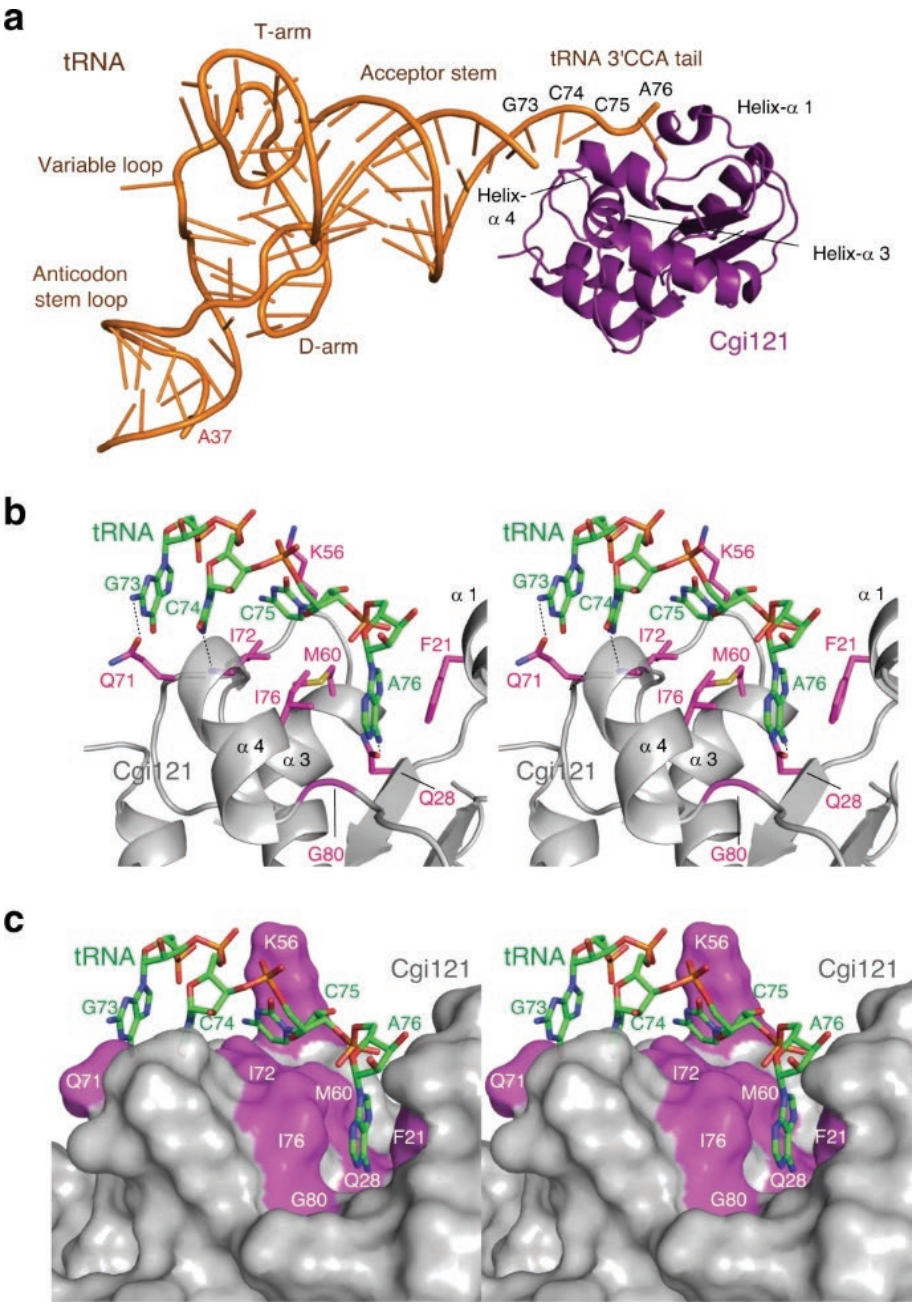


a) Ribbon representation of the mjCgi121 (purple) bound to mjtRNALysUUU (orange). b) c) Zoom-in stereo views of the binding interface between mjCgi121 and mjtRNALysUUU. For ease of viewing, only the tRNA tail region encompassing 5'-73GCCA76-3' tail (green) and side chains of Cgi121 mediating direct contacts are shown in stick representation

## CMCF

The KEOPS complex, which is conserved across archaea and eukaryotes, is composed of four core subunits; Pcc1, Kae1, Bud32 and Cgi121. KEOPS is crucial for the fitness of all organisms examined. In humans, pathogenic mutations in KEOPS genes lead to Galloway-Mowat syndrome, an autosomal-recessive disease causing childhood lethality. Kae1 catalyzes the universal and essential tRNA modification $N^6$-threonylcarbamoyl adenosine, but the precise roles of all other KEOPS subunits remain an enigma. Here we show using structure-guided studies that Cgi121 recruits tRNA to KEOPS by binding to its 3' CCA tail. A composite model of KEOPS bound to tRNA reveals that all KEOPS subunits form an extended tRNA-binding surface that we have validated in vitro and in vivo to mediate the interaction with the tRNA substrate and its modification. These findings provide a framework for understanding the inner workings of KEOPS and delineate why all KEOPS subunits are essential.

**Corresponding author:**
**Dr. Frank Sicheri**

# Vascular supply of the human spiral ganglion: novel three-dimensional analysis using synchrotron phase-contrast imaging and histology

Mei, Xueshuang; Glueckert, Rudolf; Schrott-Fischer, Annelies et al. (2020). Vascular Supply of the Human Spiral Ganglion: Novel Three-Dimensional Analysis Using Synchrotron Phase-Contrast Imaging and Histology. *Scientific Reports* 10(1), 5877. DOI: 10.1038/s41598-020-62653-0.

## BMIT

Human spiral ganglion (HSG) cell bodies located in the bony cochlea depend on a rich vascular supply to maintain excitability. These neurons are targeted by cochlear implantation (CI) to treat deafness, and their viability is critical to ensure successful clinical outcomes. The blood supply of the HSG is difficult to study due to its helical structure and encasement in hard bone. The objective of this study was to present the first three-dimensional (3D) reconstruction and analysis of the HSG blood supply using synchrotron radiation phase-contrast imaging (SR-PCI) in combination with histological analyses of archival human cochlear sections. Twenty-six human temporal bones underwent SR-PCI. Data were processed using volume-rendering software, and a representative three-dimensional (3D) model was created to allow visualization of the vascular anatomy. Histologic analysis was used to verify the segmentations. Results revealed that the HSG is supplied by radial vascular twigs which are separate from the rest of the inner ear and encased in bone. Unlike with most organs, the arteries and veins in the human cochlea do not follow the same conduits. There is a dual venous outflow and a modiolar arterial supply. This organization may explain why the HSG may endure even in cases of advanced cochlear pathology.

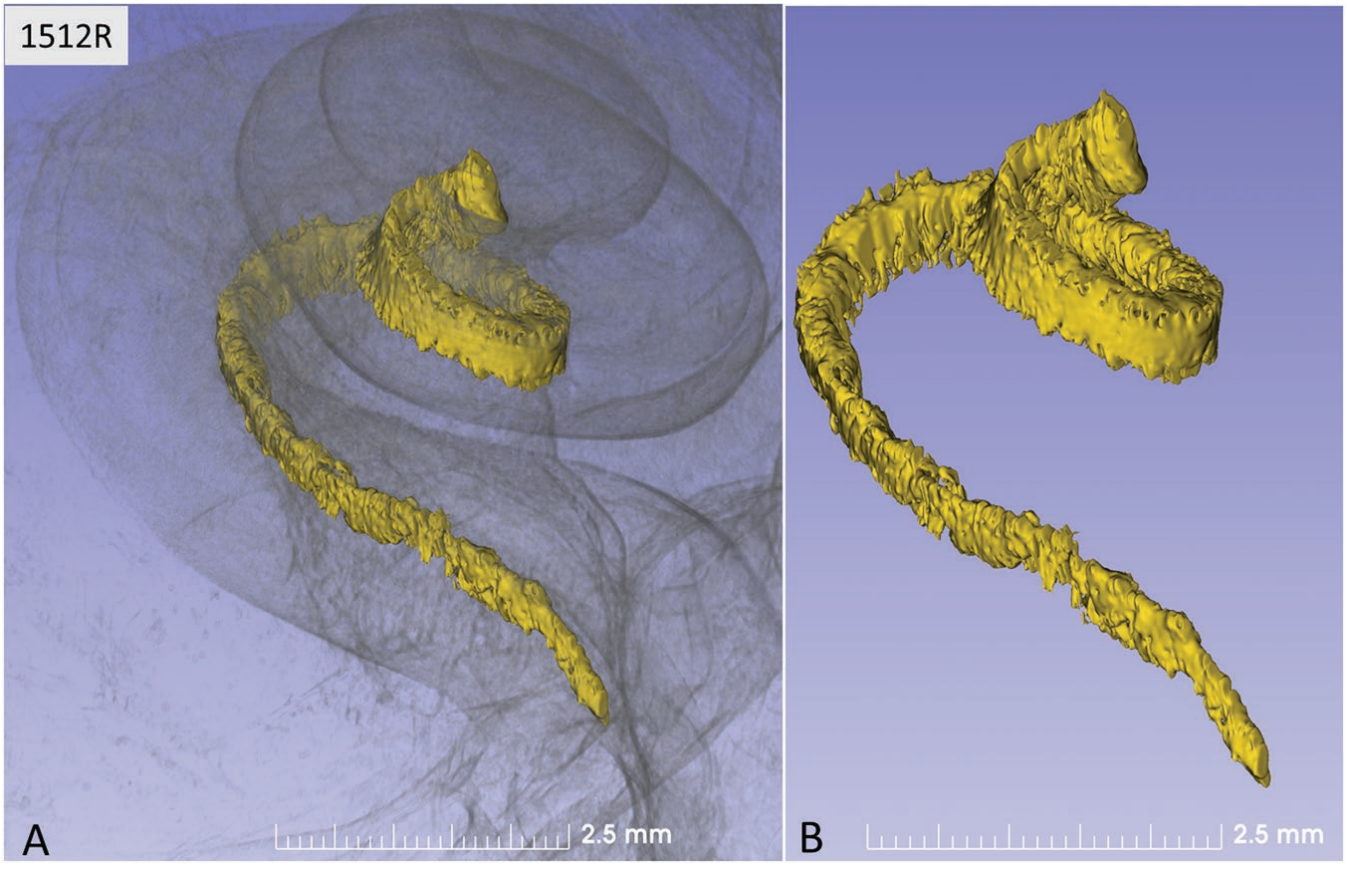


Corresponding author:
Dr. Helge Rask-Andersen

**(A, B) Synchrotron radiation phase-contrast imaging (SR-PCI) and orthographic rendering with 3D view of a left Rosenthal canal (yellow) and its topographic relationship in the semi-transparent cochlea.**

# Plasmodium falciparum circumsporozoite protein repeat motifs

Murugan, Rajagopal; Scally, Stephen W.; Costa, Giulia et al. (2020). Evolution of protective human antibodies against Plasmodium falciparum circumsporozoite protein repeat motifs. *Nature Medicine,* DOI: 10.1038/s41591-020-0881-9. [PDB: 6ulf]

## CMCF

The circumsporozoite protein of the human malaria parasite Plasmodium falciparum (PfCSP) is the main target of antibodies that prevent the infection and disease, as shown in animal models. However, the limited efficacy of the PfCSP-based vaccine RTS,S calls for a better understanding of the mechanisms driving the development of the most potent human PfCSP antibodies and identification of their target epitopes. By characterizing 200 human monoclonal PfCSP antibodies induced by sporozoite immunization, we establish that the most potent antibodies bind around a conserved (N/D)PNANPN(V/A) core. High antibody affinity to the core correlates with protection from parasitemia in mice and evolves around the recognition of NANP motifs. The data suggest that the rational design of a next-generation PfCSP vaccine that elicits high-affinity antibody responses against the core epitope will promote the induction of protective humoral immune responses.

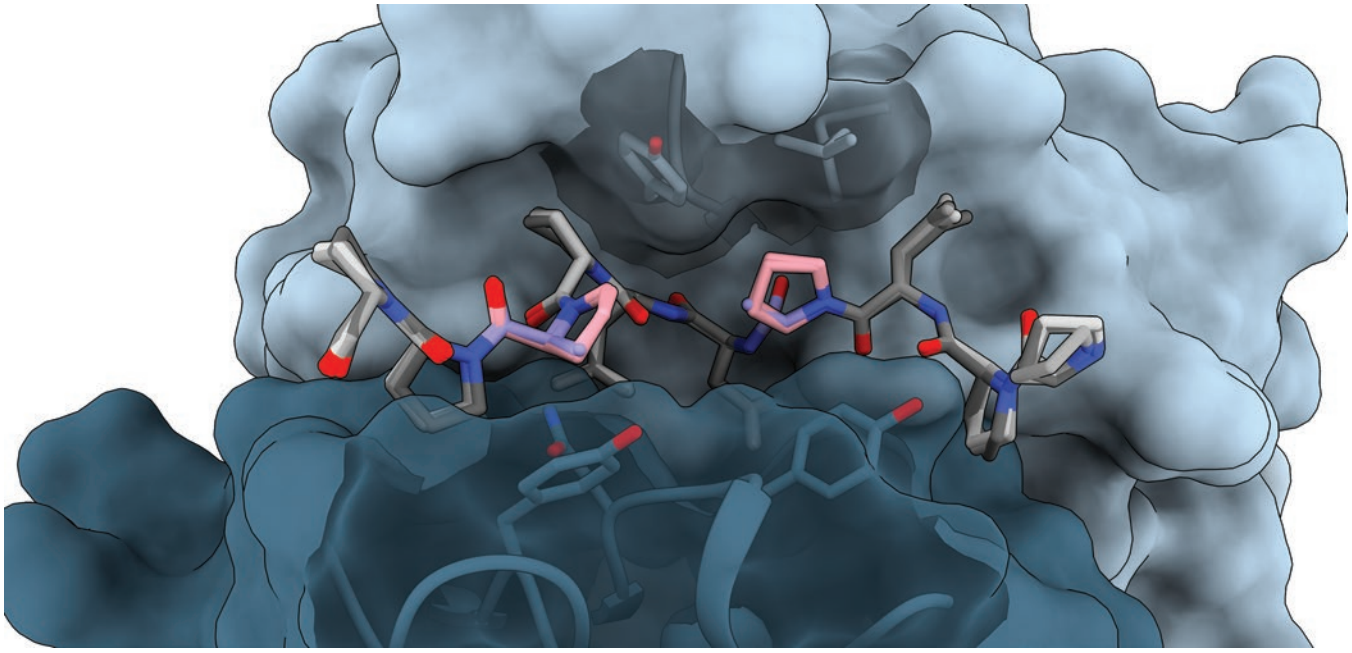

**Neutralizing antibody 3D11 binds each subtle variant of the Plasmodium berghei circumsporozoite protein repeat motif in the same conformation, deep within the paratope. Complementary structural studies in this work reveal common mechanisms of antibody evolution in mammals against the circumsporozoite repeats of Plasmodium sporozoites.**

**Corresponding authors: Jean-Philippe Julien, Elena A. Levashina, Hedda Wardemann**

# AGRICULTURE

## Pathophysiology and pathological remodelling associated with dilated cardiomyopathy in broiler chickens predisposed to heart pump failure

Olkowski, A. A.; Wojnarowicz, C.; Laarveld, B. (2020). Pathophysiology and Pathological Remodeling Associated with Dilated Cardiomyopathy in Broiler Chickens Predisposed to Heart Pump Failure. *Avian Pathology*, 1-41.
DOI: 10.1080/03079457.2020.1757620

### Mid-IR

Broiler chickens selected for rapid growth are highly susceptible to dilated cardiomyopathy (DCM). In order to elucidate the pathophysiology of DCM, the present study examines the fundamental features of pathological remodelling associated with DCM in broiler chickens using light microscopy, transmission electron microscopy (TEM), and synchrotron Fourier Transform Infrared (FTIR) micro-spectroscopy. The morphological features and FTIR spectra of the left ventricular myocardium were compared among broiler chickens affected by DCM with clinical signs of heart pump failure, apparently normal fast-growing broiler chickens showing signs of subclinical DCM (high risk of heart failure), slow-growing broiler chickens (low risk of heart failure) and Leghorn chickens (resistant to heart failure, used here as physiological reference). The findings indicate that DCM and heart pump failure in fast-growing broiler chickens are a result of a complex metabolic syndrome involving multiple catabolic pathways. Our data indicate that a good deal of DCM pathophysiology in chickens selected for rapid growth is associated with conformational changes of cardiac proteins, and pathological changes indicative of accumulation of misfolded and aggregated proteins in the affected cardiomyocytes. From TEM image analysis it is evident that the affected cardiomyocytes demonstrate significant difficulty in the disposal of damaged proteins and maintenance of proteostasis, which leads to pathological remodelling of the heart and contractile dysfunction. It appears that the underlying causes of accumulation of damaged proteins are associated with dysregulated auto phagosome and proteasome systems, which, in susceptible individuals, create a milieu conducive for the development of DCM and heart failure.

**Corresponding author:**
**Andrew Olkowski**

# The effects of sodium reduction on the gas phase of bread doughs using synchrotron X-ray microtomography

Sun, Xinyang; Scanlon, Martin G.; Guillermic, Reine-Marie; Belev, George S.; Webb, M. Adam et al. (2020). The effects of sodium reduction on the gas phase of bread doughs using synchrotron X-ray microtomography. *Food Research International,* 130, 108919. DOI: 10.1016/j.foodres.2019.108919.

## BMIT

Globally, the bakery industry has a target of reducing sodium content in bread products. However, removing salt results in changes in the quality of bread through effects on dough's gas phase during the breadmaking process. Using synchrotron X-ray microtomography, the objective of this study was to investigate how sodium reduction induced changes in the gas phase parameters (i.e., gas volume fraction, bubble size distribution (BSD) and its time evolution) of non-yeasted doughs made from a wide range of formulations (i.e., wheat cultivar and water content) prepared with different mixing times. As salt content was reduced, a lower gas volume was retained in the dough by the end of mixing. Less gas bubbles were also retained if doughs were prepared from a stronger wheat cultivar, higher water content, and/or mixed for a shorter time. Rates of change in the median (R0) and the width (ε) of the fitted lognormal radius dependence of bubble volume fraction [BVF(R)] indicated that reduced sodium content permitted disproportionation to proceed more rapidly. Higher water content or longer mixing time also resulted in faster disproportionation, indicating that water content and mixing time can be manipulated as a means of increasing bubble stability against disproportionation during low-sodium breadmaking. An examination of relative changes in dough's gas phase parameters arising from sodium reduction demonstrated that wheat cultivar, water content and mixing time all affected dough's tolerance to sodium reduction. Therefore, attainment of good bread crumb cell structure in low-sodium bread formulas is a function of salt's effects on dough rheology in addition to its effect on yeast activity, so that dough formulation and mixing conditions also need to be considered.

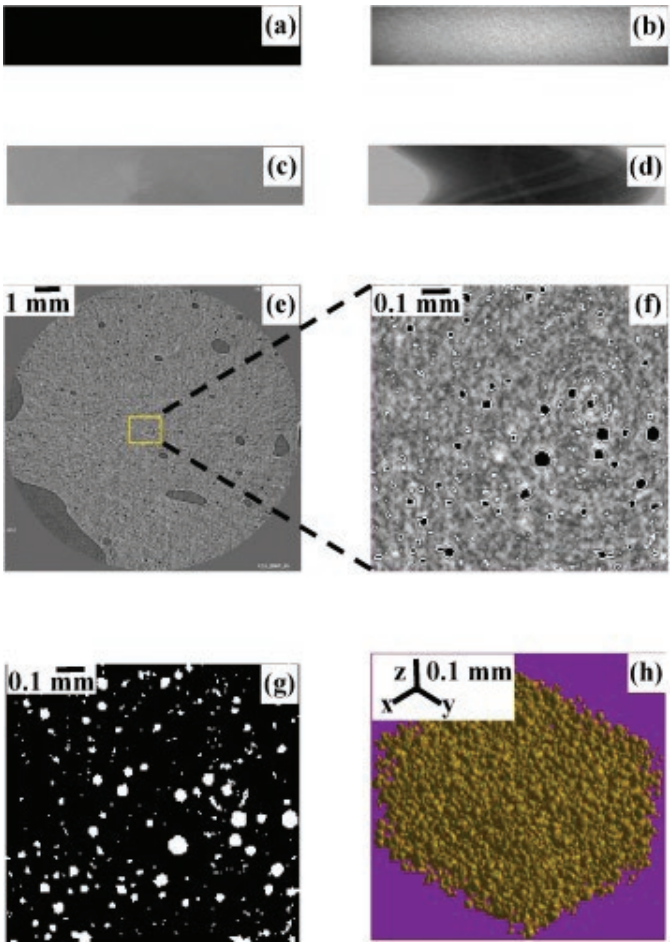


**Procedures of X-ray microtomography image reconstruction and analysis: (a) a representative dark image; (b) a representative flat image; (c) a representative projection image; (d) a representative sinogram; (e) a representative 2D cross-sectional image; (f) a magnified 2D cross-sectional image after image intensity enhancement where bubbles are circled in white for ease of identification; (g) a 2D cross-sectional image after image segmentation where bubbles are white and dough matrix is black; (h) a representative 3D volume of interest converted from a stack of the segmented 2D cross-sectional images where bubbles are yellow-green. (For interpretation of the references to color in this figure legend, the reader is referred to the web version of this article.)**

**Corresponding author:**
**Filiz Koksel**

# Quantifying uncertainties in sequential chemical extraction of soil phosphorus using XANES Spectroscopy

Gu, Chunhao; Dam, Than; Hart, Stephen C.; Turner, Benjamin L.; Chadwick, Oliver A. et al. (2020). Quantifying Uncertainties in Sequential Chemical Extraction of Soil Phosphorus Using XANES Spectroscopy. *Environmental Science & Technology,* 54(4), 2257-2267. DOI: 10.1021/acs.est.9b05278.

## SXRMB

Sequential chemical extraction has been widely used to study soil phosphorus (P) dynamics and inform nutrient management, but its efficacy for assigning P into biologically meaningful pools remains unknown. Here, we evaluated the accuracy of the modified Hedley extraction scheme using P K-edge X-ray absorption near-edge structure (XANES) spectroscopy for nine carbonate-free soil samples with diverse chemical and mineralogical properties resulting from different degrees of soil development. For most samples, the extraction markedly overestimated the pool size of calcium-bound P (Ca-P, extracted by 1 M HCl) due to (1) P redistribution during the alkaline extractions (0.5 M NaHCO3 and then 0.1 M NaOH), creating new Ca-P via formation of Ca phosphates between NaOH-desorbed phosphate and exchangeable $Ca^{2+}$ and/or (2) dissolution of poorly crystalline Fe and Al oxides by 1 M HCl, releasing P occluded by these oxides into solution. The first mechanism may occur in soils rich in well-crystallized minerals and exchangeable $Ca^{2+}$ regardless of the presence or absence of $CaCO_3$, whereas the second mechanism likely operates in soils rich in poorly crystalline Fe and Al minerals. The overestimation of Ca-P simultaneously caused underestimation of the pools extracted by the alkaline solutions. Our findings identify key edaphic parameters that remarkably influenced the extractions, which will strengthen our understanding of soil P dynamics using this widely accepted procedure.

P K-edge XANES Spectroscopy

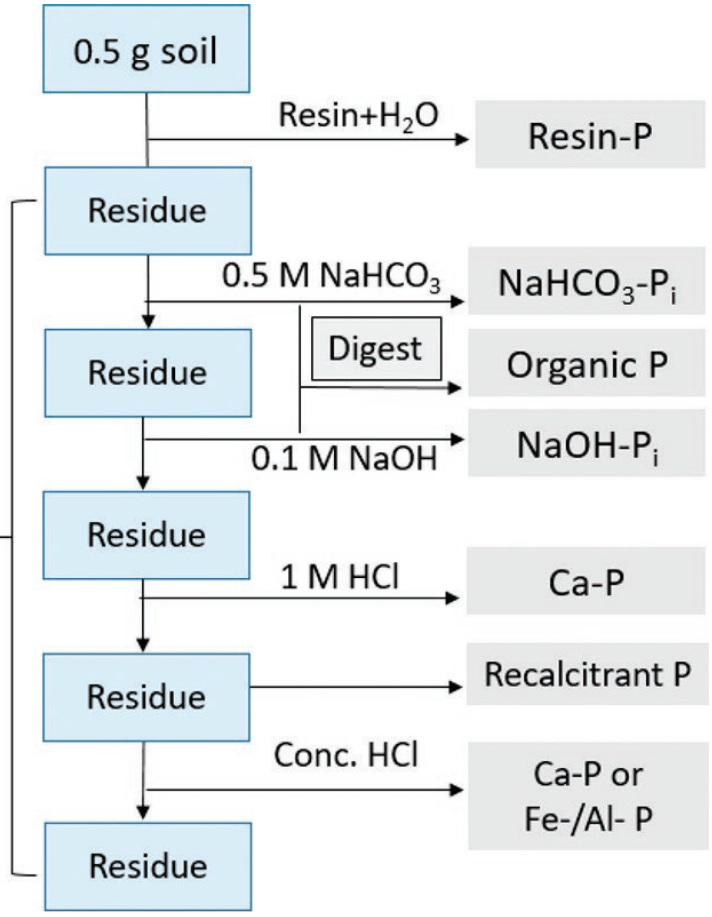


**Flow chart for modified Hedley fractionations combined with phosphorus K-edge X-ray absorption near-edge structure (XANES) spectroscopic analysis.**

**Corresponding author:**
**Mengqiang Zhu**

# Nitrogen speciation and transformations in fire-derived organic matter

Torres-Rojas, Dorisel; Hestrin, Rachel; Solomon, Dawit; Gillespie, Adam W.; Dynes, James J. et al. (2020). Nitrogen speciation and transformations in fire-derived organic matter. *Geochimica et Cosmochimica Acta.* 276, 170-185.
DOI: 10.1016/j.gca.2020.02.034.

## SGM

Vegetation fires are known to have broad geochemical effects on carbon (C) cycles in the Earth system, yet limited information is available for nitrogen (N). In this study, we evaluated how charring organic matter (OM) to pyrogenic OM (PyOM) altered the N molecular structure and affected subsequent C and N mineralization. Nitrogen near-edge X-ray absorption fine structure (NEXAFS) of uncharred OM, PyOM, PyOM toluene extract, and PyOM after toluene extraction were used to predict PyOM-C and -N mineralization potentials. PyOM was produced from three different plants (e.g. Maize-*Zea mays* L.; Ryegrass-*Lollium perenne* L.; and Willow-*Salix viminalix* L.) each with varying initial N contents at three pyrolysis temperatures (350, 500 and 700 °C). Mineralization of C and N was measured from incubations of uncharred OM and PyOM in a sand matrix for 256 days at 30 °C. As pyrolysis temperature increased from 350 to 700 °C, aromatic CN in 6-membered rings (putative) increased threefold. Aromatic CN in 6-membered oxygenated ring increased sevenfold, and quaternary aromatic N doubled. Initial uncharred OM-N content was positively correlated with the proportion of heterocyclic aromatic N in PyOM ($R^2 = 0.44$; $P < 0.0001$; n = 42). A 55% increase of aromatic N heterocycles at high OM-N content, when compared to low OM-N content, suggests that higher concentrations of N favor the incorporation of N atoms into aromatic structures by overcoming the energy barrier associated with the electronic and atomic configuration of the C structure. A ten-fold increase of aromatic CN in 6-membered rings (putative) in PyOM (as proportion of all PyOM-N) decreased C mineralization by 87%, whereas total N contents and C:N ratios of PyOM had no effects on C mineralization of PyOM-C for both pyrolysis temperatures (for PyOM-350 °C, $R^2 = 0.15$; $P < 0.27$; for PyOM-700 °C, $R^2 = 0.22$; $P < 0.21$). Oxidized aromatic N in PyOM toluene extracts correlated with higher C mineralization, whereas aromatic N in 6-membered heterocycles correlated with reduced C mineralization ($R^2 = 0.56$; $P = 0.001$; n = 100). Similarly, aromatic N in 6-membered heterocycles in PyOM remaining after toluene extraction reduced PyOM-C mineralization ($R^2 = 0.49$; $P = 0.0006$; n = 100). PyOM-C mineralization increased when N atoms were located at the edge of the C network in the form of oxidized N functionalities or when more N was found in PyOM toluene extracts and was more accessible to microbial oxidation. These results confirm the hypothesis that C persistence of fire-derived OM is significantly affected by its molecular N structure and the presented quantitative structure-activity relationship can be utilized for predictive modeling purposes.

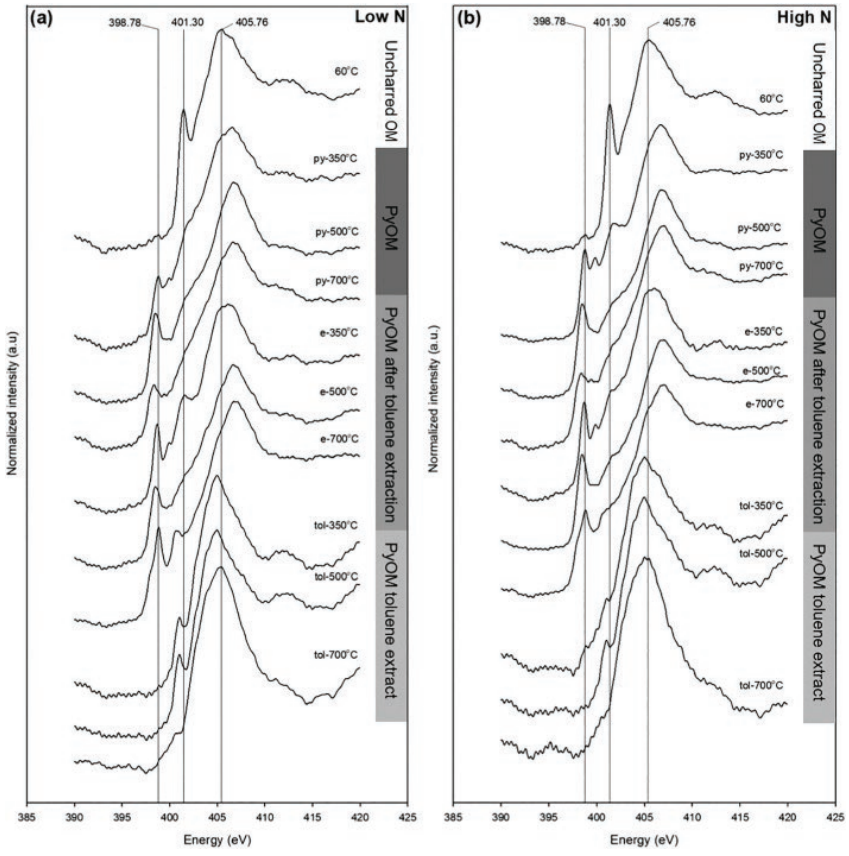


**Nitrogen K-edge NEXAFS spectra of uncharred initial OM, entire PyOM (py-), extracted PyOM (e-), and the toluene extract of PyOM (tol-) as a function of pyrolysis temperature for maize leaves. (a) Low N-containing maize leaves, and (b) high N-containing maize leaves. Black lines represent the peak centers associated with selected key spectral features: 398.78 eV for CN bonds in aromatic six-membered rings, 401.30 eV for amide N/CN bonds in aromatic five-membered rings, and 405.76 eV for NH bonds.**

**Corresponding author:**
**Johannes Lehmann**

# ENVIRONMENT

## Magnetotaxis as an adaptation to enable bacterial shuttling of microbial sulfur and sulfur cycling across aquatic oxic-anoxic interfaces

Li, Jinhua; Liu, Peiyu; Wang, Jian et al. (2020). Magnetotaxis as an adaptation to enable bacterial shuttling of microbial sulfur and sulfur cycling across aquatic oxic-anoxic interfaces. *Journal of Geophysical Research Biogeosciences.* DOI: 10.1029/2020jg006012.

### SM

Magnetotactic bacteria (MTB) widely inhabit the oxic-anoxic interface (OAI) of sediments and water columns, with their motility guided by geomagnetic fields (a behavior known as magnetotaxis). Beside biomineralizing membrane-enveloped magnetite or greigite nanocrystals called magnetosomes, cells of many MTB groups contain numerous sulfur globules within their cells. Here, by combining transmission electron microscopy and synchrotron-based scanning transmission X-ray microscopy, we investigated the cellular structure and chemistry of *Candidatus* Magnetobacterium casensis (Mcas), a giant rod-shaped MTB from the Nitrospirae phylum. We find that nitrate-storing vacuoles and linearly polymeric sulfur globules occur exclusively within some Mcas cells along with magnetosomal magnetite. Genomic prediction indicates that Mcas cells have the potential to oxidize sulfide to sulfate (i.e., $S^{2-} \rightarrow S^0 \rightarrow SO_3^{2-} \rightarrow SO_4^{2-}$), to reduce sulfate to sulfide (i.e., $SO_4^{2-} \rightarrow SO_3^{2-} \rightarrow S^{2-}$), and to reduce nitrate to $NH_4^+/N_2$. Together with previous environmental observations, comparative genomic analysis allows us to propose a model for Mcas involving the microbial sulfur cycle across aquatic OAIs based on magnetotaxis. Via directional movement guided by geomagnetic fields, Mcas cells shuttle either upward to upper microoxic zones for sulfur oxidation and nitrate accumulation in the OAI, or downward to deeper anoxic zones for sulfur deposition by coupling sulfide oxidation and nitrate reduction. Development of magnetotaxis makes MTB an efficient bacterial shuttle for C, N, S, and Fe across aquatic OAI environments and likely contributes significantly to their global biogeochemical cycling. It also benefits cell growth and magnetosomal magnetite formation in MTB.

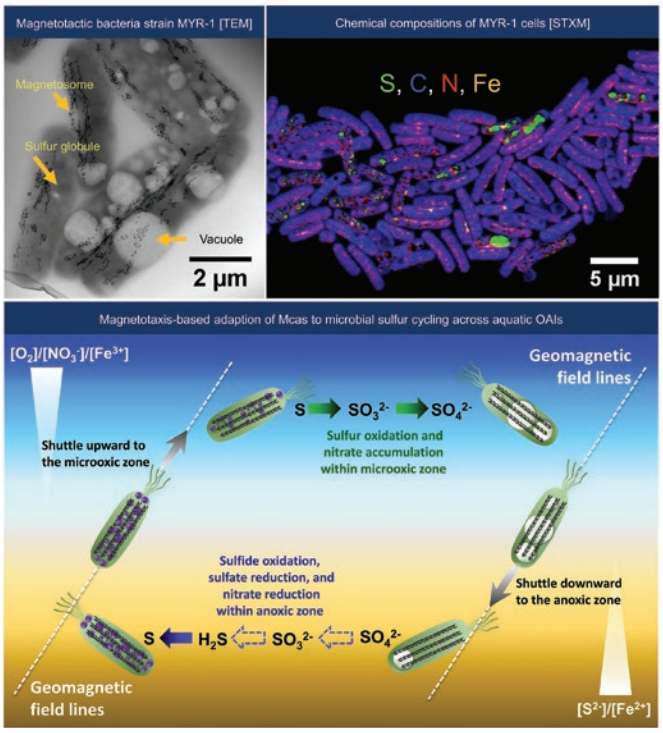


**Microbial sulfur cycling across the oxic-anoxic interface (OAI) of sediments and the water column is an important component of the global sulfur cycle. However, hydrogen sulfide (H2S) are generally produced in anoxic zones below the OAI.They have to transferred to oxic zones above the OAI for complete oxidization. Magnetotactic bacteria (MTB) widely inhabit the OAI of sediments and water columns, with their motility guided by geomagnetic fields (a behavior known as magnetotaxis). A combination of transmission electron microscopy, synchrotron-based scanning transmission X-ray microscopy, and genomic studies on Candidatus Magnetobacterium casensis strain MYR-1, a giant rod-shaped MTB from the Nitrospirae phylum, revealed that MTB may provide a new adaptation to the microbial sulfur cycle in the OAI based on magnetotaxix. Via directional movement guided by geomagnetic fields, MTB cells shuttle either upward to upper microoxic zones for sulfur oxidation and nitrate accumulation in the OAI, or downward to deeper anoxic zones for sulfur deposition by coupling sulfide oxidation and nitrate reduction. Development of magnetotaxis makes MTB an efficient bacterial shuttle for C, N, S, and Fe across aquatic OAI environments and likely contributes significantly to their global biogeochemical cycling. It also benefits cell growth and magnetosomal magnetite formation in MTB.**

**Corresponding author:**
**Jinhua Li**

# Aqueous vanadate removal by iron(II)-bearing phases under anoxic conditions

Vessey, Colton J.; Lindsay, Matthew B. J. (2020). Aqueous Vanadate Removal by Iron(II)-Bearing Phases under Anoxic Conditions. *Environmental Science & Technology* 54(7), 4006-4015.
DOI: 10.1021/acs.est.9b06250

## SXRMB

Vanadium contamination is a growing environmental hazard worldwide. Aqueous vanadate ($HxV^{V}O^{(3-X)-}$) concentrations are often controlled by surface complexation with metal (oxyhydr)oxides in oxic environments. However, the geochemical behavior of this toxic redox-sensitive oxyanion in anoxic environments is poorly constrained. Here, we describe results of batch experiments to determine kinetics and mechanisms of aqueous $H_2V^{V}O_4$ (100 μM) removal under anoxic conditions in suspensions (2.0 g $L^{-1}$) of magnetite, siderite, pyrite, and mackinawite. We present results of parallel experiments using ferrihydrite (2.0 g $L^{-1}$) and $Fe^{2+}$ (200 μM) for comparison. Siderite and mackinawite reached near complete removal (46 μmol $g^{-1}$) of aqueous vanadate after 3 h and rates were generally consistent with ferrihydrite, whereas magnetite removed 18 μmol $g^{-1}$ of aqueous vanadate after 48 h and uptake by pyrite was limited. Removal during reaction with $Fe^{2+}$ was observed after 8 h, concomitant with precipitation of secondary Fe phases. X-ray absorption spectroscopy revealed V(V) reduction to V(IV) and formation of bidentate corner-sharing surface complexes on magnetite and siderite, and with $Fe^{2+}$ reaction products. These data also suggest that V(IV) is incorporated into the mackinawite structure. Overall, we demonstrate that Fe(II)-bearing phases can promote aqueous vanadate attenuation and, therefore, limit dissolved V concentrations in anoxic environments.

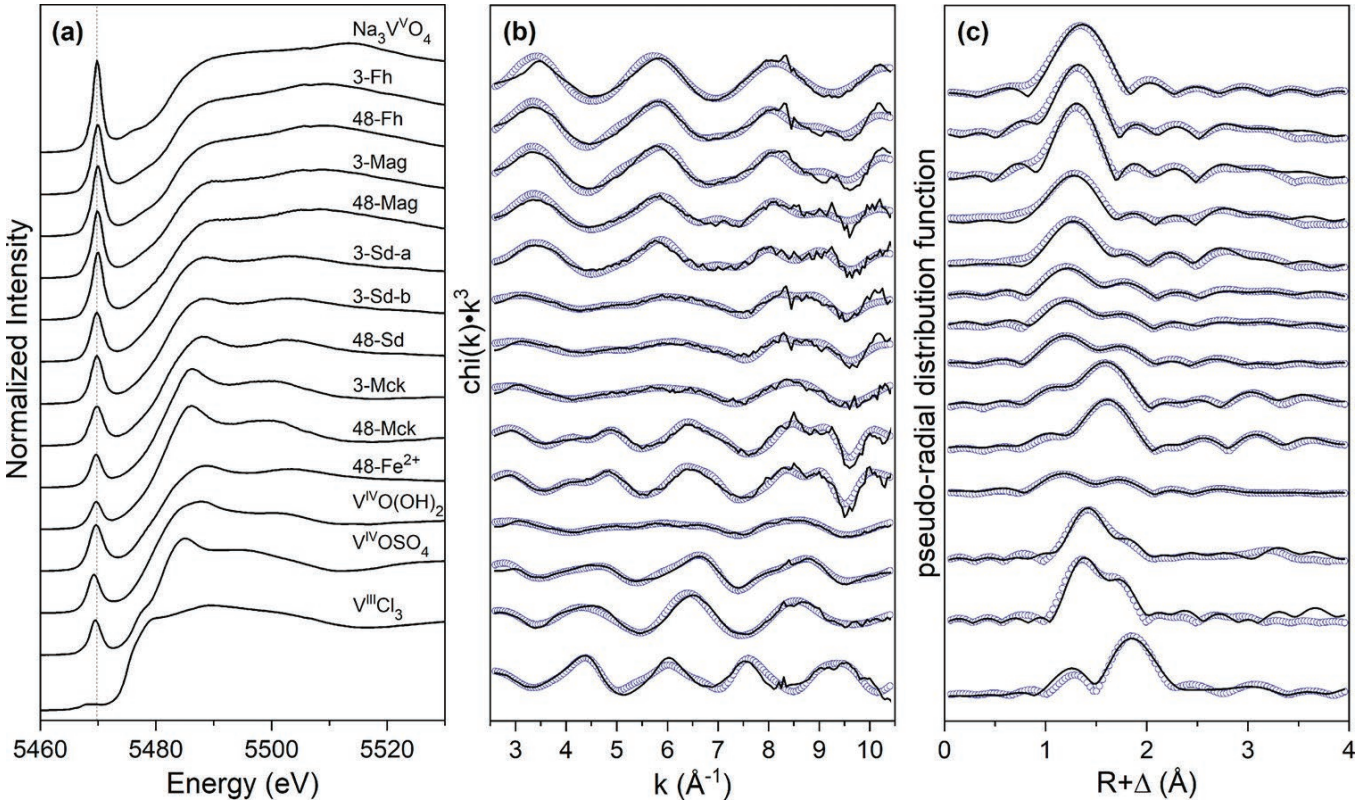


**Corresponding author:**
**Matthew Lindsay**

**(a) Normalized absorbance of V K-edge XANES spectra for selected reference compounds and samples. Vertical dashed line indicates the theoretical V pre-edge peak position (5468.9 eV). (b) Measured (solid black lines) and modeled EXAFS (open blue circles) k3-weighted EXAFS spectra. (c) Pseudoradial distribution functions for reference compounds and samples. Reference and sample spectra in panels b and c are ordered for consistency with panel a.**

# Functional PVDF ultrafiltration membrane for Tetrabromobisphenol-A (TBBPA) removal with high water recovery

Chen, Xiujuan; Huang, Gordon; Li, Yongping; An, Chunjiang; Feng, Renfei et al. (2020). Functional PVDF ultrafiltration membrane for Tetrabromobisphenol-A (TBBPA) removal with high water recovery. *Water Research* 181, 115952. DOI: 10.1016/j.watres.2020.115952.

## VESPERS, Mid-IR

Tetrabromobisphenol-A (TBBPA) is one of the most important brominated flame retardants (BFRs), accounting for 60% of the total commercial BFR market. Increasing amounts of TBBPA and byproducts are released to the aquatic environment due to their extensive utilization in various sectors. However, research on the treatment of TBBPA contaminated wastewater using membrane filtration is still lacked. Herein, a PVDF10-PAA-$ZrO_2$ membrane was successfully developed and applied for the treatment of high-concentration TBBPA wastewater with super-high water recovery. The membrane was obtained through surface functionalization with nano-$ZrO_2$ from commercial PVDF ultrafiltration (UF) membrane. Compared to the commercial PVDF membrane, the developed membrane exhibited 4 times of permeate flux which was up to 200 L/m$^2$ min with comparable TBBPA rejection rate. Furthermore, the mechanisms of membrane development and TBBPA rejection were explored through synchrotron-based ATR-FTIR and X-ray analyses. It was revealed that $ZrO_2$ NPs were immobilized into membrane surface through binding with PAA layer, where the O of the carboxyl group combined with the $Zr^{4+}$ on the $ZrO_2$ NP surface to form C-O-Zr bond through monodentate and bridging-bidentate modes. The sieving function of membrane could be the main mechanism of TBBPA removal. This research demonstrated a practical route and solid insight toward the development of highly efficient membrane for TBBPA removal. The proposed PVDF10-PAA-$ZrO_2$ membrane can also be promising for other industrial separation and purification applications.

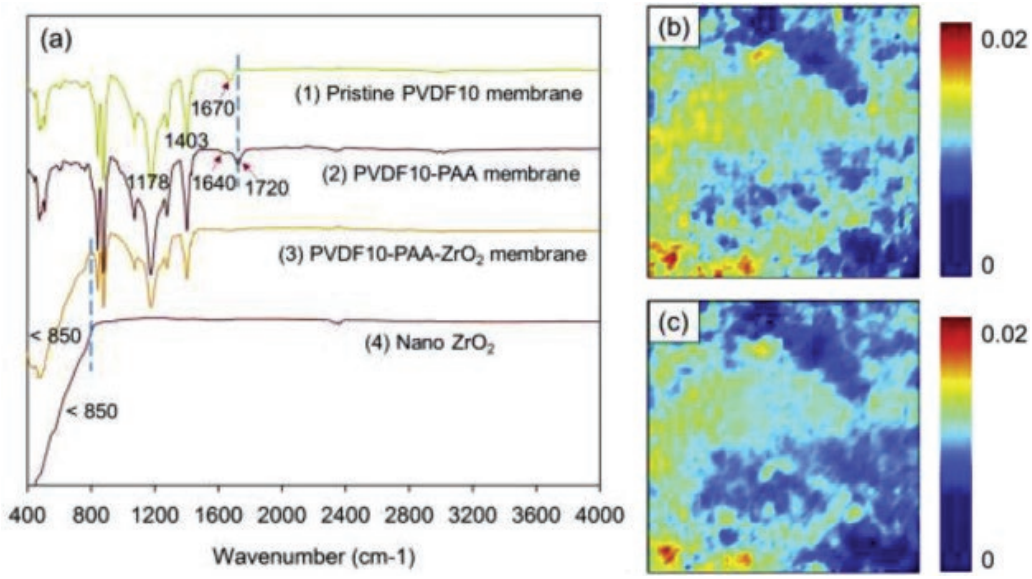


**Synchrotron ATR-FTIR spectra of membrane surfaces and $ZrO_2$ NPs, (b) and (c) Synchrotron ATR-FTIR mappings of PVDF10-PAA membrane surface under different wavenumbers (b: 1640 cm$^{-1}$; c: 1720 cm$^{-1}$). The mapping area is 300 × 300 μm$^2$.**

**Corrsponding author:**
**Gordon Huang**

# Spatially resolved organomineral interactions across a permafrost chronosequence

Sowers, Tyler D.; Wani, Rucha; Coward, Elizabeth et al. (2020). Spatially-resolved organomineral interactions across a permafrost chronosequence. *Environmental Science & Technology.* DOI: 10.1021/acs.est.9b06558.

## SM

Permafrost contains a large (1700 Pg C) terrestrial pool of organic matter (OM) that is susceptible to degradation as global temperatures increase. Of particular importance is syngenetic Yedoma permafrost containing high OM content. Reactive iron phases promote stabilizing interactions between OM and soil minerals and this stabilization may be of increasing importance in permafrost as the thawed surface region ("active layer") deepens. However, there is limited understanding of Fe and other soil mineral phase associations with OM carbon (C) moieties in permafrost soils. To elucidate the elemental associations involved in organomineral complexation within permafrost systems, soil cores spanning a Pleistocene permafrost chronosequence (19,000, 27,000, and 36,000 years old) were collected from an underground tunnel near Fairbanks, Alaska. Subsamples were analyzed via scanning transmission X-ray microscopy–near edge X-ray absorption fine structure spectroscopy at the nano- to microscale. Amino acid-rich moieties decreased in abundance across the chronosequence. Strong correlations between C and Fe with discrete Fe(III) or Fe(II) regions selectively associated with specific OM moieties were observed. Additionally, Ca coassociated with C through potential cation bridging mechanisms. Results indicate Fe(III), Fe(II), and mixed valence phases associated with OM throughout diverse permafrost environments, suggesting that organomineral complexation is crucial to predict C stability as permafrost systems warm.

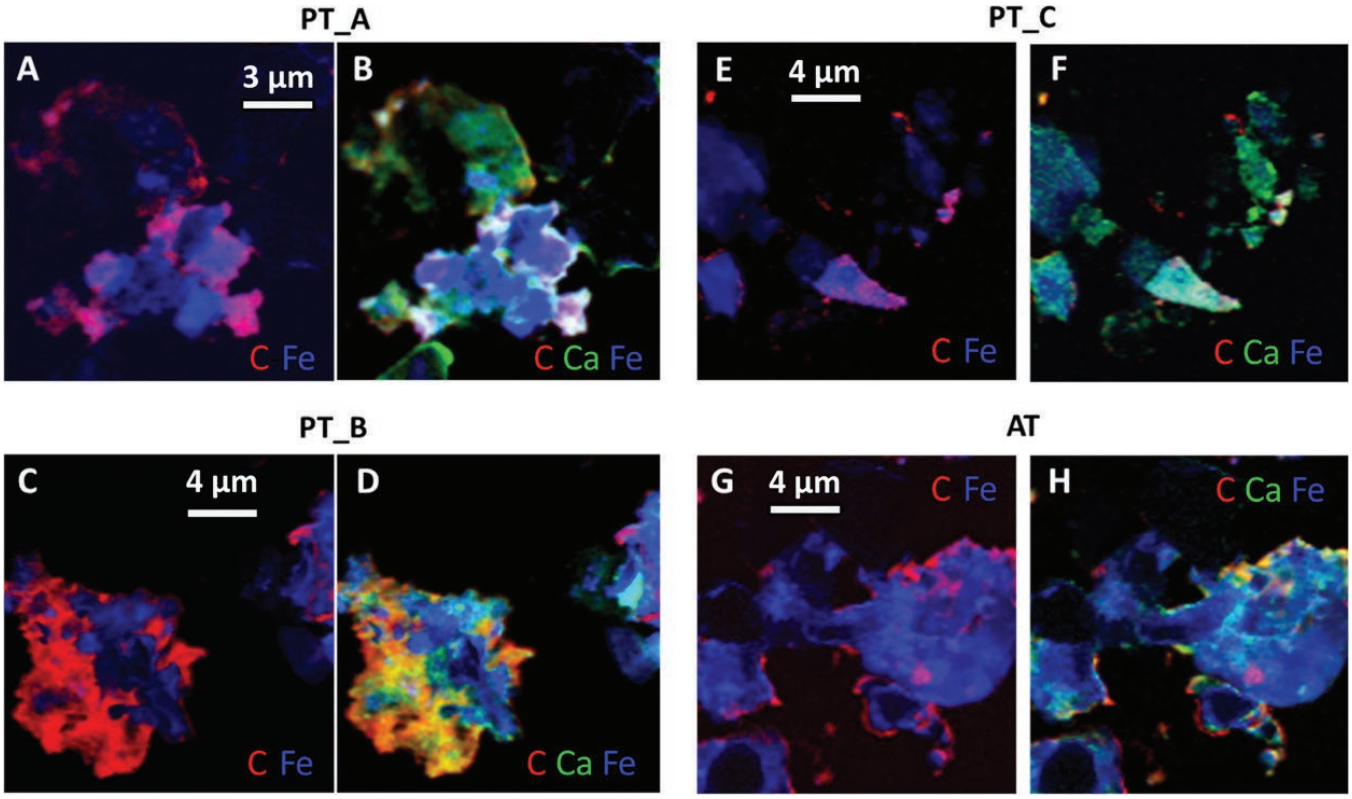


**Color-coded composite RB and RGB optical density maps created from STXM–NEXAFS data. Red, green, and blue represent carbon, calcium, and iron, respectively. Maps are shown for soils PT_A (A,B), PT_B (C,D; 27 kya PT soil), PT_C (E,F), and AT (G,H).**

**Corresponding author:**
**Tyler Sowers**

# ADVANCED MATERIALS

## Efficient electrically powered $CO_2$-to-ethanol via suppression of deoxygenation

Wang, Xue; Wang, Ziyun; García de Arquer, Pelayo et al. (2020). Efficient electrically powered $CO_2$-to-ethanol via suppression of deoxygenation. *Nature Energy* 5(6), 478-486.
DOI: 10.1038/s41560-020-0607-8.

### SXRMB, CLS@APS

The carbon dioxide electroreduction reaction ($CO_2RR$) provides ways to produce ethanol but its Faradaic efficiency could be further improved, especially in $CO_2RR$ studies reported at a total current density exceeding 10 mA $cm^{-2}$. Here we report a class of catalysts that achieve an ethanol Faradaic efficiency of (52 ± 1)% and an ethanol cathodic energy efficiency of 31%. We exploit the fact that suppression of the deoxygenation of the intermediate HOCCH* to ethylene promotes ethanol production, and hence that confinement using capping layers having strong electron-donating ability on active catalysts promotes C–C coupling and increases the reaction energy of HOCCH* deoxygenation. Thus, we have developed an electrocatalyst with confined reaction volume by coating Cu catalysts with nitrogen-doped carbon. Spectroscopy suggests that the strong electron-donating ability and confinement of the nitrogen-doped carbon layers leads to the observed pronounced selectivity towards ethanol.

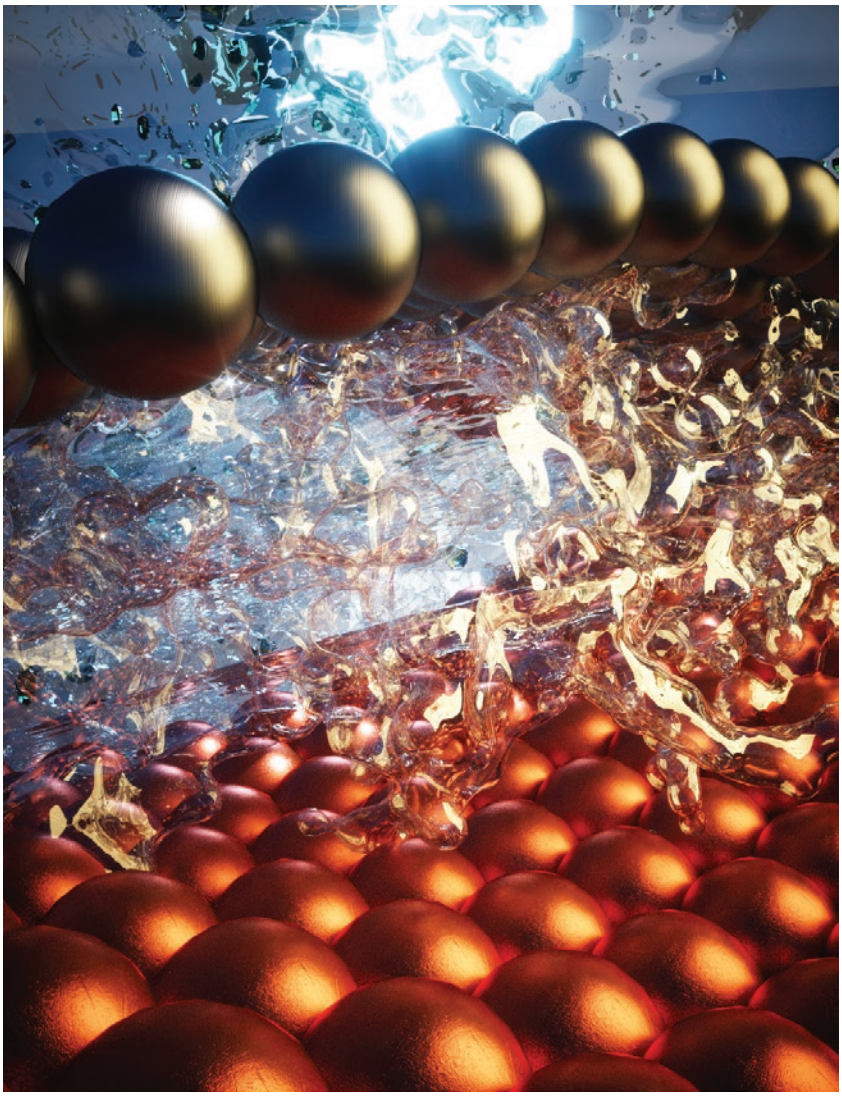

**Confined Cu by nitrogen-doped carbon for ethanol production from $CO_2$.**

**Corresponding author:**
**Edward Sargent**

# Suppressed lattice disorder for large emission enhancement and structural robustness in hybrid lead iodide perovskite discovered by high-pressure isotope effect

Lingping Kong, Jue Gong, Qingyang Hu,Francesco Capitani, Anna Celeste, Takanori Hattori, Asami Sano-Furukawa, Nana Li, Wenge Yang, Gang Liu, Ho-kwang Mao. Suppressed Lattice Disorder for Large Emission Enhancement and Structural Robustness in Hybrid Lead Iodide Perovskite Discovered by High-Pressure Isotope Effect.
*Advanced Functional Materials.* 2021 Feb; 31(9):2009131. DOI: 10.1002/adfm.202009131

## Far-IR

The soft nature of organic–inorganic halide perovskites renders their lattice particularly tunable to external stimuli such as pressure, undoubtedly offering an effective way to modify their structure for extraordinary optoelectronic properties. Here, using the methylammonium lead iodide as a representative exploratory platform, it is observed that the pressure-driven lattice disorder can be significantly suppressed via hydrogen isotope effect, which is crucial for better optical and mechanical properties previously unattainable. By a comprehensive in situ neutron/synchrotron-based analysis and optical characterizations, a remarkable photoluminescence (PL) enhancement by threefold is convinced in deuterated $CD_3ND_3PbI_3$, which also shows much greater structural robustness with retainable PL after high peak-pressure compression–decompression cycle. With the first-principles calculations, an atomic level understanding of the strong correlation among the organic sublattice and lead iodide octahedral framework and structural photonics is proposed, where the less dynamic $CD_3ND_3^+$ cations are vital to maintain the long-range crystalline order through steric and Coulombic interactions. These results also show that $CD_3ND_3PbI_3$-based solar cell has comparable photovoltaic performance as $CH_3NH_3PbI_3$-based device but exhibits considerably slower degradation behavior, thus representing a paradigm by suggesting isotope-functionalized perovskite materials for better materials-by-design and more stable photovoltaic application.

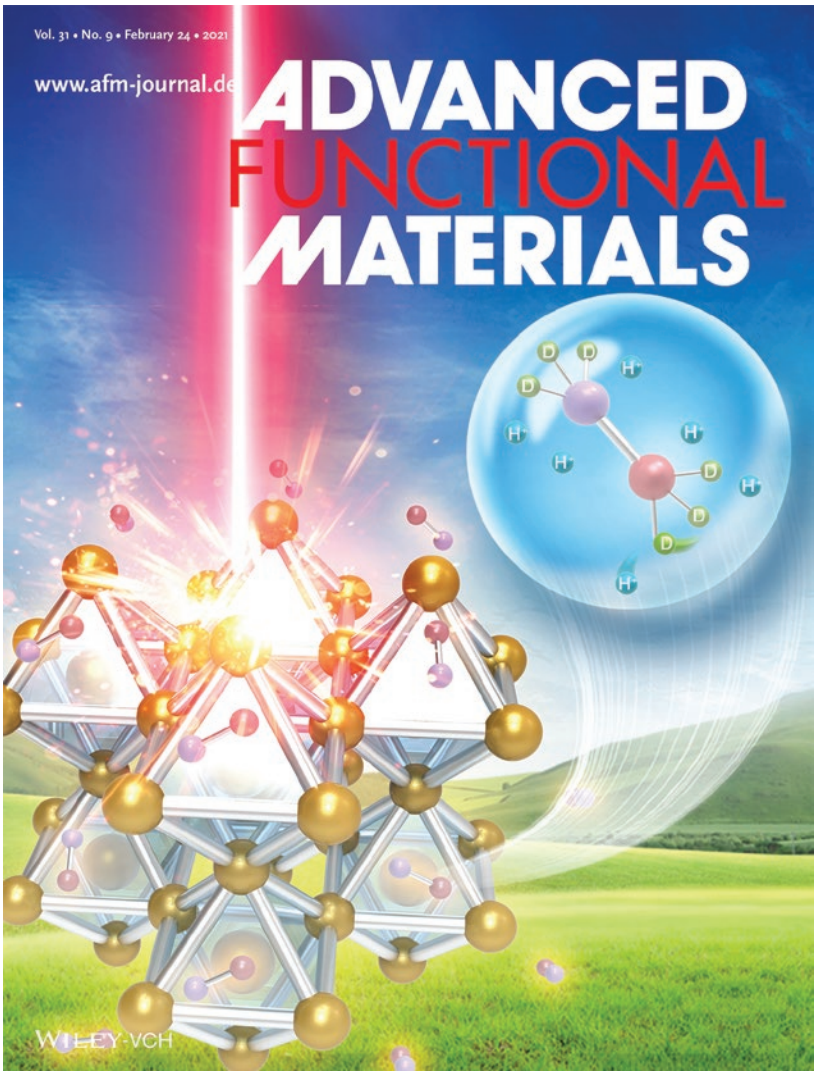


**The research on hybrid perovskites features a journal cover, published in Advanced Functional Materials. CLS Far-IR beamline user, Dr. Gang Liu from HPSTAR and team designed a high-pressure isotope study, enabling them to discover a significantly suppressed lattice disorder realized by H/D substitution in hybrid halide perovskites. Their results reveal a large emission enhancement and strong structural robustness in isotope-functionalized perovskite materials. CD3ND3PbI3-based device also exhibits slower degradation of photovoltaic performance, promising for better materials-by-design and more stable photovoltaic application.**

**Corresponding author:**
**Gang Liu**

# Elucidation of active oxygen sites upon delithiation of $Li_3IrO_4$

Li, Haifeng; Perez, Arnaud J.; Taudul, Beata; Boyko, Teak D.; Freeland, John W. et al. (2020). Elucidation of Active Oxygen Sites upon Delithiation of Li3Ir04. *ACS Energy Letters*, 140-147. DOI: 10.1021/acsenergylett.0c02040.

## REIXS

Transformational increases in the storage capacity of battery cathodes could be achieved by tapping into the redox activity at oxide ligands in addition to conventional transition metal couples. However, the key signatures that govern such lattice oxygen redox (LOR) have not been ascertained. $Li_3IrO_4$ has the largest reversible LOR, rendering it a unique model system. Here, X-ray spectroscopy and computational simulations reveal that LOR in $Li_3IrO_4$ is selectively compensated via O sites with three lone pairs, which are activated by Li/Ir disorder. The two-electron LOR can be reversed to regenerate the initial state without unlocking competing bulk reactions observed in many other compounds. We uncover an intricate interplay between stoichiometry, O coordination, and nonbonding states in LOR and pinpoint spectroscopic signatures. This interplay is indispensable for designing materials with 3d metals that fulfill the promise of LOR to overcome the bottlenecks of current cathodes for future implementation in practical batteries.

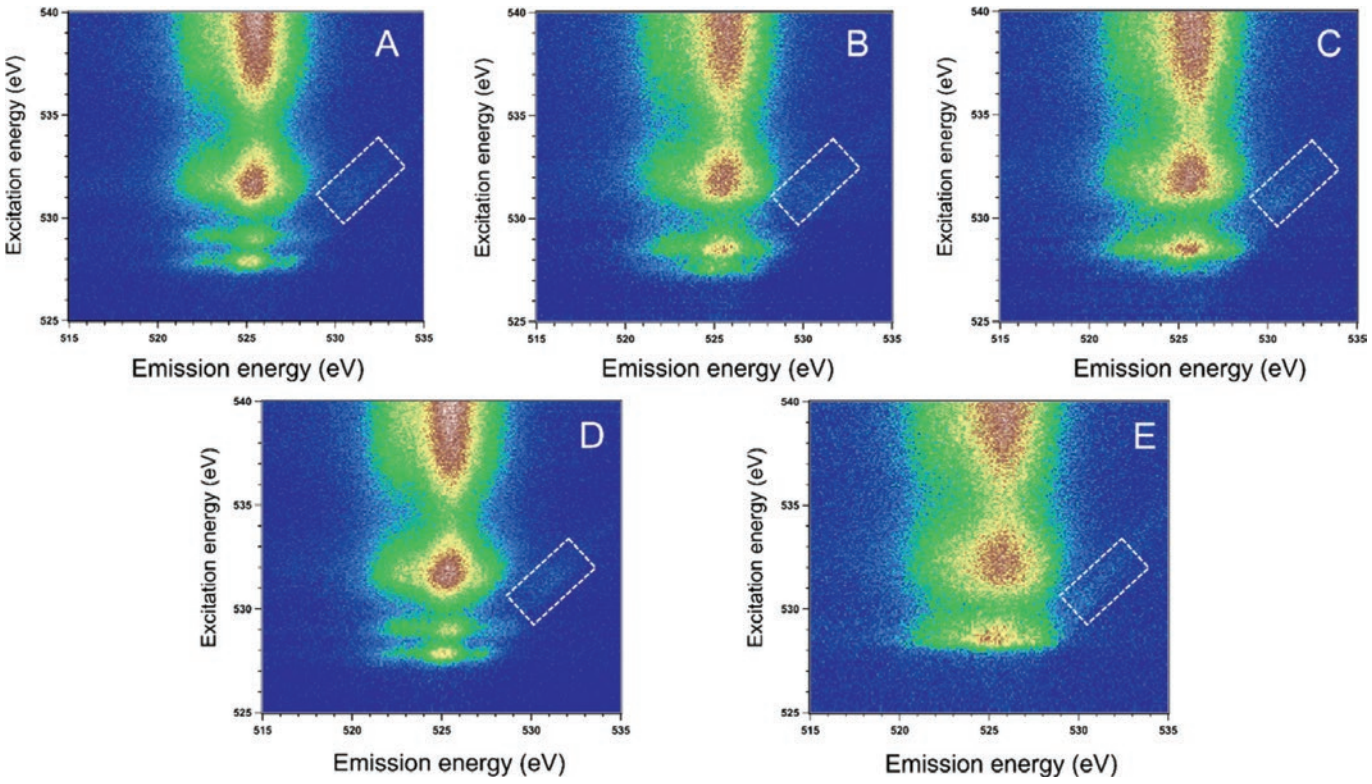


**Ex situ O K-edge RIXS maps of $Li_3IrO_4$ at the different electrochemical states indicated. The white rectangular regions identify the elastic peak.**

**Corresponding author:**
**Jordi Cabana**

# Dynamic electrocatalyst with current-driven oxyhydroxide shell for rechargeable zinc-air battery

Deng, Ya-Ping; Jiang, Yi; Liang, Ruilin; Zhang, Shao-Jian; Luo, Dan et al. (2020). Dynamic electrocatalyst with current-driven oxyhydroxide shell for rechargeable zinc-air battery. *Nature Communications* 11(1). DOI: 10.1038/s41467-020-15853-1.

## BXDS , SXRMB

Recent fruitful studies on rechargeable zinc-air battery have led to emergence of various bifunctional oxygen electrocatalysts, especially metal-based materials. However, their electrocatalytic configuration and evolution pathway during battery operation are rarely spotlighted. Herein, to depict the underlying behaviors, a concept named dynamic electrocatalyst is proposed. By selecting a bimetal nitride as representation, a current-driven "shell-bulk" configuration is visualized via time-resolved X-ray and electron spectroscopy analyses. A dynamic picture sketching the generation and maturation of nanoscale oxyhydroxide shell is presented, and periodic valence swings of performance-dominant element are observed. Upon maturation, zinc-air battery experiences a near two-fold enlargement in power density to 234 mW $cm^{-2}$, a gradual narrowing of voltage gap to 0.85 V at 30 mA $cm^{-2}$, followed by stable cycling for hundreds of hours. The revealed configuration can serve as the basis to construct future blueprints for metal-based electrocatalysts, and push zinc-air battery toward practical application.

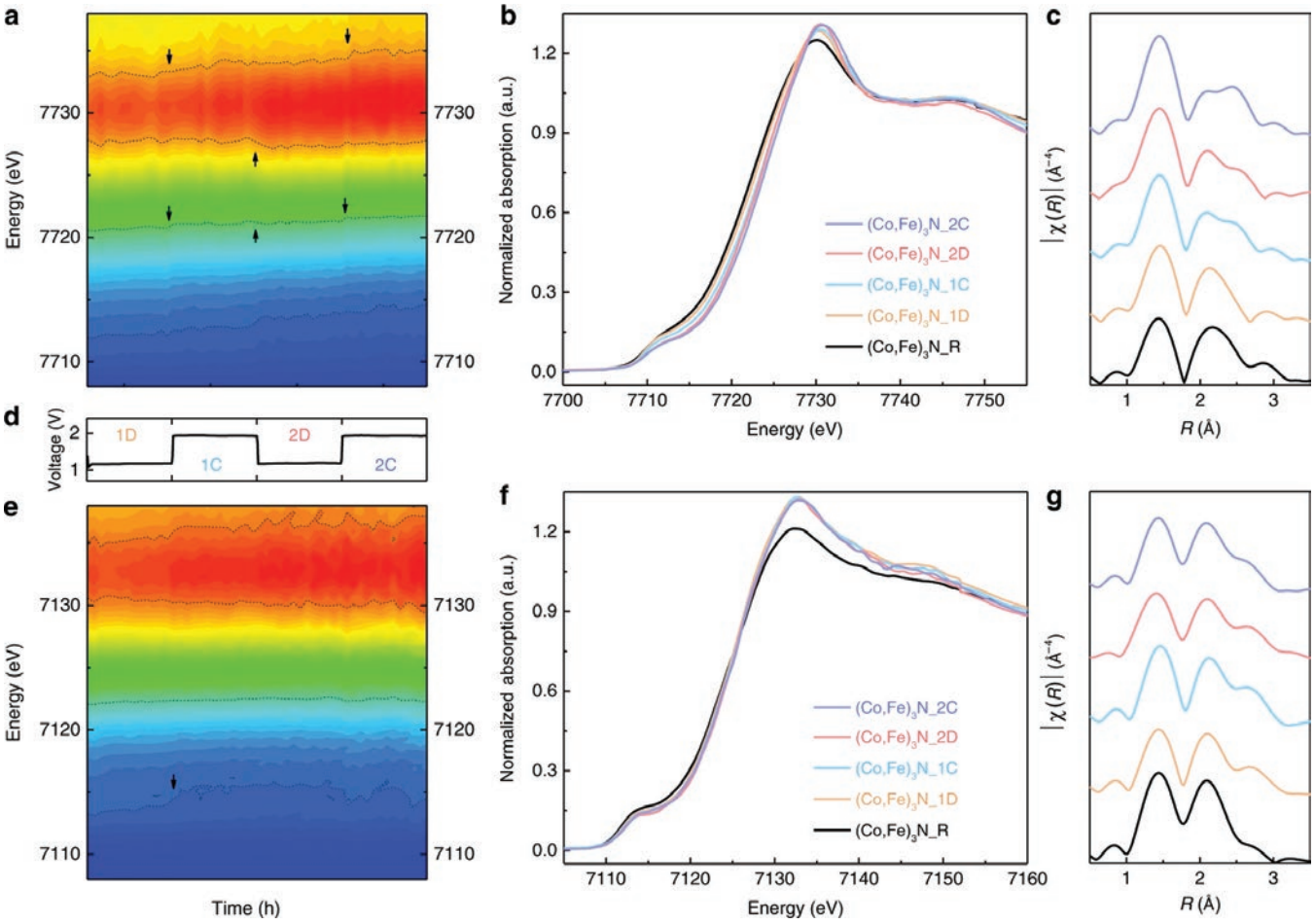


**Corresponding author:**
**Zhongwei Chen**

**The operando XANES contour maps of a Co and e Fe K edge, and the corresponding d voltage profile in the first two cycles; the red and blue contours, respectively, represent high and low adsorption intensities. Operando XANES and the k3-weighted FT spectra of d, e Co and f, g Fe K edge at different electrochemical stages.**

# Research to fight COVID-19

**In 2020, our research program was focused on supporting the fight against COVID-19. In an effort to help fight this global pandemic, we opened a special call for research proposals for any work that would actively contribute to finding COVID-related treatments or vaccines, or improve conditions for frontline workers. The call remains open to researchers from any institution, in any location.**

## Towards a treatment for COVID-19

Much of the research addressed the need for treatments for this disease, with structure-functional research being conducted on our CMCF beamline. University of Alberta researchers studied slightly altered chemical compounds they had previously made for the inhibition of the original SARS-CoV 3CL protease, using X-ray crystal structures of the SARS-CoV-2 3CL protease with these potential drugs to facilitate further inhibitor design. Another U of A team used the beamline to analyze the papain-like protease—a protein that the SARS-CoV-2 virus needs to establish a COVID-19 infection—in order to find small molecules that could bind to the protease and inhibit its activity.

Meanwhile University of Calgary scientists are studying the polymerase of the SARS-CoV-2 virus, in order to design new drugs that will inhibit the polymerase and prevent the virus from replicating and stop the infection in its tracks. A University of Toronto-led team has developed and are studying synthetic antibodies that could be used to protect frontline health workers, or as therapeutics for patients struggling to fight the virus.

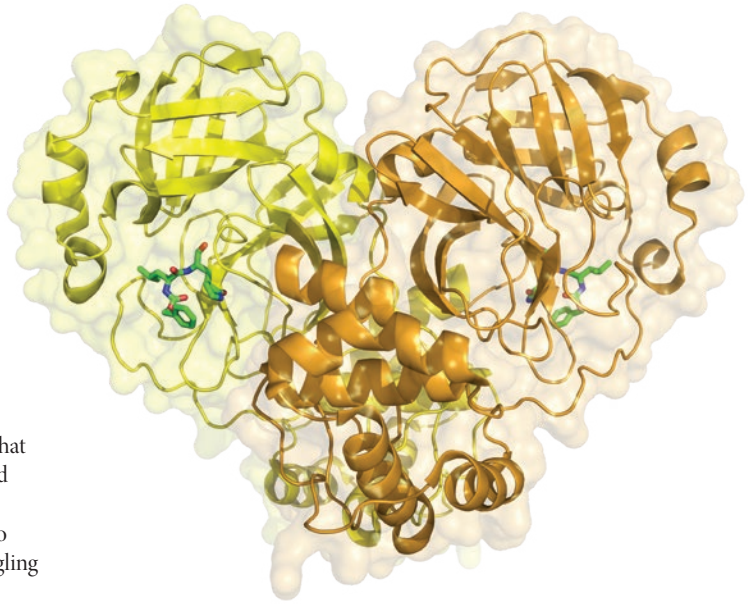

The crystal structure of COVID-19 main protease in complex with GC376. Protein Data Bank: 7c8u.

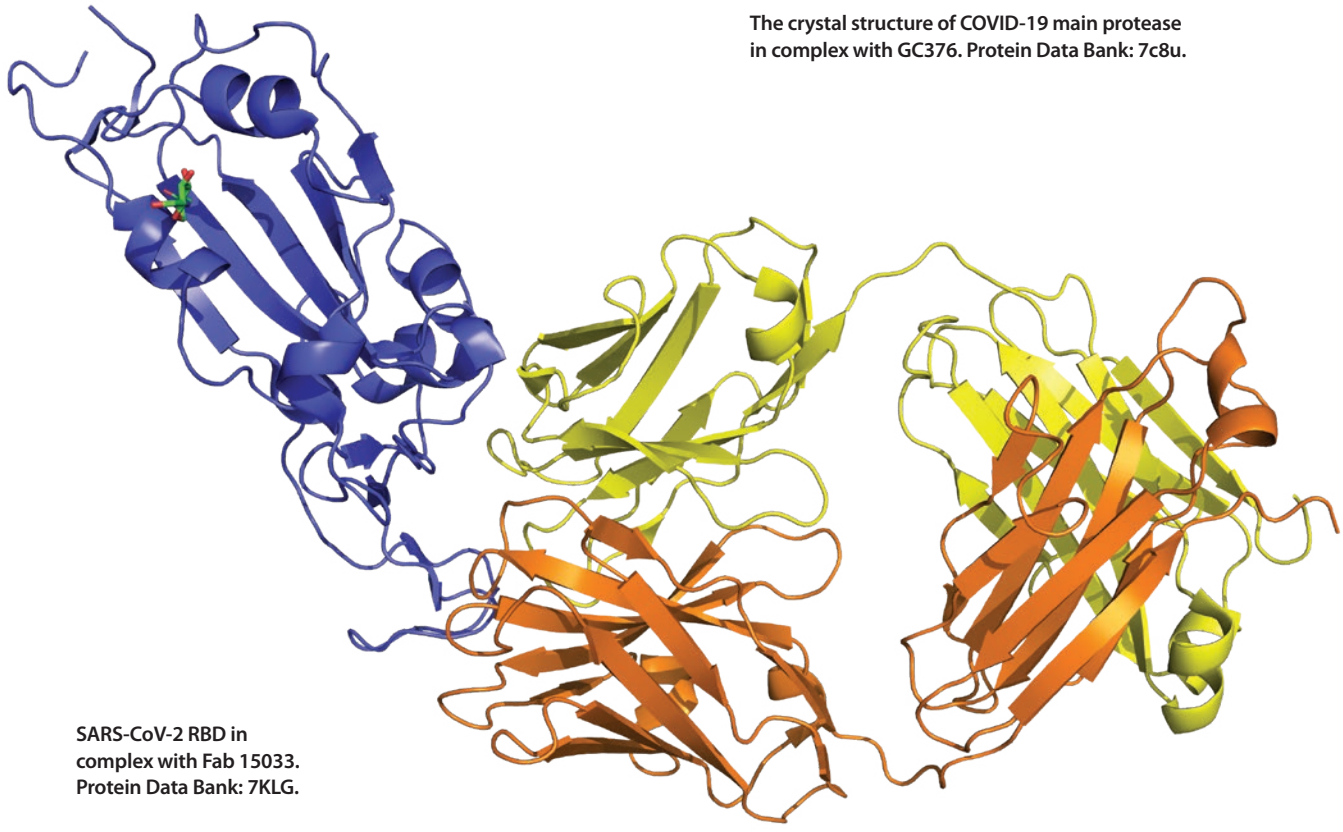

SARS-CoV-2 RBD in complex with Fab 15033. Protein Data Bank: 7KLG.

## Helping remove SARS-COV-2 from the air we breathe

A University of Saskatchewan research team has designed a device that can sanitize the air and could help protect us from catching the SARS-CoV-2 virus. The scientists are using SXRMB to test the device's effectiveness and the feasibility of integrating it into current air conditioning systems. The team is using the CLS to take high resolution images of their device while it is in action to gain a deeper knowledge of the sanitation process and optimize its performance.

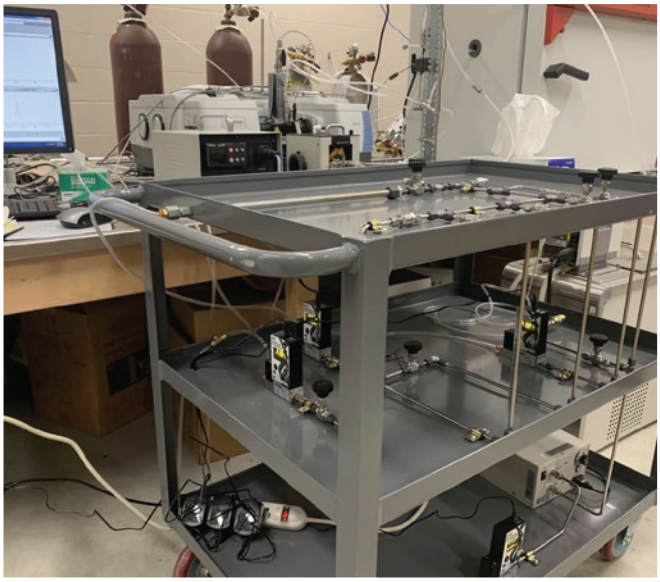

**A University of Saskatchewan team hopes to design an affordable, shoebox sized air filter. Image courtesy Nazanin Charchi.**

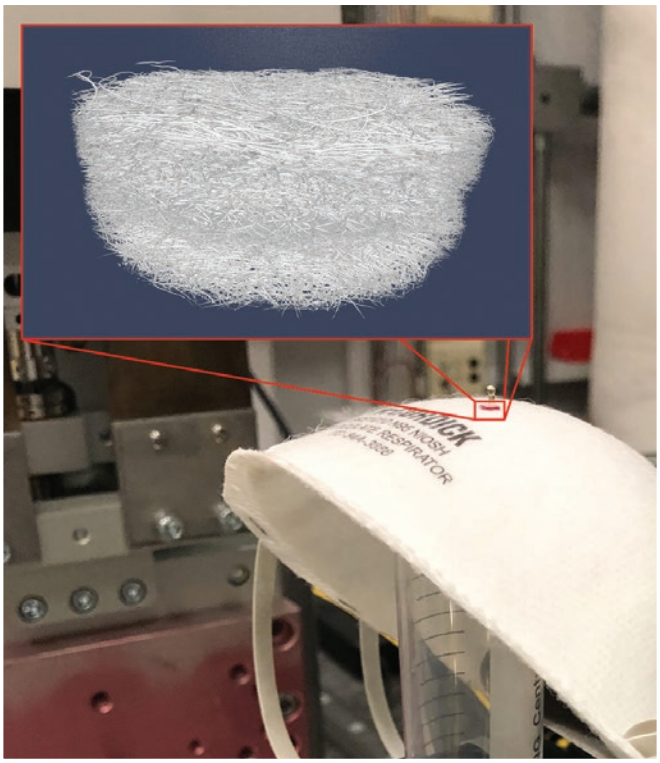

## Extending the lifespan of N95 masks

Through a collaboration between the CLS and the Vaccine and Infectious Disease Organization-International Vaccine Centre (VIDO-InterVac), scientists hope to understand the structural changes happening inside N95 respirator masks after being sterilized for reuse. The BMIT beamline has been used to visualize these changes.

## Micron-etching for better COVID-19 testing

**Researchers from the CLS and Université Laval are using our SyLMAND beamline to develop a device with multiple narrow channels through which a small fluid sample from a patient could flow. Meanwhile, they are creating an accessory that could systematically run tests through the channels to determine if the patient has coronavirus. If successful, this project could improve Canada's testing and contact tracing performance.**

A laser writer in our SyLMAND facility

**For videos and stories about our COVID research program, visit: www.lightsource.ca/covid19_research.html**

# ADDITIONAL HIGHLIGHTS

## Using automation to keep the data flowing at the CLS

In March of 2020 the CLS went into a shutdown that coincided with the declaration of a provincial state of emergency. When operations resumed again in the summer of 2020, restricted travel and facility access meant that new approaches were required to keep beamlines operating at high capacity. Automation of beamline optimization and scanning suddenly became a necessity for keeping the data flowing. Most synchrotron experiments rely heavily on the work of visiting scientists and students who are responsible for the preparation of samples, sample loading and general beamline operation. For some experiments the work can be quite technical and demanding, involving long hours at the beamline. But for other experiments, much of the work can be repetitive, making it suitable for automation. On many beamlines, automation was always part of the plans but the COVID pandemic accelerated development and beamline automation is now being used to deliver user data 24 hours a day through a highly efficient mail-in program. In 2020, several beamlines made the move to more automated delivery. While not all experiments can be performed using automation, many routine measurements can be made without users being present and research programs relying on these measurements can continue to move forward.

The first stage of the mail-in procedure involves research groups preparing their samples for shipment to the CLS. Specific instructions are produced by the users for the preparation and handling of each sample along with a request for the specific measurements required. Once the samples arrive at the CLS they are prepared by staff and loaded into the beamline.

Using SGM as an example, automated procedures are used to map the sample holder, identify the sample positions and configure the beamline for a series of measurements. Very little intervention is required during measurement as the automation handles beamline optimization, watches for the occurrence of beam dumps and notifies staff when the measurements are complete. Using automation in this way, a handful of staff members are able to maintain full time operations and keep the data flowing to scientists around the globe.

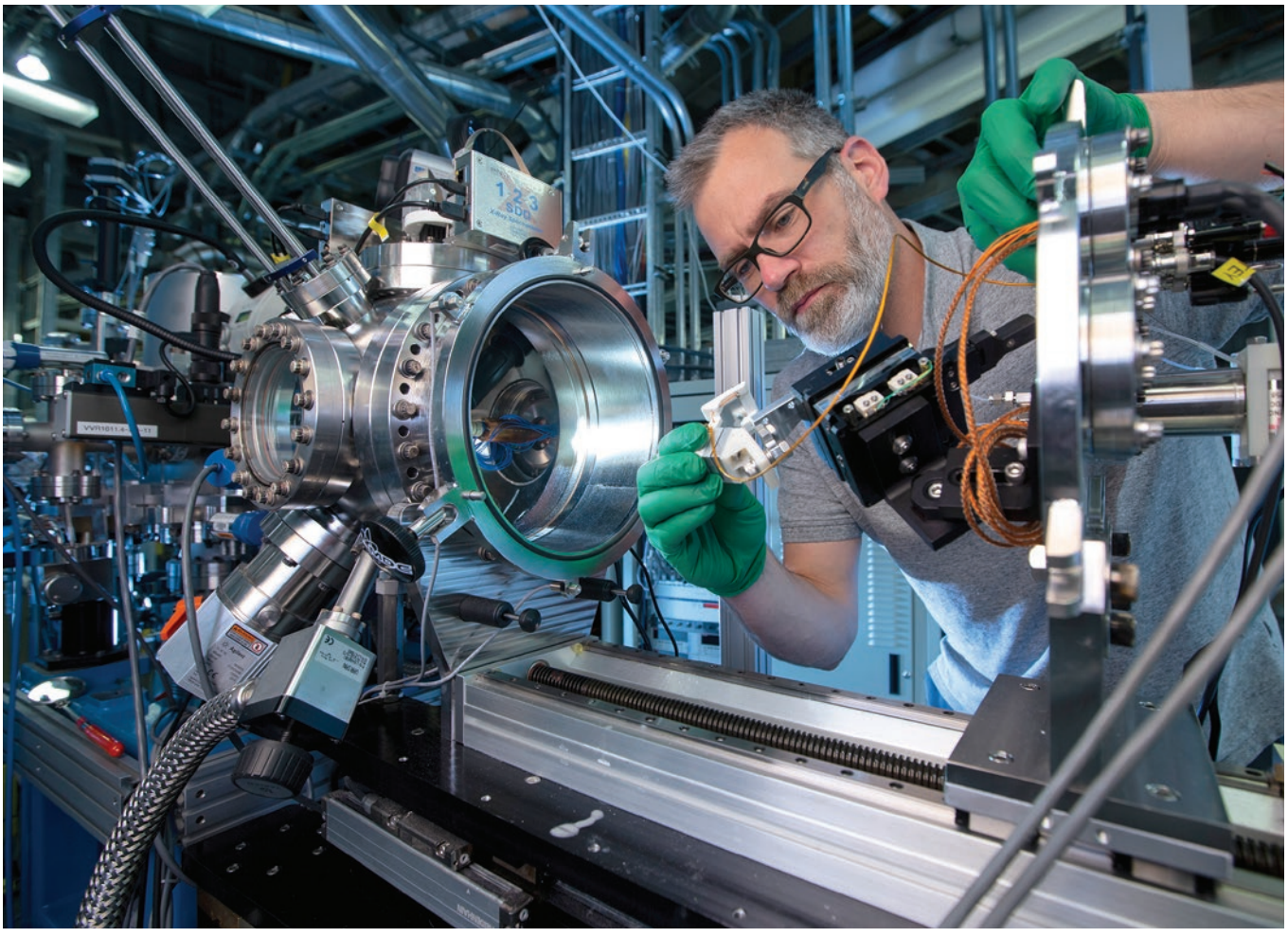

FAR-IR

# Astrophysical research at the Far-Infrared beamline: Decoding the sky

Photons from celestial bodies unimaginable distances away carry information about all of the space through which they have traveled. Spectrometers attached to telescopes and satellites collect these photons and record the information they offer.

To understand the rich spectral information we gather from astrological bodies, we have the know what we are looking for. The Far-Infrared beamline helps to collect and analyze spectra here on earth to interpret the data collected from space, and many exciting astrophysical projects were completed in 2020.

Methanol is highly pervasive in the interstellar medium and star-forming regions, serving as an important probe of the complex isotopic chemistry and excitation mechanisms in protostars. It also it has a complicated spectrum thanks to the large-amplitude internal rotation of its methyl group. Dr. Ron Lees et al. are decoding the transition network that governs the molecular excitation in warm regions. [1] and are exploring patterns observed for the CSH-bending and CH3-rocking bands of methyl mercaptan [2]. Important work has been done by Dr. Kobayashi et. al to characterize the low-lying torsions and vibrations of methyl formate, which have been observed in the giant molecular clouds Sagittarius B2 and Orion KL. [3].

Propane has been observed on Titan, Jupiter, and Saturn; to aid in its analysis Dr. Duant et. al have analyzed several bands of the spectrum of 2-C13-propane. [4] Ammonia is commonly observed in astrophysical measurements and has been seen in the atmospheres of Earth, Jupiter, Saturn, and other planets, while work by Cane et al. has improved the accuracy of the parameters needed for understanding ammonia's bending states. [5]

It is also important to understand the effects of the environment that key gases are found in. To this end, Bernath and co-workers have measured absorption cross-sections of neopentane, broadened by nitrogen, and ethane and isobutane broadened by both nitrogen and hydrogen. All of which are relevant to the atmospheres of Titan, a moon of Saturn, and the giant planets among other astronomical bodies. [6-9].

The final paper we will mention here is the work of Godin et. al, who addressed the question as to whether collision-induced absorption of $CH_4$-$CO_2$ and $H_2$-$CO_2$ could have produced a greenhouse effect in the ancient martian atmosphere strong enough to allow liquid water to be present. Using data collected at the CLS, they showed that collision-induced absorption of $H_2$-$CO_2$ may provide sufficient warming to account for the presence of liquid water on the planet. [10]

While much work has been done there are many more molecules to study and many more parameters to probe. In the future, the Far-IR beamline will continue its work enabling a deeper understanding of the universe.


1. Lees, R.M.; Xu, Li-Hong; Billinghurst, Brant et al. (2020). Patterns in synchrotron near-free-rotor FIR spectra of $CH_3OH$ and $CD_3OH$ – The tau of methanol. *Journal of Molecular Structure*, 127960. DOI: 10.1016/j.molstruc.2020.127960.

2. Lees, R.M.; Reid, E.M; Xu, Li-Hong; Billinghurst, B.E. (2020). Synchrotron spectroscopy of the CSH-bending and $CH_3$-rocking bands of methyl mercaptan. *Canadian Journal of Physics* 98(6), 519-529. DOI: 10.1139/cjp-2019-0487.

3. Kobayashi, Kaori; Sakai, Yusuke; Fujitake et al. (2020). Identification of a vibrationally excited level in methyl formate through microwave and far-infrared spectroscopy. *Canadian Journal of Physics*. DOI: 10.1139/cjp-2019-0578.

4. Daunt, Stephen J.; Grzywacz, Robert, Western et al. (2020). First high-resolution infrared spectra of 2–13C-propane analyses of the v26 (B2) c-type and v9 (A1) b-type bands. *Journal of Molecular Structure*, 127851. DOI: 10.1016/j.molstruc.2020.127851.

5. Canè, Elisabetta; Lonardo, Gianfranco Di, Fusina et al. (2020). Spectroscopic characterization of the v2 = 3 and v2 = v4 = 1 states for $15NH_3$ from high resolution infrared spectra. *Journal of Quantitative Spectroscopy and Radiative Transfer*, 106987. DOI: 10.1016/j.jqsrt.2020.106987.

6. Bernath, Peter; Dodangodage, Randika; et al. (2020). Absorption cross sections for neopentane broadened by nitrogen in the 3.3 micron region. *Journal of Quantitative Spectroscopy and Radiative Transfer* 251, 107034. DOI: 10.1016/j.jqsrt.2020.107034.

7. Dodangodage, Randika; Bernath, Peter F.; Zhao, Jianbao; Billinghurst, Brant (2020). Absorption cross sections for ethane broadened by hydrogen and helium in the 3.3 micron region. *Journal of Quantitative Spectroscopy and Radiative Transfer* 253, 107131. DOI: 10.1016/j.jqsrt.2020.107131.

8. Hewett, Dan; Bernath, Peter; Zhao et al. (2020). Near infrared absorption cross sections for ethane broadened by hydrogen and nitrogen. *Journal of Quantitative Spectroscopy and Radiative Transfer* 242, 106780. DOI: 10.1016/j.jqsrt.2019.106780.

9. Hewett; Dan; Bernath; Peter F.; Wong et al. (2019). N2 and H2 broadened isobutane infrared absorption cross sections and butane upper limits on Titan. *Icarus*, 113460. DOI: 10.1016/j.icarus.2019.113460

10. Godin, Paul J.; Ramirez, Ramses M.; Campbell et al. (2020). Collision-Induced Absorption of CH 4 -C0 2 and H 2 -C0 2 Complexes and Their Effect on the Ancient Martian Atmosphere. *Journal of Geophysical Research Planets*. DOI: 10.1029/2019je006357.

## Mid-IR

# IRsweep F1 IRis Dual-comb Spectrometer

The millisecond to microsecond time regime spans many dynamic processes such as reaction kinetics, molecular dynamics and complex system evolution. Accessing this time regime in the mid-infrared can be challenging. A new laser-based instrument at the beamline capable of accessing these fast timescales with reasonable spectral bandwidth has recently been commissioned and is open for general user proposals.

Lins, Erick; Read, Stuart; Unni, Bipinla et al, Microsecond Resolved Infrared Spectroelectrochemistry Using Dual Frequency Comb IR Lasers. *Analytical Chemistry*. 92, 6241-6244. DOI: 10.1021/acs.analchem.0c00260

# Updates to the Agilent Infrared Microscope System

The Agilent Cary 670 FTIR Interferometer with Cary 620 Microscope at the beamline underwent a few upgrades this past year to increase useability, capacity and capabilities. The most significant of these upgrades was improving the spatial resolution and reproducibility of the microscope stage from 5um to 100nm. Additional enhancements included an automated liquid nitrogen fill system for the full field (focal plane array detector) and remote operational controls.

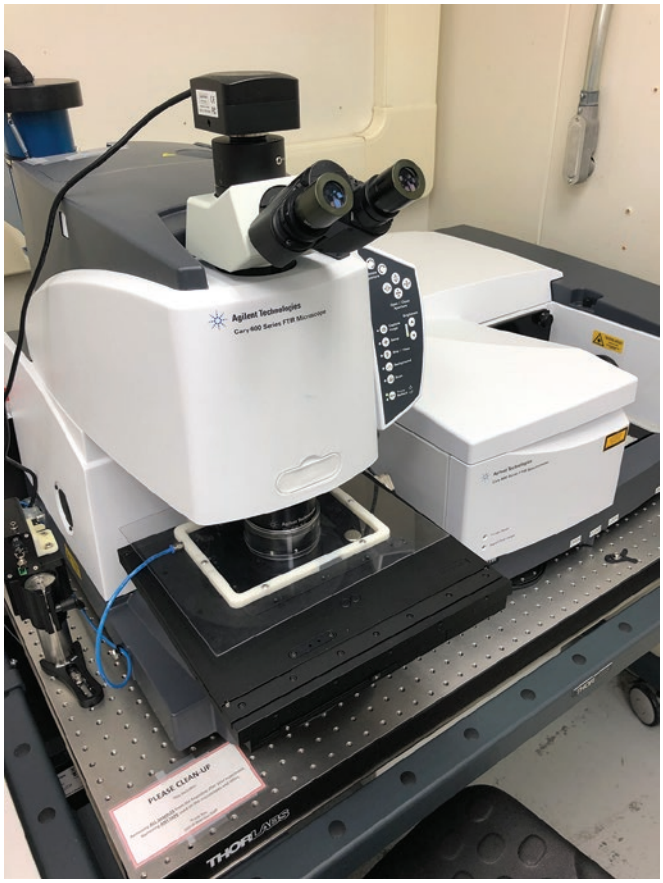


# Quasar: Open Source Data Analysis Tool

Having access to high quality data analyzing tools is important to process data from better detectors and more complex experimental setups.To this end, in 2020 CLS contributed to the development of visible image overlays and tile-by-tile processing in Quasar, an effort by many institutions to build an open-source collection of spectroscopic analytical tools.

## SXRMB

# An in situ XES endstation

Up to now, there have been limited synchrotron-based XES endstations at beamlines. Most of these endstations are designed mainly for hard X-ray (>5 keV) applications in ambient environments. There are fewer XES endstations for elements in the medium/tender energy range (between 1 and 5 keV), and these have rarely accommodated in-situ experiments. These endstations, used alongside XAS, are essential for understanding the local geometry, charge density and type of ligands attached to elements of interest, used in materials science, chemistry, catalysis, medicine, earth and environmental sciences.

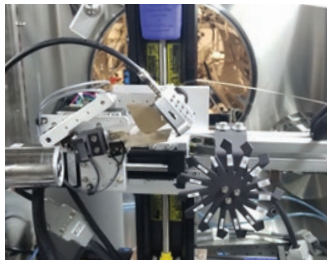

In 2019, an XES spectrometer optimized for the tender X-ray region (2–5 keV) was successfully installed into an inert atmosphere glovebox, and the entire system was successfully integrated into the SXRMB CLS [1]. High energy resolution of ~1 eV or better has been achieved for the spectrometer in the tender energy X-ray ranges. Because of the compact design of the spectrometer, it is possible to fit the spectrometer into a helium gas filled and low moisture and oxygen content (below 1 ppm) glovebox, which not only makes the low energy x-ray penetration feasible but it can also be used for in situ and in operando studies. In addition, the endstation can be equipped with a Silicon Drift Detector (SDD) for XAS measurements in fluorescence yield mode. This state of art glovebox-integrated XES spectrometer, combined with XAS, has a great capability for in-situ studies in earth and environmental sciences, battery development, and catalysis research.

Shakouri M, Holden WM, Hu Y, Xiao Q, Igarashi R, Schreiner B, Bree M, Li M, Li W, Sun X, Sham TK. Glovebox-integrated XES and XAS station for in situ studies in tender x-ray region. Electronic Structure. 2020 Oct 6;2(4):047001. DOI: 10.1088/2516-1075/abb932

# INDUSTRY

**2020 was a challenging year shared by many due to the global pandemic, but it was already going to be a challenging year for the Industry group. The primary revenue-generating beamline for the Industrial Services group, CMCF-ID, started a major upgrade, which is currently scheduled to be complete in June 2021, after some delays attributed to the pandemic.**

There are several exciting initiatives that the Industry team will be involved with in 2021. The Industry group will host a post-doctoral fellow in the coming year working on a project entitled "In-Situ X-Ray Imaging of Carbon Fibre Composite Manufacturing Processes", this work will be on the BMIT beamline.

The Industrial Services team is currently partnering with PSI Technologies and PSI Mining to investigate molecular scale processes associated with using recycled products. This mechanistic understanding will then be applied to develop models for real world applications. Another project related to materials infrastructure is discussed in more detail below.

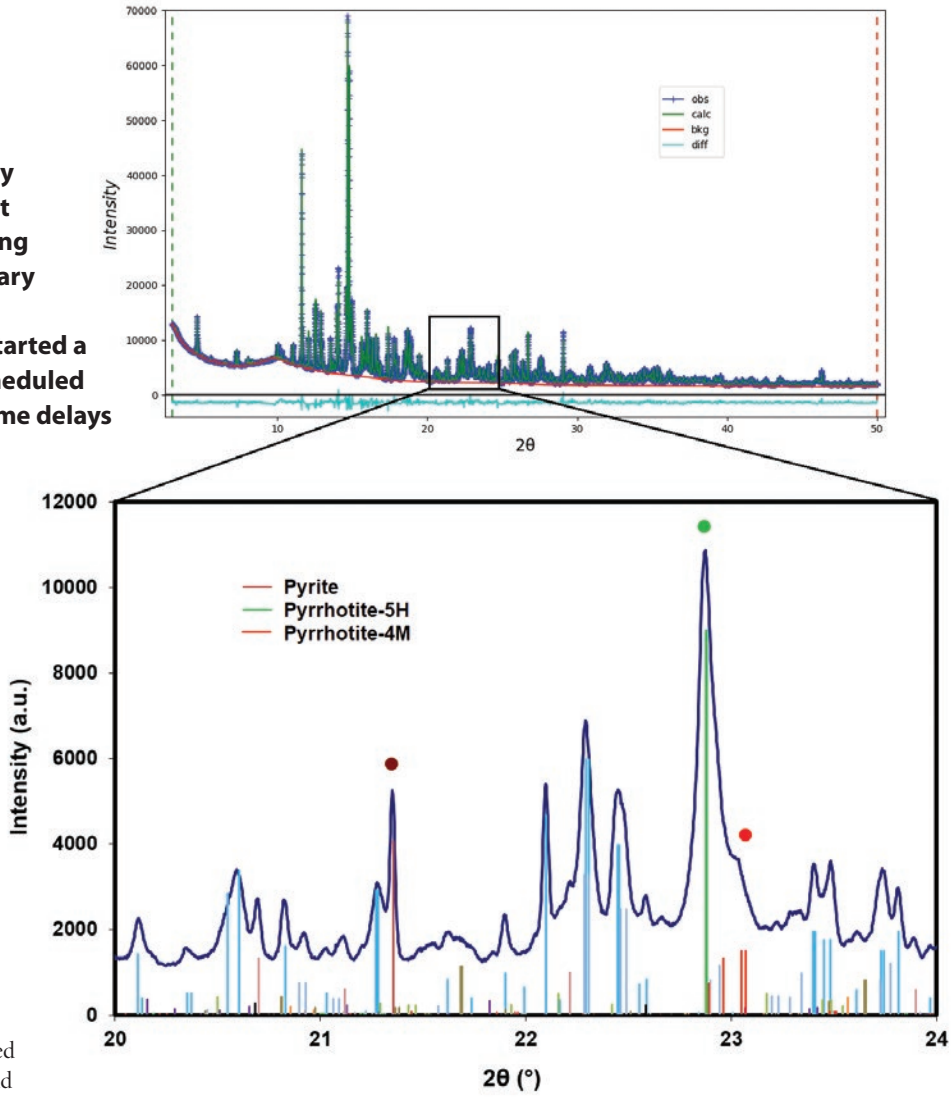


**A Rietveld refinement of synchrotron PXRD data (top), with a magnified view of a small region of the pattern illustrating the location of some Bragg reflections characteristic of pyrite (FeS2) and pyrrhotite (Fe1-xS).**

In collaboration with NRC staff members, Jon Makar and Rana Masoudi, the CLS has investigated high resolution measurements on pyrite (FeS2) and pyrrhotite (Fe1-xS) in coarse concrete aggregate. Concrete aggregates are granular materials with sizes of 5-20 mm and controlled composition, which when combined with water and cement form concrete. Trace reactive sulfide mineral impurities, like pyrrhotite and pyrite, in aggregate can have a major deleterious impact on the long term structural integrity of the final concrete product. Iron sulfides are susceptible to oxidation over time, creating sulfuric acid and ferrous ions [1], which initiate secondary reactions that can cause expansion, cracking and ultimately, concrete failure. In Canada, concrete failures due to sulfide oxidation have been a prominent problem in Trois-Rivières, Quebec, and similar concrete issues are a widespread phenomenon with occurrences in Connecticut (U.S.), southwest England, and Scandinavia, among other places [2].

Pyrrhotite is sufficiently reactive that concentrations on the order of tenths of a percent are sufficient to cause concrete damage [3]. Therefore, sensitive analytical techniques are required to detect and quantify pyrrhotite and pyrite content in aggregate materials. Synchrotron powder X-ray diffraction (PXRD) has been conducted at the CLS on concrete aggregate materials using both the CMCF-BM and BXDS-WLE beamlines, with quantification performed using Rietveld refinement.

Even in complicated aggregate matrices with 10 to 16 different mineral phases present, pyrite and multiple polymorphs of pyrrhotite have been detected and quantified at levels below 0.5 wt.%. This work will contribute to improved understanding of the distribution and range of sulfide impurities in aggregate materials, and assist with development of additional enhanced techniques for the detection and quantification of trace sulfide impurities [3].

1. Belzile, N., Chen, Y.-W., Cai, M.-F., and Li, Y. 'A review on pyrrhotite oxidation,' J. Geochem. Exploration 84 (2004) 65-76.

2. Nordic Concrete Federation. 'Impact of sulphide minerals (pyrrhotite) in concrete aggregate on concrete behaviour,' Workshop Proceedings No. 14; Oslo, Norway, November 15-16, 2018.

3. Makar, J., Reid, J., Ridsdale, A., and Masoudi, R. 'High Resolution Measurements of Pyrrhotite and Other Minerals in Coarse Concrete Aggregate,' Presented at the 56th Annual Meeting of the Northeastern Section, Geological Society of America, March 14, 2021.

Check out our new Virtual Classroom

## EDUCATION PROGRAMS

# 2020 Vision: Looking through the eyes of our users

The CLS's education programs use research as a tool for learning science in depth, with a variety of entry points and participants: large, easy entry point research opportunities, teacher professional development, and detailed-student led research programs are all offered under the CLS education umbrella.

These programs all continued through 2020, but like everyone, the pandemic changed how we operate. This year, all education programming successfully went virtual. Background information, videos, and lesson plans were created to populate a new Virtual Classroom space where all of the Light Source Student Experience (LiSSE) classes, Transcanadian Research & Environmental Education (TREE), and Students on the Beamlines (SotB) groups can connect directly with CLS to continue existing projects and begin new ones. These virtual opportunities have opened the door for international participation for the first time, with individuals from 5 countries outside of Canada connecting with our programs.

Making Indigenous connections at the Canadian Indigenous Science and Engineering Society (.caISES) conference

(L to R) Robert Blyth, CLS Science Projects Manager; Bernie Petit, Annishnaabe, CLS Education Coordinator-Indigenous Programs; Corey Gray, Blackfoot and member of the Siksika Nation, Caltech LIGO Hanford Observatory Detector Operator

One of the last in-person SotB groups get ready to prep their samples of flax plants in our Life Sciences lab. These students are from Balmoral Hall in Winnipeg.

(L to R: Alice Xu; Dr. Patricia Mitchler, teacher; Alyssa Wang; Irina Znamirowski; Bonnie Luo; Matt Gelley, teacher; Dr. Susan Koziel, mentor, InnoTech Alberta Life Sciences Research Technologist; Missing: Cassy Appelt, mentor, Usask PhD student.

### Canadian high school student comments:

*" Before I had always seen researchers and scientists as people in laboratories, working with chemicals and such… It has broadened my view of what exactly scientists do, as I now see that there are many different paths a person can follow, that are all stimulating and rewarding."*

*"This virtual meeting was an amazing and new experience for me. I appreciate the CLS team for providing us this opportunity. Looking forward to more opportunities like this!"*

*"The critical questions and depth of experience concerning the issues of governance and the intersection of science and society [was interesting]."*

### Mirwat Uzair, physics teacher in Pakistan said:

*"Thank you for an insight to Indigenous Teaching. Now I am looking at my classrooms in quite a different way. I do have some students from tribal regions of my country where females are not encouraged to pursue education for some reasons. And now I would be more careful to have them fully engaged in my classroom thru TKK and other strategies you talked about."*


Students from Bishop Carroll High School in Calgary AB present their award-winning SotB poster at CLS' virtual Annual Users Meeting.

| | |
|---|---|
| 9 PROVINCES \| 5 COUNTRIES | Participants (teachers & students) from 9 provinces & 5 countries |
| 598 | 598 high school students across all programs & virtual sessions |
| 24 | Students from 24 schools |
| 119 | 119 educators in all programs & PD sessions |
| 19 | Collaborative relationships and projects with 19 organizations |

Throughout all of this we have been developing learning approaches grounded in Traditional Indigenous Knowledge and that synchrotron techniques can contribute to. New projects and programs are developing from this work that provide space for Indigenous student to explore projects stemming from their conversations with Elders and Traditional Knowledge Keepers. For example, we will have a video connecting physics, chemistry, and Traditional teaching concepts to making bannock. LiSSE students are exploring nutrients available in wild berries and we are learning the untold (her)story of the near extinction of bison.

A group of teachers attending a virtual professional development workshop discuss soil chemistry.

# PUBLICATIONS

## PEER-REVIEWED


Abdelrasoul, Amira; Doan, Huu; Lohi, Ali; Zhu, Ning (2020). Synchrotron based Micro Tomography (SR-μCT), Experimental, and Computational Studies to Investigate the Influences of Cross Flow Air Injection in Ultrafiltration Process. Journal of Environmental Chemical Engineering,10.1016/jjece.2020.104611

Adair, Keegan R.; Banis, Mohammad Norouzi; Zhao, Yang; Bond, Toby; Li, Ruying et al. (2020). Temperature-Dependent Chemical and Physical Microstructure of Li Metal Anodes Revealed through Synchrotron-Based Imaging Techniques. Advanced Materials 32(32), 2002550.10.1002/adma.202002550

Adams, Alexis M.; Gillespie, Adam W.; Dhillon, Gurbir S.; Kar, Gourango; Minielly, Colin et al. (2020). Long-term effects of integrated soil fertility management practices on soil chemical properties in the Sahel. Geoderma 366, 114207.10.1016/j.geoderma.2020.114207

Adsetts, Jonathan Ralph; Hoesterey, Salena; Love, David A; Ding, Zhifeng (2020). Structural Origins of Carbon Quantum Dot Luminescence by Synchrotron X-Ray Spectroscopy. Electronic Structure. 10.1088/2516-1075/abd61c

Ahmad, Shehryar; Tsang, Kara K; Sachar, Kartik; Quentin, Dennis; Tashin, Tahmid M et al. (2020). Structural basis for effector transmembrane domain recognition by type VI secretion system chaperones. 10.7554/elife.62816

Akhter, Fardausi; Fairhurst, Graham D.; Blanchard, Peter E. R.; Machin, Karen L.; Blyth, Rob I. R. et al. (2020). Experimental variation in the spatial deposition of trace metals in feathers revealed using synchrotron X-ray fluorescence. X-Ray Spectrometry. 10.1002/xrs.3140

Al Fattah, Md Fahim; Amin, Muhammad Ruhul; Mallmann, Mathias; Kasap, Safa; Schnick, Wolfgang et al. (2020). Electronic structure investigation of wide band gap semiconductors—Mg2PN3 and Zn2PN3: experiment and theory. Journal of Physics Condensed Matter.10.1088/1361-648x/ab8f8a

Alabi, Wahab O.; Sulaiman, Kazeem O.; Wang, Hui (2020). Sensitivity of the properties and performance of Co catalyst to the nature of support for CO2 reforming of CH4. Chemical Engineering Journal 390, 124486.10.1016/j.cej.2020.124486

Alabi, Wahab O.; Sulaiman, Kazeem O.; Wang, Hui; Hu, Yongfeng; Patzig, Christian et al. (2020). Effect of spinel inversion and metal-support interaction on the site activity of Mg-Al-Ox supported Co catalyst for CO2 reforming of CH4. Journal of CO2 Utilization 37, 180-187.10.1016/j.jcou.2019.12.006

Alam, Md. Samrat; Bishop, Brendan; Chen, Ning; Safari, Salman; Warter, Viola et al. (2020). Reusable magnetite nanoparticles–biochar composites for the efficient removal of chromate from water. Scientific Reports 10(1). 10.1038/s41598-020-75924-7

Alonzo, Diego A.; Chiche-Lapierre, Clarisse; Tarry, Michael J.; Wang, Jimin; Schmeing, T. Martin et al. (2020). Structural basis of keto acid utilization in nonribosomal depsipeptide synthesis. Nature Chemical Biology.10.1038/s41589-020-0481-5

Amin, Muhammad Ruhul; Strobel, Philipp; Qamar, Amir; Giftthaler, Tobias; Schnick, Wolfgang et al. (2020). Understanding of Luminescence Properties Using Direct Measurements on Eu2+ -Doped Wide Bandgap Phosphors. Advanced Optical Materials, 2000504.10.1002/adom.202000504

Anderson, Alexander C.; Burnett, Alysha J.N.; Hiscock, Lana; Maly, Kenneth E.; Weadge, Joel T. et al. (2020). The Escherichia coli cellulose synthase subunit G (BcsG) is a Zn2+-dependent phosphoethanolamine transferase. Journal of Biological Chemistry 295(18), 6225-6235.10.1074/jbc.ra119.011668

Andronowski, Janna M.; Cole, Mary E. (2020). Current and emerging histomorphometric and imaging techniques for assessing age-at-death and cortical bone quality. Wiley Interdisciplinary Reviews Forensic Science, e1399.10.1002/wfs2.1399

Andronowski, Janna M.; Davis, Reed A.; Holyoke, Caleb W. (2020). A Sectioning, Coring, and Image Processing Guide for High-Throughput Cortical Bone Sample Procurement and Analysis for Synchrotron Micro-CT. Journal of Visualized Experiments (160), e61081.10.3791/61081

Athanasiadou, Dimitra; Jiang, Wenge; Reznikov, Natalie; Rodríguez-Navarro, Alejandro B.; Kröger, Roland et al. (2020). Nanostructure of mouse otoconia. Journal of Structural Biology , 107489.10.1016/j.jsb.2020.107489

Ay, Birol; Parolia, Kushagra; Liddell, Robert S.; Qiu, Yusheng; Grasselli, Giovanni et al. (2020). Hyperglycemia compromises Rat Cortical Bone by Increasing Osteocyte Lacunar Density and Decreasing Vascular Canal Volume. Communications Biology 3(20) , 1-9.10.1038/s42003-019-0747-1

Bai, Risheng; Navarro, M. Teresa; Song, Yue; Zhang, Tianjun; Zou, Yongcun et al. (2020). Titanosilicate zeolite precursors for highly efficient oxidation reactions. Chemical Science 11(45) , 12341-12349. 10.1039/d0sc04603e

Balakrishnan, Manojkumar; Shrestha, Pranay; Ge, Nan; Lee, ChungHyuk; Fahy, Kieran F. et al. (2020). Designing Tailored Gas Diffusion Layers with Pore Size Gradients via Electrospinning for Polymer Electrolyte Membrane Fuel Cells. Applied Energy Materials 3(3) , 2695-2707.10.1021/acsaem.9b02371

Barrett, William; Nasr, Somaye; Shen, Jing; Hu, Yongfeng; Hayes, Robert E. et al. (2020). Strong metal–support interactions in Pd/Co3O4 catalyst in wet methane combustion: in situ X-ray absorption study. Catalysis Science and Technology 10(13) , 4229-4236. 10.1039/d0cy00465k

Beenstock, Jonah; Ona, Samara Mishelle; Porat, Jennifer; Orlicky, Stephen; Wan, Leo C. K. et al. (2020). A substrate binding model for the KEOPS tRNA modifying complex. Nature Communications 11(1). 10.1038/s41467-020-19990-5

Bergsveinson, Jordyn; Roy, Julie; Maynard, Christine; Sanschagrin, Sylvie; Freeman, Claire N. et al. (2020). Metatranscriptomic Insights Into the Response of River Biofilm Communities to Ionic and Nano-Zinc Oxide Exposures. Frontiers in Microbiology 11. 10.3389/fmicb.2020.00267

Bernath, Peter; Dodangodage, Randika; Dulick, Michael; Zhao, Jianbao; Billinghurst, Brant et al. (2020). Absorption cross sections for neopentane broadened by nitrogen in the 3.3 micron region. Journal of Quantitative Spectroscopy and Radiative Transfer, 107034.10.1016/j.jqsrt.2020.107034

Bewer, Brian (2020). Comparison of dose values predicted by FLUKA to measured values using Luxel+ Ta type dosimeters. Nuclear Instruments and Methods in Physics Research. Section B: Beam Interactions with Materials and Atoms 464, 12-18. 10.1016/j.nimb.2019.11.042

Bhagavathula, KB; Parcon, JS; Azar, A; Ouellet, S; Satapathy, S et al. (2020). Quasistatic response of a shear-thickening foam: Microstructure evolution and infrared thermography. Journal of Cellular Plastics, 0021955X2096398. 10.1177/0021955x20963989

Billinghurst, Brant E. (2020). Preface: Special Issue: 10th International Workshop on Infrared Microscopy and Spectroscopy with Accelerator Based Sources (WIRMS 2019). Infrared Physics and Technology, 103330. 10.1016/j.infrared.2020.103330

Blanchard, Peter; Babichuk, Nicole; Sarkar, Atanu (2020). Evaluating the use of synchrotron X-ray spectroscopy in investigating brominated flame retardants in indoor dust. Environmental Science and Pollution Research .10.1007/s11356-020-10623-4

Cabral, Cyril; Lavoie, Christian; Murray, Conal; Pyzyna, Adam; Rodbell, Ken et al. (2020). Thin film deposition research and its impact on microelectronics scaling. Journal of Vacuum Science and Technology A: Vacuum. Surfaces and Films 38(4), 040803. 10.1116/6.0000230

Canè, Elisabetta; Lonardo, Gianfranco Di; Fusina, Luciano; Tamassia, Filippo; Predoi-Cross, Adriana et al. (2020). Spectroscopic characterization of the v2 = 3 and v2 = v4 = 1 states for 15NH3 from high resolution infrared spectra. Journal of Quantitative Spectroscopy and Radiative Transfer , 106987. 10.1016/j.jqsrt.2020.106987

Cao, Chuntian; Toney, Michael F.; Sham, Tsun-Kong; Harder, Ross; Shearing, Paul R. et al. (2020). Emerging X-ray imaging technologies for energy materials. Materials Today 34, 132-147. 10.1016/j.mattod.2019.08.011

Cardenas, Daniel; Turyanskaya, Anna; Rauwolf, Mirjam; Panahifar, Arash; Cooper, David et al. (2020). Determining elemental strontium distribution in rat bones treated with strontium ranelate and strontium citrate using 2D micro-XRF and 3D dual energy K-edge subtraction synchrotron imaging. X-Ray Spectrometry 49(3), 424-433. 10.1002/xrs.3127

Casali, Juliana; Hao, Chunyi; Ghorbani, Zohreh; Cavallin, Hannah; Loon, Lisa Van et al. (2020). Application of Large-scale Synchrotron X-Ray Fluorescence 2D Mapping of Alteration Styles to Understand Gold Mineralization at the Monument Bay Project, Stull Lake Greenstone Belt, Manitoba, Canada. Microscopy and Microanalysis, 1-3.10.1017/s1431927620024198

Caveney, N. A.; Serapio-Palacios, A.; Woodward, S. E.; Bozorgmehr, T.; Caballero, G. et al. (2020). Structural and cellular insights into the L,D-transpeptidase YcbB as a therapeutic target in C. rodentium, S. Typhimurium, and S. Typhi infections. Antimicrobial Agents and Chemotherapy . 10.1128/aac.01592-20

Chen, Jiatang; Yiu, Yun Mui; Wang, Zhiqiang; Covelli, Danielle; Sammynaiken, Ramaswami et al. (2020). Elucidating the Many-Body Effect and Anomalous Pt and Ni Core Level Shifts in X-ray Photoelectron Spectroscopy of Pt–Ni Alloys. Journal of Physical Chemistry C 124(4), 2313-2318. 10.1021/acs.jpcc.9b09940

Chen, Ning; Alam, Md Samrat; Alessi, Daniel S. (2020). XAS characterization of nano-chromite particles precipitated on magnetite-biochar composites. Radiation Physics and Chemistry 175, 108544. 10.1016/j.radphyschem.2019.108544

Chen, Shuo; Wu, Jia-Le; Liang, Ying; Tang, Yi-Gang; Song, Hua-Xin et al. (2020). Arsenic Trioxide Rescues Structural p53 Mutations through a Cryptic Allosteric Site. Cancer Cell . 10.1016/j.ccell.2020.11.013

Chen, Xiujuan; Huang, Gordon; Li, Yongping; An, Chunjiang; Feng, Renfei et al. (2020). Functional PVDF ultrafiltration membrane for Tetrabromobisphenol-A (TBBPA) removal with high water recovery. Water Research 181, 115952. 10.1016/j.watres.2020.115952

Chevrier, Daniel M.; Conn, Brian E.; Li, Bo; Jiang, De-en; Bigioni, Terry P. et al. (2020). Interactions between Ultrastable Na4Ag44(SR)30 Nanoclusters and Coordinating Solvents: Uncovering the Atomic-Scale Mechanism. ACS Nano 14(7) , 8433-8441. 10.1021/acsnano.0c02615

Chicilo, F; Hanson, A L; Geisler, F H; Belev, G; Edgar, A et al. (2020). Dose profiles and x-ray energy optimization for microbeam radiation therapy by high-dose, high resolution dosimetry using

Sm-doped fluoroaluminate glass plates and Monte Carlo transport simulation. Physics in Medicine and Biology 65(7), 075010. 10.1088/1361-6560/ab7361

Chicilo, F; Okada, G; Belev, G; Chapman, D; Edgar, A et al. (2020). Instrumentation for high-dose, high-resolution dosimetry for microbeam radiation therapy using samarium-doped fluoroaluminate and fluorophosphate glass plates. Measurement Science and Technology (31), 015201-1 - 015201-13. 10.1088/1361-6501/ab404e

Chivers, Brandon A.; Scott, Robert W. J. (2020). Selective oxidation of crotyl alcohol by AuxPd bimetallic pseudo-single-atom catalysts. Catalysis Science and Technology 10(22) , 7706-7718. 10.1039/d0cy01387k

Choi, Jang Hyun; Hong, Jung-A; Son, Ye Rim; Wang, Jian; Kim, Hyun Sung et al. (2020). Comparison of Enhanced Photocatalytic Degradation Efficiency and Toxicity Evaluations of CeO2 Nanoparticles Synthesized Through Double-Modulation. Nanomaterials 10(8) , 1543. 10.3390/nano10081543

Chung, Chun-wa; Dai, Han; Fernandez, Esther; Tinworth, Christopher P.; Churcher, Ian et al. (2020). Structural insights into PROTAC-mediated degradation of Bcl-xL. ACS Chemical Biology. 10.1021/acschembio.0c00266

Colocho Hurtarte, Luis Carlos; Santana Amorim, Helen Carla; Kruse, Jens; Criginski Cezar, Julio; Klysubun, Wantana et al. (2020). A Novel Approach for the Quantification of Different Inorganic and Organic Phosphorus Compounds in Environmental Samples by P L2,3-Edge X-ray Absorption Near-Edge Structure (XANES) Spectroscopy. Environmental Science & Technology 54, 2812-2820. 10.1021/acs.est.9b07018

Das, Soumya; Essilfie-Dughan, Joseph; Hendry, M. Jim (2020). Characterization and environmental implications of selenate co-precipitation with barite. Environmental Research 186, 109607. 10.1016/j.envres.2020.109607

Daunt, Stephen J.; Grzywacz, Robert; Western, Colin M.; Lafferty, Walter J.; Flaud, Jean-Marie et al. (2020). First high-resolution infrared spectra of 2–13C-propane analyses of the v26 (B2) c-type and v9 (A1) b-type bandsJournal of Molecular Structure, 127851. 10.1016/j.molstruc.2020.127851

Dawkins, Jeremy I. G.; Ghavidel, Mohammadreza Z.; Chhin, Danny; Beaulieu, Isabelle; Hossain, Md Sazzad et al. (2020). Operando Tracking of Solution-Phase Concentration Profiles in Li-ion Battery Positive Electrodes using X-Ray Fluorescence. Analytical Chemistry. 10.1021/acs.analchem.0c02086

DeRocher, Karen A.; Smeets, Paul J. M.; Goodge, Berit H.; Zachman, Michael J.; Balachandran, Prasanna V. et al. (2020). Chemical gradients in human enamel crystallites. Nature 583(7814), 66-71. 10.1038/s41586-020-2433-3

Deng, Sixu; Li, Xia; Ren, Zhouhong; Li, Weihan; Luo, Jing et al. (2020). Dual-functional interfaces for highly stable Ni-rich layered cathodes in sulfide all-solid-state batteries. Energy Storage Materials 27, 117-123. 10.1016/j.ensm.2020.01.009

Deng, Sixu; Sun, Qian; Li, Minsi; Adair, Keegan; Yu, Chuang et al. (2020). Insight into Cathode Surface to Boost the Performance of Solid-State Batteries. Energy Storage Materials. 10.1016/j.ensm.2020.12.003

Deng, Sixu; Sun, Yipeng; Li, Xia; Ren, Zhouhong; Liang, Jianwen et al. (2020). Eliminating the Detrimental Effects of Conductive Agents in Sulfide-Based Solid-State Batteries. ACS Energy Letters 5(4) , 1243-1251. 10.1021/acsenergylett.0c00256

Deng, Ya-Ping; Jiang, Yi; Liang, Ruilin; Zhang, Shao-Jian; Luo, Dan et al. (2020). Dynamic electrocatalyst with current-driven oxyhydroxide shell for rechargeable zinc-air battery. Nature Communications 11(1). 10.1038/s41467-020-15853-1

Dodangodage, Randika; Bernath, Peter F.; Zhao, Jianbao; Billinghurst, Brant (2020). Absorption cross sections for ethane broadened by hydrogen and helium in the 3.3 micron region. Journal of Quantitative Spectroscopy and Radiative Transfer 253, 107131. 10.1016/j.jqsrt.2020.107131

Donato, Giovanni; Grosvenor, Andrew P. (2020). Effect of glass composition on the crystallization of CePO4–borosilicate glass composite materials. Canadian Journal of Chemistry 98(11), 701-707. 10.1139/cjc-2020-0234

Donato, Giovanni; Grosvenor, Andrew P. (2020). Crystallization of Rare-Earth Phosphate-Borosilicate Glass Composites Synthesized by a One-Step Coprecipitation Method. Crystal Growth and Design 20(4), 2217-2231. 10.1021/acs.cgd.9b01321

Dong, Cheng; Chen, Shun-Jia; Melnykov, Artem; Weirich, Sara; Sun, Kelly et al. (2020). Recognition of nonproline N-terminal residues by the Pro/N-degron pathway. Proceedings of the National Academy of Sciences of the United States of America 117(25), 14158-14167. 10.1073/pnas.2007085117

Dong, Cheng; Nakagawa, Reiko; Oyama, Kyohei; Yamamoto, Yusuke; Zhang, Weilian et al. (2020). Structural basis for histone variant H3tK27me3 recognition by PHF1 and PHF19. 10.7554/elife.58675

Eifert, László; Bevilacqua, Nico; Köble, Kerstin; Fahy, Kieran; Xiao, Liusheng et al. (2020). Synchrotron X-ray Radiography and Tomography of Vanadium Redox Flow Batteries - Cell Design, Electrolyte Flow Geometry, and Gas Bubble Formation. ChemSusChem 13, 3154 –3165. 10.1002/cssc.202000541

Enomoto, Masahiro; Nishikawa, Tadateru; Back, Sung-In; Ishiyama, Noboru; Zheng, Le et al. (2020). Coordination of a Single Calcium Ion in the EF-hand Maintains the Off State of the Stromal Interaction Molecule Luminal Domain. Journal of Molecular Biology 432(2) , 367-383. 10.1016/j.jmb.2019.10.003

Feng, Yu; Liu, Peng; Wang, Yanxin; Finfrock, Y. Zou; Xie, Xianjun et al. (2020). Distribution and speciation of iron in Fe-modified biochars and its application in removal of As(V), As(III), Cr(VI), and Hg(II): An X-ray absorption study. Journal of Hazardous Materials 384, 121342. 10.1016/j.jhazmat.2019.121342

Feng, Yu; Liu, Peng; Wang, Yanxin; Liu, Wenfu; Liu, YingYing et al. (2020). Mechanistic investigation of mercury removal by unmodified and Fe-modified biochars based on synchrotron-based methods. Science of the Total Environment, 137435.10.1016/j.scitotenv.2020.137435

Feng, Yu; Wang, Jiancheng; Hu, Yongfeng; Lu, Jianjun; Zhang, Man et al. (2020). Microwave heating motivated performance promotion and kinetic study of iron oxide sorbent for coal gas desulfurization. Fuel 267, 117215. 10.1016/j.fuel.2020.117215

Ferri, Elena; Le Thomas, Adrien; Wallweber, Heidi Ackerly; Day, Eric S.; Walters, Benjamin T. et al. (2020). Activation of the IRE1 RNase through remodeling of the kinase front pocket by ATP-competitive ligands. Nature Communications 11(1). 10.1038/s41467-020-19974-5

Fodje, Michel; Mundboth, Kiran; Labiuk, Shaunivan; Janzen, Kathryn; Gorin, James et al. (2020). Macromolecular crystallography beamlines at the Canadian Light Source: building on success. Acta Crystallographica Section D: Structural Biology 76(7). 10.1107/s2059798320007603

Fox, Patricia M.; Bill, Markus; Heckman, Katherine; Conrad, Mark; Anderson, Carolyn et al. (2020). Shale as a Source of Organic Carbon in Floodplain Sediments of a Mountainous Watershed. Journal of Geophysical Research Biogeosciences 125(2). 10.1029/2019jg005419

Fraund, Matthew; Bonanno, Daniel J.; China, Swarup; Pham, Don Q.; Veghte, Daniel et al. (2020). Optical properties and composition of viscous organic particles found in the Southern Great Plains. Atmospheric Chemistry and Physics 20(19) , 11593-11606. 10.5194/acp-20-11593-2020

Ghavami, M.; Soltan, J.; Chen, N. (2020). Synthesis of MnOx/Al2O3 Catalyst by Polyol Method and Its Application in Room Temperature Ozonation of Toluene in Air. Catalysis Letters. 10.1007/s10562-020-03393-8

Ghavami, Mehraneh; Aghbolaghy, Mostafa; Soltan, Jafar; Chen, Ning (2020). Room temperature oxidation of acetone by ozone over alumina-supported manganese and cobalt mixed oxides. Frontiers of Chemical Science and Engineering . 10.1007/s11705-019-1900-6

Ghorbani, Zohreh; Casali, Juliana; Hao, Chunyi; Cavallin, Hannah; Van Loon, Lisa et al. (2020). Biogeochemical Exploration at the Twin Lakes Au Deposit Using Synchrotron Radiation Micro X-ray Fluorescence and X-ray Absorption Near-Edge Structure Spectroscopy. Microscopy and Microanalysis, 1-5.10.1017/s1431927620017547

"Godin, Paul J.; Ramirez, Ramses M.; Campbell, Charissa L.; Wizenberg, Tyler; Nguyen, Tue Giang et al. (2020). Collision-Induced Absorption of CH4-CO2 and H2 -CO2 Complexes and Their Effect on the Ancient Martian Atmosphere. Journal of Geophysical Research Planets. 10.1029/2019je006357

Goff, Kira L.; Ellis, Thomas H.; Wilson, Kenneth E. (2020). Synchrotron FTIR spectromicroscopy as a tool for studying populations and individual living cells of green algae. Analyst. The. 10.1039/d0an01386b

Gorelik, Alexei; Labriola, Jonathan M.; Illes, Katalin; Nagar, Bhushan (2020). Crystal structure of the nucleotide-metabolizing enzyme NTPDase4. Protein Science. 10.1002/pro.3926

Gourgas, Ophélie; Khan, Kashif; Schwertani, Adel; Cerruti, Marta (2020). Differences in mineral composition and morphology between men and women in aortic valve calcification. Acta Biomaterialia 106, 342-350. 10.1016/j.actbio.2020.02.030

Grant, Benjamin M. M.; Enomoto, Masahiro; Back, Sung-In; Lee, Ki-Young; Gebregiworgis, Teklab et al. (2020). Calmodulin disrupts plasma membrane localization of farnesylated KRAS4b by sequestering its lipid moiety. Science Signaling 13(625), eaaz0344. 10.1126/scisignal.aaz0344

Green, R. J.; Sutarto, R.; He, F.; Hepting, M.; Hawthorn,, D. G. et al. (2020). Resonant Soft X-ray Reflectometry and Diffraction Studies of Emergent Phenomena in Oxide Heterostructures. Synchrotron Radiation News 33(2), 20-24. 10.1080/08940886.2020.1725797

Gu, Chunhao; Dam, Than; Hart, Stephen C.; Turner, Benjamin L.; Chadwick, Oliver A. et al. (2020). Quantifying Uncertainties in Sequential Chemical Extraction of Soil Phosphorus Using XANES Spectroscopy. Environmental Science & Technology 54(4), 2257-2267. 10.1021/acs.est.9b05278

Guan, Anxiang; Chen, Zheng; Quan, Yueli; Peng, Chen; Wang, Zhiqiang et al. (2020). Boosting CO2 Electroreduction to CH4 via Tuning Neighboring Single Copper Sites. ACS Energy Letters.10.1021/acsenergylett.0c00018

Hao, Chunyi; Casali, Juliana; Ghorbani, Zohreh; Cavallin, Hannah; Van Loon, Lisa et al. (2020). Multi-scale SR-µXRF Imaging and Characterization of Gold Mineralization at the Monument Bay Deposit, Stull Lake Greenstone Belt, Manitoba, Canada. Microscopy and Microanalysis 26(S2), 1256-1259. 10.1017/s1431927620017493

Hao, Chunyi; Casali, Juliana; Ghorbani, Zohreh; Cavallin, Hannah; Van Loon, Lisa et al. (2020). EPMA Characterization of Gold Associated with Different Sulfide Textures at

the Monument Bay Deposit, Manitoba, Canada. Microscopy and Microanalysis, 1-4. 10.1017/s1431927620020723

Harikrishnan, Lalgudi S.; Gill, Patrice; Kamau, Muthoni G.; Qin, Lan-Ying; Ruan, Zheming et al. (2020). Substituted benzyloxytricyclic compounds as retinoic acid-related orphan receptor gamma t (RORγt) agonists. Bioorganic and Medicinal Chemistry Letters 30(12), 127204. 10.1016/j.bmcl.2020.127204

Helpard, Luke; Li, Hao; Rask-Andersen, Helge; Ladak, Hanif M.; Agrawal, Sumit K. et al. (2020). Characterization of the human helicotrema: implications for cochlear duct length and frequency mapping. Journal of Otolaryngology - Head and Neck Surgery 49(2). 10.1186/s40463-019-0398-8

Helwig, Kate; Monaghan, Meaghan; Poulin, Jennifer; Henderson, Eric J.; Moriarty, Maeve et al. (2020). Rita Letendre's Oil Paintings from the 1960s: The Effect of Artist's Materials on Degradation Phenomena. Studies in Conservation, 1-15. 0.1080/00393630.2020.1773055

Hersch, Steven J.; Watanabe, Nobuhiko; Stietz, Maria Silvina; Manera, Kevin; Kamal, Fatima et al. (2020). Envelope stress responses defend against type six secretion system attacks independently of immunity proteins. Nature Microbiology . 10.1038/s41564-020-0672-6

Hewett, Dan; Bernath, Peter; Zhao, Jianbao; Billinghurst, Brant (2020). Near infrared absorption cross sections for ethane broadened by hydrogen and nitrogen. Journal of Quantitative Spectroscopy and Radiative Transfer 242, 106780. 10.1016/j.jqsrt.2019.106780

Hilger, David M.; Hamilton, Jordan G.; Peak, Derek (2020). The Influences of Magnesium upon Calcium Phosphate Mineral Formation and Structure as Monitored by X-ray and Vibrational Spectroscopy. Soil Systems 4(1), 8. 10.3390/soilsystems4010008

Hirpara, Viral; Patel, Virat; Zhang, Yuzhou; Anderson, Ryan; Zhu, Ning et al. (2020). Investigating the effect of operating temperature on dynamic behavior of droplets for proton exchange membrane fuel cells International Journal of Hydrogen Energy 45(27), 14145-14155. 10.1016/j.ijhydene.2020.03.128

Ho, Josha; de Boer, Tristan; Braun, Patrick M.; Leedahl, Brett; Manikandan, Dhamodaran et al. (2020). Origin and control of room temperature ferromagnetism in Co,Zn-doped SnO2: oxygen vacancies and their local environment. Journal of Materials Chemistry C . 10.1039/c9tc06830a

Hogan, David T.; Gelfand, Benjamin S.; Spasyuk, Denis M.; Sutherland, Todd C. (2020). Subtle substitution controls the rainbow chromatic behaviour of multi-stimuli responsive core-expanded pyrenes. Materials Chemistry Frontiers 4(1), 268-276. 10.1039/c9qm00710e

Holt, Christian; Hamborg, Louise; Lau, Kelvin; Brohus, Malene; Sørensen, Anders Bundgaard et al. (2020). The arrhythmogenic N53I variant subtly changes the structure and dynamics in the calmodulin N-domain, altering its interaction with the cardiac ryanodine receptor. Journal of Biological Chemistry , jbc.RA120.013430. 10.1074/jbc.ra120.013430

Hu, Zilun; Wang, Cailan; Glunz, Peter W.; Li, Julia; Cheadle, Nathan L. et al. (2020). Discovery of a phenylpyrazole amide ROCK inhibitor as a tool molecule for in vivo studies. Bioorganic and Medicinal Chemistry Letters 30(21), 127495. 10.1016/j.bmcl.2020.127495

Huang, Jing; Huang, Guohe; An, Chunjiang; Xin, Xiaying; Chen, Xiujuan et al. (2020). Exploring the use of ceramic disk filter coated with Ag/ZnO nanocomposites as an innovative approach for removing Escherichia coli from household drinking water. Chemosphere 245, 125545. 10.1016/j.chemosphere.2019.125545

Huhn, Annissa J.; Gardberg, Anna S.; Poy, Florence; Brucelle, Francois; Vivat, Valerie et al. (2020). Early Drug Discovery Efforts Towards the Identification of EP300/CBP Histone Acetyltransferase (HAT) Inhibitors. ChemMedChem. 10.1002/cmdc.202000007

Hömberg, Annkathrin; Obst, Martin; Knorr, Klaus-Holger; Kalbitz, Karsten; Schaller, Jörg et al. (2020). Increased silicon concentration in fen peat leads to a release of iron and phosphate and changes in the composition of dissolved organic matter. Geoderma 374, 114422. 10.1016/j.geoderma.2020.114422

Jia, Xiaocen; Zhou, Jianwei; Liu, Jing; Liu, Peng; Yu, Lu et al. (2020). The antimony sorption and transport mechanisms in removal experiment by Mn-coated biochar. Science of the Total Environment 724, 138158. 10.1016/j.scitotenv.2020.138158

Jiang, Yi; Deng, Ya-Ping; Liang, Ruilin; Fu, Jing; Gao, Rui et al. (2020). d-Orbital steered active sites through ligand editing on heterometal imidazole frameworks for rechargeable zinc-air battery. Nature Communications 11(1). 10.1038/s41467-020-19709-6

Jiang, Ying-Ying; Wang, Zhi-Qiang; Chen, Jia-Tang; Li, Jun; Zhu, Ying-Jie et al. (2020). Tracking the interaction of drug molecules with individual mesoporous amorphous calcium phosphate/ATP nanocomposites – an X-ray spectromicroscopy study. Physical Chemistry Chemical Physics. 10.1039/d0cp00797h

Jones, Carys S.; Sychantha, David; Howell, P. Lynne; Clarke, Anthony J. (2020). Structural basis for the O-acetyltransferase function of the extracytoplasmic domain of OatA from Staphylococcus aureus. Journal of Biological Chemistry, jbc.RA120.013108. 10.1074/jbc.ra120.013108

Jones, Darryl R.; Xing, Xiaohui; Tingley, Jeffrey P.; Klassen, Leeann; King, Marissa L. et al. (2020). Analysis of Active Site Architecture and Reaction Product Linkage Chemistry Reveals a Conserved Cleavage Substrate for an Endo-alpha-mannanase within Diverse Yeast Mannans. Journal of Molecular Biology 432(4), 1083-1097. 10.1016/j.jmb.2019.12.048

Kaliyappan, Karthikeyan; Or, Tyler; Deng, Ya-Ping; Hu, Yongfeng; Bai, Zhengyu et al. (2020). Constructing Safe and Durable High-Voltage P2 Layered Cathodes for Sodium Ion Batteries Enabled by Molecular Layer Deposition of Alucone. Advanced Functional Materials, 1910251. 10.1002/adfm.201910251

Kamath, Girish; Badoga, Sandeep; Shakouri, Mohsen; Hu, Yongfeng; Dalai, Ajay K. et al. (2020). Influence of calcination on physico-chemical properties and Ficher–Tropsch activity of titanosilicate supported cobalt catalysts with different pore sizes. Applied Catalysis A: General 598, 117563. 10.1016/j.apcata.2020.117563

Khatami, Zahra; Bleczewski, Lyndia; Neville, John J.; Mascher, Peter (2020). X-ray Absorption Spectroscopy of Silicon Carbide Thin Films Improved by Nitrogen for All-Silicon Solar Cells. ECS Journal of Solid State Science and Technology 9(8), 083002. 10.1149/2162-8777/abb2b1

Kim, Chang-Yong (2020). Carbon Deposition on Hematite (α-Fe2O3) Nanocubes by Annealing in the Air: Morphology Study with Grazing Incidence Small Angle X-ray Scattering (GISAXS). Condensed Matter 5(3), 54.10.3390/condmat5030054

Kim, Chang-Yong (2020). Atomic structure of hematite (α-Fe2O3) nanocube surface; synchrotron X-ray diffraction study. Nano-Structures and Nano-Objects 23, 100497. 10.1016/j.nanoso.2020.100497

Kim, P. J.; Lee, CH.; Lee, J. K.; Fahy, K.F.; Bazylak, A. et al. (2020). In-Plane Transport in Water Electrolyzer Porous Transport Layers with Through Pores. Journal of the Electrochemical Society 167(12), 124522.10.1149/1945-7111/abb173

King, Graham (2020). New examples of non-cooperative octahedral tilting in a double perovskite: phase transitions in K3GaF6. Acta Crystallographica Section B: Structural Science. Crystal Engineering and Materials 76(5) .10.1107/s2052520620009695

King, Graham; Celikin, Mert; Gomez, Mario Alberto; Becze, Levente; Petkov, Valeri et al. (2020). Revealing the structures and relationships of Ca(ii)–Fe(iii)–AsO4 minerals: arseniosiderite and yukonite. Environmental Science: Nano.10.1039/d0en00503g

Kleebusch, Enrico; Patzig, Christian; Krause, Michael; Hu, Yongfeng; Höche, Thomas et al. (2020). The titanium coordination state and its temporal evolution in Li2O–Al2O3–SiO2 (LAS) glasses with ZrO2 and TiO2 as nucleation agents - A XANES investigation. Ceramics International 46(3), 3498-3501.10.1016/j.ceramint.2019.10.064

Kobayashi, Kaori; Sakai, Yusuke; Fujitake, Masaharu; Tokaryk, Dennis W.; Billinghurst, Brant E. et al. (2020). Identification of a vibrationally excited level in methyl formate through microwave and far-infrared spectroscopy. Canadian Journal of Physics .10.1139/cjp-2019-0578

Kodur, Moses; Kumar, Rishi E.; Luo, Yanqi; Cakan, Deniz N.; Li, Xueying et al. (2020). X-Ray Microscopy of Halide Perovskites: Techniques, Applications, and Prospects. Advanced Energy Materials, 1903170. 10.1002/aenm.201903170

Kong, Fanpeng; Ren, Zhouhong; Norouzi Banis, Mohammad; Du, Lei; Zhou, Xin et al. (2020). Active and Stable Pt-Ni Alloy Octahedra Catalyst for Oxygen Reduction via Near-Surface Atomical Engineering. ACS Catalysi .10.1021/acscatal.9b05133

Kong, Huating; Zhang, Jichao; Li, Jiang; Wang, Jian; Shin, Hyun-Joon et al. (2020). Genetically encoded X-ray cellular imaging for nanoscale protein localization. National Science Review.10.1093/nsr/nwaa055

Kong, Lingping; Gong, Jue; Hu, Qingyang; Capitani, Francesco; Celeste, Anna et al. (2020). Suppressed Lattice Disorder for Large Emission Enhancement and Structural Robustness in Hybrid Lead Iodide Perovskite Discovered by High-Pressure Isotope Effect. Advanced Functional Materials, 2009131. 10.1002/adfm.202009131

Kozachuk, M. S.; Sham, T. K.; Martin, R. R.; Nelson, A. J. (2020). Bromine, a possible marine diet indicator? A hypothesis revisited. Archaeometry. 10.1111/arcm.12590

Kozlov, Guennadi; Funato, Yosuke; Chen, Yu Seby; Zhang, Zhidian; Illes, Katalin et al. (2020). PRL3 pseudophosphatase activity is necessary and sufficient to promote metastatic growth. Journal of Biological Chemistry 295(33), 11682-11692. 10.1074/jbc.ra120.014464

Krounbi, Leilah; Enders, Akio; Anderton, Christopher R.; Engelhard, Mark H.; Hestrin, Rachel et al. (2020). Sequential Ammonia and Carbon Dioxide Adsorption on Pyrolyzed Biomass to Recover Waste Stream Nutrients. ACS Sustainable Chemistry & Engineering 8(18), 7121-7131. 10.1021/acssuschemeng.0c01427

Kruse, Jens; Koch, Maximilian; Khoi, Chau Minh; Braun, Gianna; Sebesvari, Zita et al. (2020). Land use change from permanent rice to alternating rice-shrimp or permanent shrimp in the coastal Mekong Delta, Vietnam: Changes in the nutrient status and binding forms. Science of the Total Environment 703, 134758. 10.1016/j.scitotenv.2019.134758

Langman, Jeff B.; Behrens, David; Moberly, James G. (2020). Seasonal formation and stability of dissolved metal particles in mining-impacted, lacustrine sediments. Journal of Contaminant Hydrology 232, 103655. 10.1016/j.jconhyd.2020.103655

Langman, Jeff; Ali, Jaabir; Child, Andrew; Wilhelm, Frank; Moberly, James et al. (2020). Sulfur Species, Bonding Environment, and Metal Mobilization in Mining-Impacted Lake Sediments: Column Experiments Replicating Seasonal Anoxia and Deposition of Algal Detritus. Minerals 10(10 , 849.10.3390/min10100849

Lawrence, John R.; Paule, Armelle; Swerhone, George

D.W.; Roy, Julie; Grigoryan, Alexander A. et al. (2020). Microscale and molecular analyses of river biofilm communities treated with microgram levels of cerium oxide nanoparticles indicate limited but significant effects. Environmental Pollution 256, 113515. 10.1016/j.envpol.2019.113515

Lee, CH.; Lee, J. K.; Zhao, B.; Fahy, K. F.; Bazylak, A. et al. (2020). Transient Gas Distribution in Porous Transport Layers of Polymer Electrolyte Membrane Electrolyzers. Journal of the Electrochemical Society 167(2), 024508. 10.1149/1945-7111/ab68c8

Lee, Jason K.; Lee, ChungHyuk; Fahy, Kieran F.; Kim, Pascal J.; Krause, Kevin et al. (2020). Accelerating bubble detachment in porous transport layers with patterned through pores. ACS Applied Energy Materials 3(10), 9676–9684. 10.1021/acsaem.0c01239

Lees, R.M.; Reid, E.M; Xu, Li-Hong; Billinghurst, B.E. (2020). Synchrotron spectroscopy of the CSH-bending and CH3-rocking bands of methyl mercaptan. Canadian Journal of Physics 98(6), 519-529.10.1139/cjp-2019-0487

Lees, R.M.; Xu, Li-Hong; Billinghurst, B.E. (2020). Patterns in synchrotron near-free-rotor FIR spectra of CH3OH and CD3OH – The tau of methanol. Journal of Molecular Structure, 127960. 10.1016/j.molstruc.2020.127960

Lei, Sicong; Zhu, Ling; Xue, Cong; Hong, Chengyi; Wang, Junliang et al. (2020). Mechanistic insights and multiple characterizations of cadmium binding to animal-derived biochar. Environmental Pollution 258, 113675. 10.1016/j.envpol.2019.113675

Leukkunen, Petri M.; Rani, Ekta; Sasikala Devi, Assa Aravindh; Singh, Harishchandra; King, Graham et al. (2020). Synergistic effect of Ni–Ag–rutile TiO2 ternary nanocomposite for efficient visible-light-driven photocatalytic activity. RSC Advances 10(60), 36930-36940. 10.1039/d0ra07078e

Li, Franco K.K.; Rosell, Federico I.; Gale, Robert T.; Simorre, Jean-Pierre; Brown, Eric D. et al. (2020). Crystallographic analysis of Staphylococcus aureus LcpA, the primary wall teichoic acid ligase. Journal of Biological Chemistry 295(9), 2629-2639. 10.1074/jbc.ra119.011469

Li, Haifeng; Perez, Arnaud J.; Taudul, Beata; Boyko, Teak D.; Freeland, John W. et al. (2020). Elucidation of Active Oxygen Sites upon Delithiation of Li3IrO4. ACS Energy Letters, 140-147. 10.1021/acsenergylett.0c02040

Li, Hao; Schart-Morén, Nadine; Rohani, Seyed Alireza; Ladak, Hanif M.; Rask-Andersen, Helge et al. (2020). Synchrotron Radiation-Based Reconstruction of the Human Spiral Ganglion. Ear and Hearing 41(1), 173–181. 10.1097/aud.0000000000000738

Li, Jinhua; Liu, Peiyu; Wang, Jian; Roberts, Andrew P.; Pan, Yongxin et al. (2020). Magnetotaxis as an adaptation to enable bacterial shuttling of microbial sulfur and sulfur cycling across aquatic oxic-anoxic interfaces. Journal of Geophysical Research Biogeosciences. 10.1029/2020jg006012

Li, Jun; Xu, Aoni; Li, Fengwang; Wang, Ziyun; Zou, Chengqin et al. (2020). Enhanced multi-carbon alcohol electroproduction from CO via modulated hydrogen adsorption. Nature Communications 11(1).10.1038/s41467-020-17499-5

Li, Junrui; Sharma, Shubham; Wei, Kecheng; Chen, Zitao; Morris, David et al. (2020). Anisotropic Strain Tuning of L10 Ternary Nanoparticles for Oxygen Reduction. Journal of the American Chemical Society 142(45), 19209-19216. 10.1021/jacs.0c08962

Li, Weihan; Li, Minsi; Li, Junjie; Liang, Jianneng; Adair, Keegan R. et al. (2020). Phosphorene Nanosheets Exfoliated from Low-Cost and High-Quality Black Phosphorus for Hydrogen Evolution. ACS Applied Nano Materials. 10.1021/acsanm.0c01101

Li, Weihan; Liang, Jianwen; Li, Minsi; Adair, Keegan R.; Li, Xiaona et al. (2020). Unraveling the Origin of Moisture Stability of Halide Solid-State Electrolytes by In Situ and Operando Synchrotron X-ray Analytical Techniques. Chemistry of Materials. 10.1021/acs.chemmater.0c02419

Li, Weihan; Wang, Zhiqiang; Zhao, Feipeng; Li, Minsi; Gao, Xuejie et al. (2020). Phosphorene Degradation: Visualization and Quantification of Nanoscale Phase Evolution by Scanning Transmission X-ray Microscopy. Chemistry of Materials. 10.1021/acs.chemmater.9b04811

Li, Xiaona; Liang, Jianwen; Adair, Keegan R.; Li, Junjie; Li, Weihan et al. (2020). Origin of Superionic Li3Y1−xInxCl6 Halide Solid Electrolytes with High Humidity Tolerance. Nano Letters 20(6), 4384-4392. 10.1021/acs.nanolett.0c01156

Li, Xiaona; Liang, Jianwen; Banis, Mohammad Norouzi; Luo, Jing; Wang, Changhong et al. (2020). Totally compatible P4S10+n cathodes with self-generated Li+ pathways for sulfide-based all-solid-state batteries. Energy Storage Materials 28, 325-333. 10.1016/j.ensm.2020.03.014

Li, Yingying; Walsh, Andrew G.; Li, Dashuai; Do, David; Ma, He et al. (2020). W-Doped TiO2 for photothermocatalytic CO2 reduction. Nanoscale 12(33 , 17245-17252. 10.1039/d0nr03393f

Li, Zhaoqiang; Jiang, Gaopeng; Deng, Ya-Ping; Liu, Guihua; Ren, Dezhang et al. (2020). Deep-Breathing Honeycomb-like Co-Nx-C Nanopolyhedron Bifunctional Oxygen Electrocatalysts for Rechargeable Zn-Air Batteries. 10.1016/j.isci.2020.101404

Li, Zhigen; Wang, Peng; Menzies, Neal W.; McKenna, Brigid A.; Karunakaran, Chithra et al. (2020). Examining a synchrotron-based approach for in situ analyses of Al speciation in plant roots. Journal of Synchrotron Radiation 27(1).10.1107/s1600577519014395

Liang, Jianneng; Hwang, Sooyeon; Li, Shuang; Luo, Jing; Sun, Yipeng et al. (2020). Stabilizing and understanding the interface between nickel-rich cathode and PEO-based electrolyte by lithium niobium oxide coating for high-performance all-solid-state batteries. Nano Energy, 105107. 10.1016/j.nanoen.2020.105107

Liang, Jianneng; Sun, Yipeng; Zhao, Yang; Sun, Qian; Luo, Jing et al. (2020). Engineering the conductive carbon/PEO interface to stabilize solid polymer electrolytes for all-solid-state high voltage LiCoO2 batteries. Journal of Materials Chemistry A 8(5), 2769-2776. 10.1039/c9ta08607b

Liang, Jianwen; Chen, Ning; Li, Xiaona; Li, Xia; Adair, Keegan R. et al. (2020). Li10Ge(P1−xSbx)2S12 Lithium-Ion Conductors with Enhanced Atmospheric Stability. Chemistry of Materials 32(6), 2664-2672. 10.1021/acs.chemmater.9b04764

Liang, Jianwen; Li, Xiaona; Wang, Shuo; Adair, Keegan R.; Li, Weihan et al. (2020). Site-Occupation-Tuned Superionic LixScCl3+xHalide Solid Electrolytes for All-Solid-State Batteries. Journal of the American Chemical Society 142(15) , 7012-7022. 10.1021/jacs.0c00134

Lin, Jinru; Chen, Ning; Feng, Renfei; Nilges, Mark J.; Jia, Yongfeng et al. (2020). Sequestration of Selenite and Selenate in Gypsum (CaSO4·2H2O): Insights from the Single-Crystal Electron Paramagnetic Resonance Spectroscopy and Synchrotron X-ray Absorption Spectroscopy Study. Environmental Science & Technology 54(6), 3169-3180. 10.1021/acs.est.9b05714

Lin; Jinru; Chen; Ning; Pan et al. (2020). Uptake mechanisms of arsenate in gypsum: Structural incorporation versus surface adsorption and implications for remediation of arsenic contamination. Earth Science Frontiers 27(5), 228-237. 10.13745/j.esf.sf.2020.5.40

Liu, Guihua; Luo, Dan; Gao, Rui; Hu, Yongfeng; Yu, Aiping et al. (2020). A Combined Ordered Macro-Mesoporous Architecture Design and Surface Engineering Strategy for High-Performance Sulfur Immobilizer in Lithium–Sulfur Batteries. Small 16(37), 2001089. 10.1002/smll.202001089

Liu, Jian; Yu, Younong; Kelly, Joseph; Sha, Deyou; Alhassan, Abdul-Basit et al. (2020). Discovery of Highly Selective and Potent HDAC3 Inhibitors Based on a 2-Substituted Benzamide Zinc Binding Group. ACS Medicinal Chemistry Letters 11(12), 2476-2483. 10.1021/acsmedchemlett.0c00462

Liu, Jin; Han, Chaoqun; Zhao, Yuhang; Yang, Jianjun; Cade-Menun, Barbara J. et al. (2020). The chemical nature of soil phosphorus in response to long-term fertilization practices: Implications for sustainable phosphorus management. Journal of Cleaner Production 272, 123093. 10.1016/j.jclepro.2020.123093

Liu, Kai; Ma, Shengcan; Zhang, Yuxi; Zeng, Hai; Yu, Guang et al. (2020). Magnetic-field-driven reverse martensitic transformation with multiple magneto-responsive effects by manipulating magnetic ordering in Fe-doped Co-V-Ga Heusler alloys. Journal of Materials Science and Technology 58, 145-154. 10.1016/j.jmst.2020.05.009

Liu, Lichen; Lopez-Haro, Miguel; Lopes, Christian W.; Meira, Debora M.; Concepcion, Patricia et al. (2020). Atomic-level understanding on the evolution behavior of subnanometric Pt and Sn species during high-temperature treatments for generation of dense PtSn clusters in zeolites. Journal of Catalysis 391, 11-24. 10.1016/j.jcat.2020.07.035

Liu, Lichen; Lopez-Haro, Miguel; Meira, Debora M.; Concepcion, Patricia; Calvino, Jose J. et al. (2020). Regioselective Generation of Single-Site Ir Atoms and their Evolution into Stabilized Subnanometric Ir Clusters in MWW Zeolite. 10.1002/ange.202005621

Liu, Peng; Ptacek, Carol J.; Blowes, David W.; Finfrock, Y. Zou; Liu, YingYing et al. (2020). Characterization of chromium species and distribution during Cr(VI) removal by biochar using confocal micro-X-ray fluorescence redox mapping and X-ray absorption spectroscopy. Environment International 134, 105216. 10.1016/j.envint.2019.105216

Liu, Qiming; Peng, Yi; Li, Qiaoxia; He, Ting; Morris, David et al. (2020). Atomic Dispersion and Surface Enrichment of Palladium in Nitrogen-Doped Porous Carbon Cages Lead to High-Performance Electrocatalytic Reduction of Oxygen. ACS Applied Materials & Interfaces 12(15), 17641-17650.

Liu, Yisi; Wang, Biqiong; Sun, Qian; Pan, Qiyun; Zhao, Nian et al. (2020). Controllable Synthesis of Co@CoOx/Helical Nitrogen-Doped Carbon Nanotubes toward Oxygen Reduction Reaction as Binder-free Cathodes for Al–Air Batteries. ACS Applied Materials & Interfaces. 10.1021/acsami.0c01603

Liu, Yunqiu; Huang, Gordon; An, Chunjiang; Chen, Xiujuan; Zhang, Peng et al. (2020). Use of Nano-TiO2 self-assembled flax fiber as a new initiative for immiscible oil/water separation. Journal of Cleaner Production 249, 119352. 10.1016/j.jclepro.2019.119352

Lo, Calvin; Sano, Tomoko; Hogan, James D. (2020). Deformation mechanisms and evolution of mechanical properties in damaged advanced ceramics. Journal of the European Ceramic Society 40(8), 3129-3139. 10.1016/j.jeurceramsoc.2020.02.058

Lotz, Hélène; Carrière, Charly; Bataillon, Christian; Gardes, Emmanuel; Monnet, Isabelle et al. (2020).Investigation of steel corrosion in MX80 bentonite at 120°C. Materials and Corrosion - Werkstoffe und Korrosion. 10.1002/maco.202011777

Lou, X.; Xu, H. C.; Wen, C. H. P.; Yu, T. L.; Wei, W. Z. et al. (2020). Lattice distortion and electronic structure of BaAg2As2 across its nonmagnetic phase transition. Physical Review B 101(7). 10.1103/physrevb.101.075123

Loundagin, Lindsay L.; Haider, Ifaz T.; Cooper, David M.L.; Edwards, W. Brent (2020). Association between intracortical microarchitecture and the compressive fatigue life of human bone: A pilot study. Bone Reports 12, 100254. 10.1016/j.bonr.2020.100254

Lu, Bingzhang; Liu, Qiming; Nichols, Forrest; Mercado, Rene; Morris, David et al. (2020). Oxygen Reduction Reaction Catalyzed by Carbon-Supported Platinum Few-Atom Clusters: Significant Enhancement by Doping of Atomic Cobalt. Research 2020, 1-12. 10.34133/2020/9167829

Lu, Mi; Yu, Fuda; Hu, Yongfeng; Zaghib, Karim; Schougaard, Steen B. et al. (2020). Correlative imaging of ionic transport and electronic structure in nano Li0.5FePO4 electrodes. Chemical Communications. 10.1039/c9cc09116e

Lu, Xiaocen; Wen, Yurong; Zhang, Shuce; Zhang, Wei; Chen, Yilun et al. (2020). Improved Photocleavable Proteins with Faster and More Efficient Dissociation. Journal of Nanoparticle Research. 10.1101/2020.12.10.419556

Lum, Yanwei; Huang, Jianan Erick; Wang, Ziyun; Luo, Mingchuan; Nam, Dae-Hyun et al. (2020). Tuning OH binding energy enables selective electrochemical oxidation of ethylene to ethylene glycol. Nature Catalysis 3(1), 14-22. 10.1038/s41929-019-0386-4

Luo, Dan; Zhang, Zhen; Li, Gaoran; Cheng, Shaobo; Li, Shuang et al. (2020). Revealing the Rapid Electrocatalytic Behavior of Ultrafine Amorphous Defective Nb2O5–x Nanocluster toward Superior Li–S Performance. ACS Nano 14(4), 4849-4860. 10.1021/acsnano.0c00799

"Lv, Ximeng; Shang, Longmei; Zhou, Si; Li, Si; Wang, Yuhang et al. (2020). Electron-Deficient Cu Sites on Cu3Ag1 Catalyst Promoting CO2 Electroreduction to Alcohols. Advanced Energy Materials 10(37), 2001987. 10.1002/aenm.202001987

Ma, Jinjin; McLeod, John A.; Chang, Lo-Yueh; Pao, Chih-Wen; Lin, Bi-Hsuan et al. (2020). Increasing photoluminescence yield of CsPbCl3 nanocrystals by heterovalent doping with Pr3+. Materials Research Bulletin 129, 110907. 10.1016/j.materresbull.2020.110907

Ma, Wenping; Jacobs, Gary; Sparks, Dennis E.; Todic, Branislav; Bukur, Dragomir B. et al. (2020). Quantitative comparison of iron and cobalt based catalysts for the Fischer-Tropsch synthesis under clean and poisoning conditions. Catalysis Today 343, 125-136. 10.1016/j.cattod.2019.04.011

Maciag, Bryan J.; Brenan, James M. (2020). Speciation of arsenic and antimony in basaltic magmas. Geochimica et Cosmochimica Acta 276, 198-218. 10.1016/j.gca.2020.02.022

Mahassneh, Omar; van Wijngaarden, Jennifer (2020). Analysis of the Coriolis perturbed rovibrational spectrum of the C-O asymmetric stretch and C-C symmetric stretch of trimethylene oxide. Journal of Molecular Spectroscopy, 111322. 10.1016/j.jms.2020.111322

Majdi Yazdi, Mohadeseh; Saran, Sagar; Mrozowich, Tyler; Lehnert, Cheyanne; Patel, Trushar R. et al. (2020). Asparagine-84, a regulatory allosteric site residue, helps maintain the quaternary structure of Campylobacter jejuni dihydrodipicolinate synthase. Journal of Structural Biology 209(107409). 10.1016/j.jsb.2019.107409

Majewski, Dorothy D.; Okon, Mark; Heinkel, Florian; Robb, Craig S.; Vuckovic, Marija et al. (2020). Characterization of the Pilotin-Secretin Complex from the Salmonella enterica Type III Secretion System Using Hybrid Structural Methods. Structure. 10.1016/j.str.2020.08.006

Manenda, Mahder S.; Picard, Marie-Ève; Zhang, Liping; Cyr, Normand; Zhu, Xiaojun et al. (2020). Structural analyses of the group A flavin-dependent monooxygenase PieE reveal a sliding FAD cofactor conformation bridging OUT and IN conformations. Journal of Biological Chemistry, jbc.RA119.011212. 10.1074/jbc.ra119.011212

Martens, Isaac; Melo, Lis G. A.; West, Marcia M.; Wilkinson, David P.; Bizzotto, Dan et al. (2020). Imaging Reactivity of the Pt–Ionomer Interface in Fuel-Cell Catalyst Layers. ACS Catalysis 10(15) , 8285-8292. 10.1021/acscatal.0c01594

Martin-Drumel, Marie-Aline; Porterfield, Jessica P.; Goubet, Manuel; Asselin, Pierre; Georges, Robert et al. (2020). Synchrotron-Based High Resolution Far-Infrared Spectroscopy of trans-Butadiene. Journal of Physical Chemistry A. 10.1021/acs.jpca.0c00623

Mazhar, Waqas; Klymyshyn, David M; Achenbach, Sven; Qureshi, Aqeel Ahmed; Wells, Garth et al. (2020). On the fabrication of thin-film artificial metal grid resonator antenna arrays using deep X-ray Lithography. Journal of Micromechanics and Microengineering . 10.1088/1361-6439/ab6dbd

McIntyre, Stewart; Van Loon, Lisa; Sherry, Nathaniel; Bauer, Michael; Banerjee, Neil et al. (2020). Using Multi-Element Reference Materials for Approximating Concentrations in Soils and Sediments from Micro XRF Spectra. Microscopy and Microanalysis, 1-4. 10.1017/s1431927620019327

McIntyre, Stewart; Van Loon, Lisa; Sherry, Nathaniel; Bauer, Michael; Kotzer, Tom et al. (2020). Microscopic Characterization of Uranium Ore Specimens Using the Peakaboo Analysis Platform. Microscopy and Microanalysis, 1-4. 10.1017/s1431927620017560

McMahon, Christopher; Achkar, A. J.; da Silva Neto, E. H.; Djianto, I.; Menard, J. et al. (2020). Orbital symmetries of charge density wave order in YBa2Cu3O6+x. Science advances 6(45), eaay0345. 10.1126/sciadv.aay0345

Mei, Xueshuang; Glueckert, Rudolf; Schrott-Fischer, Annelies; Li, Hao; Ladak, Hanif M. et al. (2020). Vascular Supply of the Human Spiral Ganglion: Novel Three-Dimensional Analysis Using Synchrotron Phase-Contrast Imaging and Histology. Scientific Reports 10(1), 5877. 10.1038/s41598-020-62653-0

Mendoza, Matthew N.; Jian, Mike; King, Moeko T.; Brooks, Cory L. (2020). Role of a noncanonical disulfide bond in the stability, affinity, and flexibility of a VHH specific for the Listeria virulence factor InlB. Protein Science 29(4), 1004-1017. 10.1002/pro.3831

Mercado, Rene; Wahl, Carolin; En Lu, Jia; Zhang, Tianjun; Lu, Bingzhang et al. (2020). Nitrogen-Doped Porous Carbon Cages for Electrocatalytic Reduction of Oxygen: Enhanced Performance with Iron and Cobalt Dual Metal Centers. ChemCatChem 12(12), 3230-3239. 10.1002/cctc.201902324

Miersch, Shane; Li, Zhijie; Saberianfar, Reza; Ustav, Mart; Case, James Brett et al. (2020). Tetravalent SARS-CoV-2 Neutralizing Antibodies Show Enhanced Potency and Resistance to Escape Mutations. Vibrational Spectroscopy. 10.1101/2020.10.31.362848

Miron, Caitlin E.; Staalduinen, Laura; Rangaswamy, Alana M.; Chen, Mickey; Liang, Yushi et al. (2020). Going Platinum to the Tune of a Remarkable Guanine Quadruplex Binder: Solution- and Solid-State Investigations. Angewandte Chemie - International Edition. 10.1002/anie.202012520

Mitcheltree, Matthew J.; Li, Derun; Achab, Abdelghani; Beard, Adam; Chakravarthy, Kalyan et al. (2020). Discovery and Optimization of Rationally Designed Bicyclic Inhibitors of Human Arginase to Enhance Cancer Immunotherapy. ACS Medicinal Chemistry Letters 11(4), 582-588. 10.1021/acsmedchemlett.0c00058

Moreau, Liane M.; Herve, Alexandre; Straub, Mark D.; Russo, Dominic R.; Abergel, Rebecca J. et al. (2020). Structural properties of ultra-small thorium and uranium dioxide nanoparticles embedded in a covalent organic framework. Chemical Science 11(18), 4648-4668. 10.1039/c9sc06117g

Mukhopadhyay, Indranath; Billinghurst, B.E. (2020). Very high-resolution synchrotron radiation far-infrared (FIR) spectrum of methanol-d2 (CHD2OH) & millimeter-wave (MMW) measurements involving highly excited torsional vibrational rotational states, and identification of optically pumped FIR laser lines. Infrared Physics and Technology, 103563. 10.1016/j.infrared.2020.103563

Murota, Kota; Pachoud, Elise; Attfield, J. Paul; Glaum, Robert; Sutarto, Ronny et al. (2020). Vanadium 3d charge and orbital states in V2OPO4 probed by x-ray absorption spectroscopy. Physical Review B 101(24). 10.1103/physrevb.101.245106

Murugan, Rajagopal; Scally, Stephen W.; Costa, Giulia; Mustafa, Ghulam; Thai, Elaine et al. (2020). Evolution of protective human antibodies against Plasmodium falciparum circumsporozoite protein repeat motifs. Nature Medicine. 10.1038/s41591-020-0881-9

Nelson, Nicholas C.; Chen, Linxiao; Meira, Debora; Kovarik, Libor; Szanyi, János et al. (2020). In Situ Dispersion of Palladium on TiO2 During Reverse Water–Gas Shift Reaction: Formation of Atomically Dispersed Palladium. Angewandte Chemie. 10.1002/ange.202007576

Nguyen, Minh Tho; Gusev, Dmitry; Dmitrienko, Anton; Gabidullin, Bulat M.; Spasyuk, Denis et al. (2020). Ge(0) Compound Stabilized by a Diimino-Carbene Ligand: Synthesis and Ambiphilic Reactivity. Journal of the American Chemical Society 142(12), 5852-5861. 10.1021/jacs.0c01283

Nguyen, Van At; Wang, Jian; Kuss, Christian (2020). Conducting polymer composites as water-dispersible electrode matrices for Li-Ion batteries: Synthesis and characterization. Journal of Power Sources Advances 6, 100033. 10.1016/j.powera.2020.100033

Ning, Liqun; Mehta, Riya; Cao, Cong; Theus, Andrea; Tomov, Martin et al. (2020). Embedded 3D Bioprinting of Gelatin Methacryloyl-Based Constructs with Highly Tunable Structural Fidelity. ACS Applied Materials & Interfaces 12(40), 44563–44577. 10.1021/acsami.0c15078

Noach, Ilit; Boraston, Alisdair B (2020). Structural evidence for a proline-specific glycopeptide recognition domain in an O-glycopeptidase. Glycobiology. 10.1093/glycob/cwaa095

Nordström, Charlotta Kämpfe; Li, Hao; Ladak, Hanif M.; Agrawal, Sumit; Rask-Andersen, Helge et al. (2020). A Micro-CT and Synchrotron Imaging Study of the Human Endolymphatic Duct with Special Reference to Endolymph Outflow and Meniere's Disease. Scientific Reports 10(8295). 10.1038/s41598-020-65110-0

Olaleye, Abimfoluwa; Oyedele, Durodoluwa; Akponikpe, Pierre; Kar, Gourango; Peak, Derek et al. (2020). Molecular Scale Studies of Phosphorus Speciation and Transformation in Manure Amended and Microdose Fertilized Indigenous Vegetable Production Systems of Nigeria and Republic of Benin. Soil Systems 4(1), 5. 10.3390/soilsystems4010005

Olkowski, A. A.; Wojnarowicz, C.; Laarveld, B. (2020). Pathophysiology and Pathological Remodeling Associated with Dilated Cardiomyopathy in Broiler Chickens Predisposed to Heart Pump Failure. Avian Pathology, 1-41. 0.1080/03079457.2020.1757620

O'Day, Peggy A.; Nwosu, Ugwumsinachi G.; Barnes, Morgan E.; Hart, Stephen C.; Berhe, Asmeret Asefaw et al. (2020). Phosphorus Speciation in Atmospherically Deposited Particulate Matter and Implications for Terrestrial Ecosystem Productivity. Environmental Science & Technology 54(8), 4984-4994. 10.1021/acs.est.9b06150

Palte, Rachel L.; Schneider, Sebastian E.; Altman, Michael D.; Hayes, Robert P.; Kawamura, Shuhei et al. (2020). Allosteric Modulation of Protein Arginine Methyltransferase 5 (PRMT5). ACS Medicinal Chemistry Letters. 10.1021/acsmedchemlett.9b00525

Pan, B. Y.; Xu, H. C.; Liu, Y.; Sutarto, R.; He, F. et al. (2020). Anomalous helimagnetic domain shrinkage due to the weakening of the Dzyaloshinskii-Moriya interaction in CrAs. Physical Review B 102(10). 10.1103/physrevb.102.104432

Pan, Yuanming; Li, Dien; Feng, Renfei; Wiens, Eli; Chen, Ning et al. (2020). Uranyl binding mechanism in microcrystalline silicas: A potential missing link for uranium mineralization by direct uranyl co-precipitation and environmental implications. Geochimica et Cosmochimica Acta. 10.1016/j.gca.2020.10.017

Pan; Yuanming; Chen; Ning; Zhu et al. (2020). Local structural environments of bromine in chlorine-rich minerals: Insight from Br K-edge XAS and Br MAS NMR spectroscopy. Earth Science Frontiers 27(5), 10-22. 10.13745/j.esf.sf.2020.5.54

Patel, Megha; Zhong, Jiayun; Gomez-Haibach, Konrad S.; Gomez, Maria A.; King, Graham et al. (2020). Low-energy Sr2MSbO5.5(M = Ca and Sr) structures show significant distortions near oxygen vacancies. International Journal of Quantum Chemistry. 10.1002/qua.26356

Peng, Wenfeng; Li, Junkai; Shen, Kangqi; Zheng, Lirong; Tang, Hu et al. (2020). Iron-Regulated NiPS for Accelerated Oxygen Evolution Efficiency. Journal of Materials Chemistry A. 10.1039/d0ta08123j

Petrilli, Whitney L.; Adam, Gregory C.; Erdmann, Roman S.; Abeywickrema, Pravien; Agnani, Vijayalakshmi et al. (2020). From Screening to Targeted Degradation: Strategies for the Discovery and Optimization of Small Molecule Ligands for PCSK9. Cell Chemical Biology 26(1), 32-40. 10.1093/glycob/cwz069

Pluvinage, Benjamin; Massel, Patricia M; Burak, Kristyn; Boraston, Alisdair B (2020). Structural and functional analysis of four family 84 glycoside hydrolases from the opportunistic pathogen Clostridium perfringens. Glycobiology 30(1), 49-57. 10.1093/glycob/cwz069

Pluvinage, Benjamin; Robb, Craig S.; Jeffries, Roderick; Boraston, Alisdair B. (2020). The structure of PfGH50B, an agarase from the marine bacterium Pseudoalteromonas fuliginea PS47. Acta Crystallographica Section F: Structural Biology Communications 76(9), 422-427. 10.1107/s2053230x20010328

Possinger, Angela R.; Bailey, Scott W.; Inagaki, Thiago M.; Kögel-Knabner, Ingrid; Dynes, James J. et al. (2020). Organo-mineral interactions and soil carbon mineralizability with variable saturation cycle frequency. Geoderma 375, 114483. 10.1016/j.geoderma.2020.114483

Purdy, Sarah Kendra; Spasyuk, Denis; Chitanda, Jackson Mulenga; Reaney, Martin J. T. (2020). [1−9-NαC]-Linusorb B3 (Cyclolinopeptide A) dimethyl sulfoxide monosolvate. IUCrData 5(3). 10.1107/s2414314620003181

Qi, Peng; Samadi, Nazanin; Chapman, Dean (2020). X-ray Spectral Imaging Program: XSIP. Journal of Synchrotron Radiation 27(6), 1734-1740.10.1107/s1600577520010838

ROHANI, S.A.; ALLEN, D.; GARE, B.; ZHU, N.; AGRAWAL, S. et al. (2020). High-resolution imaging of the human incudostapedial joint using synchrotron-radiation phase-contrast imaging. Journal of Microscopy 277(2), 61-70. 10.1111/jmi.12864

Rahman, Noabur; Schoenau, Jeff (2020). Response of wheat, pea, and canola to micronutrient fertilization on five contrasting prairie soils. Scientific Reports 10(1). 10.1038/s41598-020-75911-y

Ramasubramanian, Anusuya; Tennyson, Rachel; Magnay, Maureen; Kathuria, Sagar; Travaline, Tara et al. (2020). Bringing the Heavy Chain to Light: Creating a Symmetric, Bivalent IgG-Like Bispecific. Antibodies 9(4), 62. 10.3390/antib9040062

Rasool, Majid; Chiu, Hsien-Chieh; Zank, Benjamin; Zeng, Yan; Zhou, Jigang et al. (2020). PEDOT Encapsulated and Mechanochemically Engineered Silicate Nanocrystals for High Energy Density Cathodes. Advanced Materials Interfaces, 2000226. 10.1002/admi.202000226

Reid, Joel W.; Kaduk, James A.; Blanchard, Peter E. R. (2020). Crystal structure and X-ray absorption spectroscopy of trimethylarsine oxide dihydrate, (CH3)3AsO•2H2O. Powder Diffraction 35(3), 190-196. 10.1017/s0885715620000421

Reinhardt, Averie; Feng, Renfei; Xiao, Qunfeng; Hu, Yongfeng; Sham, Tsun-Kong et al. (2020). Exploring the Dzi Bead with Synchrotron Light: XRD, XRF Imaging and μ-XANES Analysis. Heritage 3(3) , 1035-1045. 10.3390/heritage3030056

Rodionov, Andrei; Bauke, Sara L.; von Sperber, Christian; Hoeschen, Carmen; Kandeler, Ellen et al. (2020). Biogeochemical cycling of phosphorus in subsoils of temperate forest ecosystems. Biogeochemistry 150(3), 313-328. 10.1007/s10533-020-00700-8

Saidaminov, Makhsud I.; Spanopoulos, Ioannis; Abed, Jehad; Ke, Weijun; Wicks, Joshua et al. (2020). Conventional Solvent Oxidizes Sn(II) in Perovskite Inks. ACS Energy Letters 5(4), 1153-1155. 10.1021/acsenergylett.0c00402

Santos, A C F; Vasconcelos, D N; MacDonald, M A; Sant'Anna, M M; Tenório, B N C et al. (2020). Evidence of Ultrafast Dissociation in the CHCl3 Molecule. Journal of Physics B: Atomic. Molecular and Optical Physics. 10.1088/1361-6455/abc9cc

Santos, David A.; Andrews, Justin L.; Bai, Yang; Stein, Peter; Luo, Yuting et al. (2020). Bending good beats breaking bad: phase separation patterns in individual cathode particles upon lithiation and delithiation. Materials Horizons. 10.1039/d0mh01240h

Schaefer, Michael V.; Bogie, Nathaniel A.; Rath, Daniel; Marklein, Alison R.; Garniwan, Abdi et al. (2020). Effect of Cover Crop on Carbon Distribution in Size and Density Separated Soil Aggregates. Soil Systems 4(1), 6. 10.3390/soilsystems4010006

Schaefer, Michael V.; Plaganas, Mariejo; Abernathy, Macon J.; Aiken, Miranda L.; Garniwan, Abdi et al. (2020). Manganese, Arsenic, and Carbonate Interactions in Model Oxic Groundwater Systems. Environmental Science & Technology 54(17) , 10621-10629. 10.1021/acs.est.0c02084

Schoepfer, Valerie A.; Qin, Kaixuan; Robertson, Jared M.; Das, Soumya; Lindsay, Matthew B. J. et al. (2020). Structural Incorporation of Sorbed Molybdate during Iron(II)-Induced Transformation of Ferrihydrite and Goethite under Advective Flow Conditions. ACS Earth and Space Chemistry 4(7), 1114-1126. 10.1021/acsearthspacechem.0c00099

Schwanke, Anderson Joel; Balzer, Rosana; Wittee Lopes, Christian; Motta Meira, Débora; Díaz, Urbano et al. (2020). Lamellar MWW zeolite with silicon and niobium oxide pillars - A catalyst for the oxidation of volatile organic compounds. Chemistry - A European Journal. 10.1002/chem.202000862

Scott, William; Lowrance, Brian; Anderson, Alexander C.; Weadge, Joel T. (2020). Identification of the Clostridial cellulose synthase and characterization of the cognate glycosyl hydrolase, CcsZ. PLoS ONE 15(12 , e0242686. 10.1371/journal.pone.0242686

Sellers, Diane G.; Braham, Erick J.; Villarreal, Ruben; Zhang, Baiyu; Parija, Abhishek et al. (2020). An Atomic Hourglass and Thermometer Based on Diffusion of a Mobile Dopant in VO2. Journal of the American Chemical Society . 10.1021/jacs.0c07152

Seyfferth, Angelia L.; Bothfeld, Frances; Vargas, Rodrigo; Stuckey, Jason W.; Wang, Jian et al. (2020). Spatial and temporal heterogeneity of geochemical controls on carbon cycling in a tidal salt marsh. Geochimica et Cosmochimica Acta. 10.1016/j.gca.2020.05.013

Shakouri, Mohsen; Hu, Yongfeng; Lehoux, Rick; Wang, Hui (2020). CO2 conversion through combined steam and CO2 reforming of methane reactions over Ni and Co catalysts. Canadian Journal of Chemical Engineering . 10.1002/cjce.23828

Shen, Yanfeng; Wang, Meijun; Wu, Yucheng; Hu, Yongfeng; Kong, Jiao et al. (2020). Role of Gas Coal in Directional Regulation of Sulfur during Coal-Blending Coking of High Organic-Sulfur Coking Coal. Energy & Fuels 34(3), 2757-2764. 10.1021/acs.energyfuels.9b03737

Shi, Jingjing; McGill, William B.; Chen, Ning; Rutherford, P. Michael; Whitcombe, Todd W. et al. (2020). Formation and Immobilization of Cr(VI) Species in Long-Term Tannery Waste Contaminated Soils. Environmental Science & Technology 54(12), 7226-7235. 10.1021/acs.est.0c00156

Shi, Ruina; Zhao, Jinxian; Quan, Yanhong; Wang, Xuhui; An, Jiangwei et al. (2020). Fabrication of Few-Layer Graphene-Supported Copper Catalysts Using a Lithium-Promoted Thermal Exfoliation Method for Methanol Oxidative Carbonylation. ACS Applied Materials & Interfaces 12(27), 10.1021/acsami.0c08366

Shin, Hyungki; Liu, Chong; Li, Fengmiao; Sutarto, Ronny; Davidson, Bruce A. et al. (2020). Controlling the electrical and magnetic ground states by doping in the complete phase diagram of titanate Eu1−xLaxTiO3 thin films. Physical Review B 101(21). 10.1103/physrevb.101.214105

Shokatian, Sadegh; Wang, Jian; Urquhart, Stephen G. (2020). Effect of Chain Length on the Near Edge X-ray Absorption Fine Structure Spectra of Liquid n-Alkanes. Chemical Physics Letters, 137564. 10.1016/j.cplett.2020.137564

Shrestha, P.; Lee, CH.; Fahy, K. F.; Balakrishnan, M.; Ge, N. et al. (2020). Formation of Liquid Water Pathways in PEM Fuel Cells: A 3-D Pore-Scale Perspective. Journal of the Electrochemical Society 167(5), 054516. 10.1149/1945-7111/ab7a0b

Siemens, Ashley M.; Dynes, James J.; Chang, Wonjae (2020). Sodium adsorption by reusable zeolite adsorbents: integrated adsorption cycles for salinised groundwater treatment. Environmental Technology (United Kingdom), 1-12. 10.1080/09593330.2020.1721567

Sirovica, Slobodan; Solheim, Johanne H.; Skoda, Maximilian W. A.; Hirschmugl, Carol J.; Mattson, Eric C. et al. (2020). Origin of micro-scale heterogeneity in polymerisation of photo-activated resin composites. Nature Communications 11(1). 10.1038/s41467-020-15669-z

Situm, Arthur; Beam, Jeremiah C.; Hughes, Kebbi A.; Rowson, John; Essilfie-Dughan, Joseph et al. (2020). An X-ray spectromicroscopy study of the calcium mineralization in the JEB tailings management facility at McClean Lake, Saskatchewan. Applied Geochemistry 112, 104459. 10.1016/j.apgeochem.2019.104459

Smiles, Danil E.; Batista, Enrique R.; Booth, Corwin H.; Clark, David L.; Keith, Jason M. et al. (2020). The duality of electron localization and covalency in lanthanide and actinide metallocenes. Chemical Science 11(10), 2796-2809. 10.1039/c9sc06114b

Sokaribo, Akosiererem; Novakovski, Brian A.A.; Cotelesage, Julien; White, Aaron P.; Sanders, David et al. (2020). Kinetic and structural analysis of Escherichia coli phosphoenolpyruvate carboxykinase mutants. Biochimica et Biophysica Acta - General Subjects 1864(4), 129517. 10.1016/j.bbagen.2020.129517

Song, Sanzhao; Bao, Hongliang; Lin, Xiao; Du, Xian-Long; Zhou, Jing et al. (2020). Molten salt-assisted synthesis of bulk CoOOH as a water oxidation catalyst. Journal of Energy Chemistry 42, 5-10. 10.1016/j.jechem.2019.05.021

Song, Xiaojing; Yang, Xiaotong; Zhang, Tianjun; Zhang, Hao; Zhang, Qiang et al. (2020). Controlling the Morphology and Titanium Coordination States of TS-1 Zeolites by Crystal Growth Modifier. Inorganic Chemistry 59(18), 13201-13210. 10.1021/acs.inorgchem.0c01518

Sowers, Tyler D.; Wani, Rucha P.; Coward, Elizabeth K.; Fischel, Matthew H.H.; Betts, Aaron R. et al. (2020). Spatially-resolved organomineral interactions across a permafrost chronosequence. Environmental Science & Technology. 10.1021/acs.est.9b06558

Stachel, Shawn J.; Ginnetti, Anthony T.; Johnson, Scott A.; Cramer, Paige; Wang, Yi et al. (2020). Identification of potent inhibitors of the sortilin-progranulin interaction.Bioorganic and Medicinal Chemistry Letters 30(17), 127403. 10.1016/j.bmcl.2020.127403

Stirling, Alexander J.; Gilbert, Stephanie E.; Conner, Megan; Mallette, Evan; Kimber, Matthew S. et al. (2020). A Key Glycine in Bacterial Steroid-Degrading Acyl-CoA Dehydrogenases Allows Flavin-Ring Repositioning and Modulates Substrate Side Chain Specificity. Biochemistry 59(42), 4081-4092. 10.1021/acs.biochem.0c00568

Sudheeshkumar, V.; Alyari, Maryam; Gangishetty, Mahesh; Scott, Robert W. J. (2020). Galvanic synthesis of AgPd bimetallic catalysts from Ag clusters dispersed in a silica matrix. Catalysis Science and Technology 10(24), 8421-8428. 10.1039/d0cy01675f

Sun, Tianxiao; Sun, Gang; Yu, Fuda; Mao, Yongzhi; Tai, Renzhong et al. (2020). Soft X-ray Ptychography Chemical Imaging of Degradation in a Composite Surface-Reconstructed Li-Rich Cathode. ACS Nano 15(1) , 1475-1485. 10.1021/acsnano.0c08891

Sun, Xinyang; Scanlon, Martin G.; Guillermic, Reine-Marie; Belev, George S.; Webb, M. Adam et al. (2020). The effects of sodium reduction on the gas phase of bread doughs using synchrotron X-ray microtomography. Food Research International 130, 108919. 10.1016/j.foodres.2019.108919

Sun, Yipeng; Amirmaleki, Maedeh; Zhao, Yang; Zhao, Changtai; Liang, Jianneng et al. (2020). Tailoring the Mechanical and Electrochemical Properties of an Artificial Interphase for High-Performance Metallic Lithium Anode. Advanced Energy Materials 10(28), 2001139. 10.1002/aenm.202001139

Ting, Michelle; Burigana, Matthew; Zhang, Leiting; Finfrock, Y. Zou; Trabesinger, Sigita et al. (2020). Impact of Nickel Substitution into Model Li-Rich Oxide Cathode Materials for Li-Ion Batteries. Chemistry of Materials. 10.1021/acs.chemmater.9b04446

Tomlin, Jay M.; Jankowski, Kevin A.; Rivera-Adorno, Felipe A.; Fraund, Matthew; China, Swarup et al. (2020). Chemical Imaging of Fine Mode Atmospheric Particles Collected from a Research Aircraft over Agricultural Fields. ACS Earth and Space Chemistry 4(11), 2171-2184. 10.1021/acsearthspacechem.0c00172

Ton, Ngoc; Goncin, Una; Panahifar, Arash; Chapman, Dean; Wiebe, Sheldon et al. (2020). Developing a Microbubble-based Contrast Agent for Synchrotron In-line Phase Contrast Imaging. IEEE Transactions on Biomedical Engineering. 10.1109/tbme.2020.3040079

Torres-Rojas, Dorisel; Hestrin, Rachel; Solomon, Dawit; Gillespie, Adam W.; Dynes, James J. et al. (2020). Nitrogen speciation and transformations in fire-derived organic matter. Geochimica et Cosmochimica Acta 276, 170-185. 10.1016/j.gca.2020.02.034

Uchagawkar, Anoop; Ramanathan, Anand; Hu, Yongfeng; Subramaniam, Bala (2020). Highly dispersed molybdenum containing mesoporous silicate (Mo-TUD-1) for olefin metathesis. Catalysis Today 343, 215-225. 10.1016/j.cattod.2019.03.073

Van Loon, Lisa; Banerjee, Neil; Brinkman, Don (2020). Synchrotron Micro Computed Tomography for Non-Destructive 3D Studies of Fossil Fish. Microscopy and Microanalysis, 1-3. 10.1017/s1431927620017481

Van Loon, Lisa; McIntyre, Stewart; Sherry, Nathaniel; Bauer, Michael; Banerjee, Neil et al. (2020). User-Friendly Software for the Analysis of Complex XRF Spectra. Microscopy and Microanalysis, 1-4. 10.1017/s1431927620014890

Vance, Tyler D.R.; Ye, Qilu; Conroy, Brigid; Davies, Peter L. (2020). Essential role of calcium in extending RTX adhesins to their target. Journal of Structural Biology: X 4, 100036. 10.1016/j.yjsbx.2020.100036

Variani, Yuri M.; Lopes, Christian W.; Nicola, Bruna P.; Meira, Debora M.; Pergher, Sibele B. C. et al. (2020). Activated carbon fibers as support for nickel diimine complexes and its application in ethylene oligomerization. New Journal of Chemistry. 10.1039/d0nj02285c

Vessey, Colton J.; Lindsay, Matthew B. J. (2020). Aqueous Vanadate Removal by Iron(II)-Bearing Phases under Anoxic Conditions. Environmental Science & Technology 54(7), 4006-4015. 10.1021/acs.est.9b06250

Vrublevskiy, Dmitry; Lussier, Joey A.; Panchuk, Jenny R.; Mauws, Cole; Beam, Jeremiah C. et al. (2020). Understanding the Interplay of Vacancy, Cation, and Charge Ordering in the Tunable Sc2VO5+δ Defect Fluorite System. Inorganic Chemistry 60(2), 872-882. 10.1021/acs.inorgchem.0c02992

Walsh, Andrew G.; Zhang, Peng (2020). Thiolate-Protected Bimetallic Nanoclusters: Understanding the Relationship between Electronic and Catalytic Properties. Journal of Physical Chemistry Letters 12(1), 257-275. 10.1021/acs.jpclett.0c03252

Wang, Jiayi; Li, Gaoran; Luo, Dan; Zhang, Yongguang; Zhao, Yan et al. (2020). Engineering the Conductive Network of Metal Oxide-Based Sulfur Cathode toward Efficient and Longevous Lithium–Sulfur Batteries. Advanced Energy Materials 10(41), 2002076. 10.1002/aenm.202002076

Wang, Lichen; Yu, Biqiong; Jing, Ran; Luo, Xiangpeng; Zeng, Junbang et al. (2020). Doping-dependent phonon anomaly and charge-order phenomena in the HgBa2CuO4+δ and HgBa2CaCu2O6+δ superconductors. Physical Review B 101(22). 10.1103/physrevb.101.220509

Wang, Lu; Dong, Yuchan; Yan, Tingjiang; Hu, Zhixin; Jelle, Abdinoor A. et al. (2020). Black indium oxide a photothermal CO2 hydrogenation catalyst. Nature Communications 11(1). 10.1038/s41467-020-16336-z

Wang, Meijun; Shen, Yanfeng; Hu, Yongfeng; Kong, Jiao; Wang, Jiancheng et al. (2020). Effect of pre-desulfurization process on the sulfur forms and their transformations during pyrolysis of Yanzhou high sulfur coal. Fuel 276, 118124. 10.1016/j.fuel.2020.118124

Wang, Qiong; Tang, Tengteng; Cooper, David; Eltit, Felipe; Fratzl, Peter et al. (2020). Globular structure of the hypermineralized tissue in human femoral neck. Journal of Structural Biology 212(2), 107606. 10.1016/j.jsb.2020.107606

Wang, Xuchun; Xie, Miao; Lyu, Fenglei; Yiu, Yun-Mui; Wang, Zhiqiang et al. (2020). Bismuth Oxyhydroxide-Pt Inverse Interface for Enhanced Methanol Electrooxidation Performance. Nano Letters 20(10), 7751-7759. 10.1021/acs.nanolett.0c03340

Wang, Xue; Wang, Ziyun; García de Arquer, F. Pelayo; Dinh, Cao-Thang; Ozden, Adnan et al. (2020). Efficient electrically powered CO2-to-ethanol via suppression of deoxygenation. Nature Energy 5(6), 478-486. 10.1038/s41560-020-0607-8

Wang, Xuewan; Wu, Dan; Dai, Chengzhi; Xu, Chenyu; Sui, Pengfei et al. (2020). Novel folic acid complex derived nitrogen and nickel co-doped carbon nanotubes with embedded Ni nanoparticles as efficient electrocatalysts for CO2 reduction. Journal of Materials Chemistry A 8(10), 5105-5114. 10.1039/c9ta12238a

Wang, Xuewan; Xi, Xiuan; Huo, Ge; Xu, Chenyu; Sui, Pengfei et al. (2020). Co- and N-doped carbon nanotubes with hierarchical pores derived from metal-organic nanotubes for oxygen reduction reaction. Journal of Energy Chemistry. 10.1016/j.jechem.2020.05.020

Wang, Zhijiang; Yuan, Qi; Shan, Jingjing; Jiang, Zhaohua; Xu, Ping et al. (2020). Highly Selective Electrocatalytic Reduction of CO2 into Methane on Cu–Bi Nanoalloys. Journal of Physical Chemistry Letters, 7261-7266. 10.1021/acs.jpclett.0c01261

Weber, Rochelle; Li, Hongyang; Chen, Weifeng; Kim, Chang-Yong; Plucknett, Kevin et al. (2020). In Situ XRD Studies During Synthesis of Single-Crystal LiNiO2, LiNi0.975Mg0.025O2, and LiNi0.95Al0.05O2 Cathode Materials. Journal of the Electrochemical Society 167(10), 100501. 10.1149/1945-7111/ab94ef

Weeks, Joseph J.; Hettiarachchi, Ganga M. (2020). Source and formulation matter: New insights into phosphorus fertilizer fate and transport in mildly calcareous soils. Soil Science Society of America Journal 84(3), 731-746. 10.1002/saj2.20054

Wen, Guobin; Ren, Bohua; Park, Moon G.; Yang, Jie; Dou, Haozhen et al. (2020). Ternary Sn-Ti-O Electrocatalyst Boosts the Stability and Energy Efficiency of CO2 Reduction. Angewandte Chemie - International Edition 59(31), 12860-12867. 10.1002/anie.202004149

Wilson, Catrina E.; Gibson, Amanda E.; Argo, Joshua J.; Loughney, Patricia A.; Xu, Wenqian et al. (2020). Accelerated microwave-assisted synthesis and in situ X-ray scattering of tungsten-substituted vanadium dioxide (V1−xW x O2). Journal of Materials Research, 1-13. 10.1557/jmr.2020.250

Wu, Jian-Feng; Ramanathan, Anand; Kersting, Reinhard; Jystad, Amy; Zhu, Hongda et al. (2020). Enhanced Olefin Metathesis Performance of Tungsten and Niobium Incorporated Bimetallic Silicates: Evidence of Synergistic Effects. ChemCatChem 12(7), 2004-2013. 10.1002/cctc.201902131

Wu, Longfei; Dzade, Nelson Y.; Chen, Ning; van Dijk, Bas; Balasubramanyam, Shashank et al. (2020). Cu Electrodeposition on Nanostructured MoS2 and WS2 and Implications for HER Active Site Determination. Journal of the Electrochemical Society 167(11), 116517. 10.1149/1945-7111/aba5d8

Wu, Mingjie; Zhang, Gaixia; Hu, Yongfeng; Wang, Jian; Sun, Tianxiao et al. (2020). Graphitic-shell encapsulated FeNi alloy/nitride nanocrystals on biomass-derived N-doped carbon as an efficient electrocatalyst for rechargeable Zn-air battery. Carbon Energy. 10.1002/cey2.52

Xia, Xing; Yang, Jianjun; Yan, Yubo; Wang, Jian; Hu, Yongfeng et al. (2020). Molecular sorption mechanisms of Cr(III) to organo-ferrihydrite coprecipitates using synchrotron-based EXAFS and STXM techniques. Environmental Science & Technology. 10.1021/acs.est.0c02872

Xiao, Biwei; Liu, Hanshuo; Chen, Ning; Banis, Mohammad Norouzi; Yu, Haijun et al. (2020). Size-Mediated Recurring Spinel Sub-nanodomains in Li and Mn-rich Layered Cathode Materials. Angewandte Chemie - International Edition . 10.1002/anie.202005337

Xiao, Xudong; Gao, Yanting; Zhang, Liping; Zhang, Jiachen; Zhang, Qun et al. (2020). A Promoted Charge Separation/Transfer System from Cu Single Atoms and C3N4 Layers for Efficient Photocatalysis. Advanced Materials, 2003082. 10.1002/adma.202003082

Xing, Zhenyu; Tan, Guoqiang; Yuan, Yifei; Wang, Bao; Ma, Lu et al. (2020). Consolidating Lithiothermic-Ready Transition Metals for Li2S-Based Cathodes.Advanced Materials 32(31), 2002403. 10.1002/adma.202002403

Xu, Shishuai; Gao, Xiang; Deshmukh, Amol; Zhou, Junshuang; Chen, Ning et al. (2020). Pressure-promoted irregular CoMoP2 nanoparticles activated by surface reconstruction for oxygen evolution reaction electrocatalysts. Journal of Materials Chemistry A 8(4), 2001-2007. 10.1039/c9ta11775j

Xu, Shishuai; Wang, Mingzhi; Saranya, Govindarajan; Chen, Ning; Zhang, Lili et al. (2020). Pressure-driven catalyst synthesis of Co-doped Fe C@Carbon nano-onions for efficient oxygen evolution reaction. Applied Catalysis B: Environmental 268, 118385. 10.1016/j.apcatb.2019.118385

Xu, Wenjing; Zhang, Tianjun; Bai, Risheng; Zhang, Peng; Yu, Jihong et al. (2020). A one-step rapid synthesis of TS-1 zeolites with highly catalytically active mononuclear TiO6 species. Journal of Materials Chemistry A 8(19), 9677-9683. 10.1039/c9ta13851j

Xu, Ziqing; Huang, Guohe; An, Chunjiang; Huang, Jing; Chen, Xiujuan et al. (2020). Low-cost microbiological purification using a new ceramic disk filter functionalized by chitosan/TiO2 nanocomposites. Separation and Purification Technology 248, 116984. 10.1016/j.seppur.2020.116984

Yang, Jianjun; Xia, Xing; Liu, Jin; Wang, Jian; Hu, Yongfeng et al. (2020). Molecular Mechanisms of Chromium(III) Immobilization by Organo–Ferrihydrite Co-precipitates: The Significant Roles of Ferrihydrite and Carboxyl. Environmental Science & Technology 54(8), 4820-4828. 10.1021/acs.est.9b06510

Yang, Xiaohan; Huang, Guohe; An, Chunjiang; Chen, Xiujuan; Shen, Jian et al. (2020). Removal of arsenic from water through ceramic filter modified by nano-CeO2: A cost-effective approach for remote areas. Science of the Total Environment, 141510. 10.1016/j.scitotenv.2020.141510

Yang, Xiaohua; Zhang, Gaixia; Du, Lei; Zhang, Jun; Chiang, Fu-Kuo et al. (2020). PGM-Free Fe/N/C and Ultralow Loading Pt/C Hybrid Cathode Catalysts with Enhanced Stability and Activity in PEM Fuel Cells. ACS Applied Materials & Interfaces 12(12), 13739-13749. 10.1021/acsami.9b18085

Yang, Yang; Qian, Yumin; Li, Haijing; Zhang, Zhenhua; Mu, Yuewen et al. (2020). O-coordinated W-Mo dual-atom catalyst for pH-universal electrocatalytic hydrogen evolution. Science advances 6(23), eaba6586. 10.1126/sciadv.aba6586

Yao, Qianting; Jiang, Yingying; Tan, Shuo; Fu, Xinyi; Li, Bo et al. (2020). Composition and bioactivity of calcium phosphate coatings on anodic oxide nanotubes formed on pure Ti and Ti-6Al-4V alloy substrates.Materials Science and Engineering C 110, 110687. 10.1016/j.msec.2020.110687

Yao, Yonggang; Liu, Zhenyu; Xie, Pengfei; Huang, Zhennan; Li, Tangyuan et al. (2020). Computationally aided, entropy-driven synthesis of highly efficient and durable multi-elemental alloy catalysts. Science advances 6(11), eaaz0510. 10.1126/sciadv.aaz0510

Ye, Qilu; Eves, Robert; Campbell, Robert L.; Davies, Peter L. (2020). Crystal structure of an insect antifreeze protein reveals ordered waters on the ice-binding surface. Biochemical Journal. 10.1042/bcj20200539

Yu, Chuang; Li, Yong; Adair, Keegan R.; Li, Weihan; Goubitz, Kees et al. (2020). Tuning ionic conductivity and electrode compatibility of Li3YBr6 for high-performance all solid-state Li batteries. Nano Energy 77, 105097. 10.1016/j.nanoen.2020.105097

Yu, Chuang; Li, Yong; Li, Weihan; Adair, Keegan R.; Zhao, Feipeng et al. (2020). Enabling ultrafast ionic conductivity in Br-based lithium argyrodite electrolytes for solid-state batteries with different anodes. Energy Storage Materials 30, 238-249. 10.1016/j.ensm.2020.04.014

Yue, Pu; Chen, Ning; Peak, Derek; Bompoti, Nefeli Maria; Chrysochoou, Maria et al. (2020). Oxygen atom release during selenium oxyanion adsorption on goethite and hematite. Applied Geochemistry 117, 104605. 10.1016/j.apgeochem.2020.104605

Zhan, Yunfeng; Xie, Fangyan; Zhang, Hao; Jin, Yanshuo; Meng, Hui et al. (2020). Highly Dispersed Nonprecious Metal Catalyst for Oxygen Reduction Reaction in Proton Exchange Membrane Fuel Cells. ACS Applied Materials & Interfaces 12(15), 17481-17491. 10.1021/acsami.0c00126

Zhang, Chunzi; Koughia, Cyril; Gunes, Ozan; Li, Xiaoju; Li, Yuanshi et al. (2020). Size, composition and alignment of VO2 microrod crystals by the reduction of V2O5 thin films, and their optical properties through insulator-metal transitions. Journal of Alloys and Compounds 827, 154150. 10.1016/j.jallcom.2020.154150

Zhang, Haiping; Lin, Hongfei; Zheng, Ying (2020). Deactivation study of unsupported nano MoS2 catalyst. Carbon Resources Conversion 3, 60-66. 10.1016/j.crcon.2019.09.003

Zhang, Longsheng; Wang, Liping; Wen, Yunzhou; Ni, Fenglou; Zhang, Bo et al. (2020). Boosting Neutral Water Oxidation through Surface Oxygen Modulation. Advanced Materials 32(31), 2002297. 10.1002/adma.202002297

Zhang, Peng; Gourgas, Ophélie; Lainé, Audrey; Murshed, Monzur; Mantovani, Diego et al. (2020). Coacervation Conditions and Cross-Linking Determines Availability of Carbonyl Groups on Elastin and its Calcification. Crystal Growth and Design 20(11), 7170-7179. 10.1021/acs.cgd.0c00759

Zhang, Qingxin; Wieler, Mackenzie; O'Connell, David; Gill, Laurence; Xiao, Qunfeng et al. (2020). Speciation of Phosphorus from Suspended Sediment Studied by Bulk and Micro-XANES. Soil Systems 4(3), 51. 10.3390/soilsystems4030051

Zhang, Tianjun; Chen, Ziyi; Walsh, Andrew G.; Li, Yi; Zhang, Peng et al. (2020). Single-Atom Catalysts Supported by Crystalline Porous Materials: Views from the Inside. Advanced Materials 32(44), 2002910. 10.1002/adma.202002910

Zhang, Yunhui; Alessi, Daniel S.; Chen, Ning; Luo, Mina; Hao, Weiduo et al. (2020). Spectroscopic and Modeling Investigation of Sorption of Pb(II) to ZSM-5 Zeolites. ACS ES&T Water 1(1), 108-116. 10.1021/acsestwater.0c00010

Zhang, Zhen; Luo, Dan; Li, Gaoran; Gao, Rui; Li, Matthew et al. (2020). Tantalum-Based Electrocatalyst for Polysulfide Catalysis and Retention for High-Performance Lithium-Sulfur Batteries. Matter. 10.1016/j.matt.2020.06.002

Zhang, Zheyu; Singh, Kalpana; Tsur, Yoed; Zhou, Jigang; Dynes, James J. et al. (2020). Studies on effect of Ca-doping on structure and electrochemical properties of garnet-type Y3-xCaxFe5O12-δ. Journal of Solid State Chemistry 290, 121530. 10.1016/j.jssc.2020.121530

Zhao, Bin; Liu, Jianwen; Wang, Xuewan; Xu, Chenyu; Sui, Pengfei et al. (2020). CO2-emission-free Electrocatalytic CH3OH Selective Upgrading with High Productivity at Large Current Densities for Energy Saved Hydrogen Co-generation. Nano Energy, 105530. 10.1016/j.nanoen.2020.105530

Zhao, Bin; Liu, Jianwen; Xu, Chenyu; Feng, Renfei; Sui, Pengfei et al. (2020). Interfacial Engineering of Cu2Se/Co3Se4 Multivalent Hetero-nanocrystals for Energy-efficient Electrocatalytic Co-generation of Value-added Chemicals and Hydrogen. Applied Catalysis B: Environmental, 119800. 10.1016/j.apcatb.2020.119800

Zhao, Bin; Liu, Jianwen; Xu, Chenyu; Feng, Renfei; Sui, Pengfei et al. (2020). Hollow NiSe Nanocrystals Heterogenized with Carbon Nanotubes for Efficient Electrocatalytic Methanol Upgrading to Boost Hydrogen Co-Production. Advanced Functional Materials, 2008812. 10.1002/adfm.202008812

Zhao, Changtai; Liang, Jianwen; Li, Xiaona; Holmes, Nathaniel; Wang, Changhong et al. (2020). Halide-based solid-state electrolyte as an interfacial modifier for high performance solid-state Li–O2 batteries. Nano Energy, 105036. 10.1016/j.nanoen.2020.105036

Zhao, Yanyun; Huang, Guohe; An, Chunjiang; Huang, Jing; Xin, Xiaying et al. (2020). Removal of Escherichia Coli from water using functionalized porous ceramic disk filter coated with Fe/TiO2 nano-composites. Journal of Water Process Engineering 33, 101013. 10.1016/j.jwpe.2019.101013

Zhou, Limin; Wang, Xingya; Shin, Hyun-Joon; Wang, Jian; Tai, Renzhong et al. (2020). Ultra-high Density of Gas Molecules Confined in Surface Nanobubbles in Ambient Water. Journal of the American Chemical Society. 10.1021/jacs.9b11303

Zhou, Qun; Jaworski, Julie; Zhou, Yanfeng; Valente, Delphine; Cotton, Joanne et al. (2020). Engineered Fc-glycosylation switch to eliminate antibody effector function. mAbs 12(1), 1814583. 10.1080/19420862.2020.1814583

Zhu, Jianbing; Li, Shuang; Xiao, Meiling; Zhao, Xiao; Li, Gaoran et al. (2020). Tensile-strained ruthenium phosphide by anion substitution for highly active and durable hydrogen evolution. Nano Energy, 105212. 10.1016/j.nanoen.2020.105212

Śmiałek, Małgorzata A.; Duflot, Denis; Jones, Nykola C.; Hoffmann, Søren Vrønning; Zuin, Lucia et al. (2020). On the electronic structure of methyl butyrate and methyl valerate. European Physical Journal D 74(7). 10.1140/epjd/e2020-10125-5

## BOOK/CHAPTER

Ian R. Willick; Jarvis Stobbs; Chithra Karunakaran; Karen K. Tanino (2020). Phenotyping Plant Cellular and Tissue Level Responses to Cold with Synchrotron-Based Fourier-Transform Infrared Spectroscopy and X-Ray Computed Tomography. In Dirk K. Hincha; Ellen Zuther(Ed.), Plant Cold Acclimation: Methods and Protocols. Humana., 141-159.

## MASTERS THESIS

Chivers; Brandon (2020). Single-Atom Catalysts: Syntheses, Characterization, and Catalytic Evaluation in Selective Oxidation and Hydrogenation Reactions. Supervisor: Scott, Robert W. J.. SK, Canada: University of Saskatchewan. https://harvest.usask.ca/handle/10388/12670

Jian; Mike (2020). Molecular Basis for the Cross-Species Specificity of the Anti-Serum Albumin Vhh M79. Supervisor: Brooks, Cory L.. California, USA: California State University, Fresno. https://search.proquest.com/docview/2419103999

Naman K. Gupta (2020). A Study of Electronic Nematicity in Cuprate Superconductors using Resonant Soft X-Ray Scattering. Supervisor: David Hawthorn. Ontario, Canada: University of Waterloo.

Subash Dhakal (2020). SYNCHROTRON RADIATION INLINE PROPAGATION BASED PHASE CONTRAST COMPUTERIZED TOMOGRAPHY (PC-CT) OF HUMAN PROSTATE SAMPLE. Supervisor: Al-Dissi, Ahmad; Buhr, Mary. Saskatchewan, Canada: University of Saskatchewan. https://harvest.usask.ca/handle/10388/12771

Tristan K. Kuehn (2020). A 3D Printed Axon-Mimetic Diffusion MRI Phantom. Supervisor: Khan, Ali R. Ontario, Canada: The University of Western Ontario. https://ir.lib.uwo.ca/etd/7238/

William F; McComb (2020). Non-destructive solid-state investigation of PEI agricultural soils. Supervisor: Kirby, Chris; Bissessur, Rabin. Prince Edward Island, Canada: University of Prince Edward Island.

William G. Barrett (2020). Galvanic Synthesis and In Situ Speciation of Methane Oxidation Catalysts. Supervisor: Scott, Robert W. J.. Saskatoon: University of Saskatchewan. https://harvest.usask.ca/handle/10388/12896

Zhang; Qingxin (2020). Speciation of Bioavailable Phosphorus in Fluvial Sediments. Supervisor: Yongfeng Hu. SK, Canada: University of Saskatchewan. http://hdl.handle.net/10388/13107

## PDB DEPOSITION

Alexander; J.A.N.; Strynadka; N.C.J. (2020). Crystal structure of Staphylococcus aureus BlaR1 antibiotic-sensor domain in complex with avibactam. Protein Data Bank: 6o9w

Alexander; J.A.N.; Strynadka; N.C.J. (2020). Crystal structure of Staphylococcus aureus MecR1 antibiotic-sensor domain in complex with avibactam. Protein Data Bank: 6o9s

Allingham; J.S.; Deng; X.; Trofimova et al. (2020). Structure of rabbit actin in complex with truncated analog of Mycalolide B. Protein Data Bank: 6w7v

Anderson; A.C.; Brenner; T.; Weadge et al. (2020). Crystal structure of the bacterial cellulose synthase subunit G (BcsG) from Escherichia coli, catalytic domain. Protein Data Bank: 6pd0

Anderson; A.C.; Brenner; T.; Weadge et al. (2020). Crystal structure of the bacterial cellulose synthase subunit G (BcsG) catalytic domain from Escherichia coli, selenomethionine variant. Protein Data Bank: 6pcz

Boniecki; M.T.; Cygler; M. (2020). N-terminal mutation of ISCU2 (L35H36) traps Nfs1 Cys loop in the active site of ISCU2 without metal present. Structure of human mitochondrial complex Nfs1-ISCU2(L35H36)-ISD11 with E.coli ACP1 at 1.9 A resolution (NIAU)2. Protein Data Bank:6wih

Boniecki; M.T.; Cygler; M. (2020). Structure of human mitochondrial complex Nfs1-ISCU2-ISD11 with E.coli ACP1 at 1.95 A resolution (NIAU)2. N-terminal mutation of ISCU2 (L35) traps Nfs1 Cys loop in the active site of ISCU2 without metal present. Protein Data Bank: 6wi2

Caveney; N.A.; Strynadka; N.C.J. (2020). C. rodentium YcbB - ertapenem complex. Protein Data Bank: 7kgm

Ceccarelli; D.F.; Beenstock; J.; Wan et al. (2020). Cgi121-tRNA complex. Protein Data Bank: 7kju

Chan; A.C.; Herrmann; J.; Smit et al. (2020). Surface-layer (S-layer) RsaA protein from Caulobacter crescentus bound to strontium and iodide. Protein Data Bank: 6p5t

Chiche-Lapierre; C.; Alonzo; D.A.; Schmeing et al. (2020). Adenylation domain of the initiation module of LgrA mutant P483M. Protein Data Bank: 6ulz

Chung; C. (2020). PROTAC6 mediated complex of VHL:EloB:EloC and Bcl-xL. Protein Data Bank: 6zhc

Cygler; M.; Voth; K. (2020). Crystal structure of the Legionella effector protein MavL. Protein Data Bank: 6omi

Cygler; M.; Voth; K.A. (2020). Crystal structure of the Legionella effector protein MavE. Protein Data Bank:6pir

Dong; A.; Li; A.; Zhang et al. (2020). Crystal structure of caltubin from the great pond snail. Protein Data Bank: 6van

Dong; C.; Bountra; C.; Edwards et al. (2020). complex structure of PHF1. Protein Data Bank: 6wat

Dong; C.; Bountra; C.; Edwards et al. (2020). Complex structure of PHF19. Protein Data Bank: 6wau

Dong; C.; Tempel; W.; Bountra et al. (2020). GID4 in complex with VGLWKS peptide. Protein Data Bank:6wzz

Gardberg; A.S.; Wilson; J.E. (2020). Crystal structure of the p300 acetyltransferase domain with AcCoA competitive inhibitor 17. Protein Data Bank: 6v8n

Gorelik; A.; Labriola; J.M.; Illes et al. (2020). Human ectonucleoside triphosphate diphosphohydrolase 4 (ENTPD4, NTPDase 4). Protein Data Bank: 6wg5

Grant; B.M.M.; Enomoto; M.; Lee et al. (2020). Calmodulin in complex with farnesyl cysteine methyl ester. Protein Data Bank: 6os4

Guarne; A.; Almawi; A.W. (2020). Crystal structure of the polo-box domain of Cdc5 from budding yeast. Protein Data Bank: 6mf4

Jones; C.J.; Sychantha; D.; Howell et al. (2020). Structure of Staphylococcus aureus peptidoglycan O-acetyltransferase A (OatA) C-terminal catalytic domain, Zn-bound. Protein Data Bank: 6wn9

Jones; D.R.; Abbott; D.W. (2020). Crystal Structure of a family 76 glycoside hydrolase from a bovine Bacteroides thetaiotaomicron strain. Protein Data Bank: 6u4z

Khan; J.A. (2020). STRUCTURE OF HUMAN PREGNANE X RECEPTOR LIGAND BINDING DOMAIN BOUND TETHERED WITH SRC CO-ACTIVATOR PEPTIDE AND COMPOUND-3 AKA 1,3,3,3-HEXAFLUORO-2-{4-[1-(4-LUOROBENZENESULFONYL) CYCLOPENTYL] PHENYL} PROPAN-2-OL. Protein Data Bank: 6nx1

Kimber; M.S.; Mallette; E.; Kamski-Hennekam et al. (2020). WbbM bifunctional glycosytransferase apo structure. Protein Data Bank: 6u4b

Kimber; M.S.; Stirling; A.J.; Seah et al. (2020). Tcur3481-Tcur3483 steroid ACAD G363A variant. Protein Data Bank: 6wy9

Klein; D.J.; Liu; J. (2020). Structure of Human HDAC2 in complex with a 2-substituted benzamide inhibitor (compound 20). Protein Data Bank: 7kbg

Lau; K.; Nielsen; L.H.; Holt et al. (2020). Calmodulin N53I variant bound to cardiac ryanodine receptor (RyR2) calmodulin binding domain. Protein Data Bank: 6y4p

Li; F.K.K.; Strynadka; N.C.J. (2020). Crystal structure of B. subtilis TagT. Protein Data Bank: 6uf5

Li; F.K.K.; Strynadka; N.C.J. (2020). Crystal structure of B. subtilis TagU. Protein Data Bank: 6uf6

Li; F.K.K.; Strynadka; N.C.J. (2020). Crystal structure of B. subtilis TagV. Protein Data Bank: 6uf3

Li; F.K.K.; Strynadka; N.C.J. (2020). Crystal structure of S. aureus LcpA in complex with octaprenyl-pyrophosphate-GlcNAc. Protein Data Bank: 6uex

Lord; D.M.; Zhou; Y.F. (2020). 2xVH Fab. Protein Data Bank: 7jkb

Luan; X.; Shang; W.; Wang et al. (2020). The crystal structure of COVID-19 main protease in complex with GC376. Protein Data Bank: 7c8u

Majewski; D.D.; Okon; M.; Heinkel et al. (2020). Crystal structure of the type III secretion pilotin InvH. Protein Data Bank: 6xfj

Mendoza; M.N.; Jian; M.; Toride King et al. (2020). VHH R303 C33A/C102A in complex withthe LRR domain of InlB. Protein Data Bank: 6u14

Mendoza; M.N.; Jian; M.; Toride King et al. (2020). VHH R303 C33A/C102A in complex withthe LRR domain of InlB. Protein Data Bank: 6u12

Miron; C.E.; van Staalduinen; L.M.; Jia et al. (2020). Crystal Structure of human telomeric DNA G-quadruplex in complex with a novel platinum(II) complex. Protein Data Bank: 6xcl

Muckelbauer; J.K. (2020). CRYSTAL STRUCTURE OF RHO-ASSOCIATED PROTEIN KINASE 1 (ROCK1) IN COMPLEX WITH A PHENYLPYRAZOLE AMIDE INHIBITOR. Protein Data Bank: 7jou

Noach; I.; Boraston; A.B. (2020). Structure of IMPa from Pseudomonas aeruginosa in complex with an O-glycopeptide. Protein Data Bank: 7jtv

Palte; R.L. (2020). Human Arginase1 Complexed with Bicyclic Inhibitor Compound 3. Protein Data Bank: 6v7c

Palte; R.L.; Schneider; S.E. (2020). PRMT5:MEP50 Complexed with Allosteric Inhibitor Compound 8. Protein Data Bank: 6uxy

Parthasarathy; G.; Soisson; S.M. (2020). Sortilin-Progranulin Interaction With Compound 17. Protein Data Bank: 6x48

Parthasarathy; G.; Soisson; S.M. (2020). Sortilin-Progranulin Interaction With Compound 2. Protein Data Bank: 6x3l

Pluvinage; B.; Boraston; A.B. (2020). Structure of PfGH50B. Protein Data Bank: 6xj9

Sachar; K.; Ahmad; S.; Whitney et al. (2020). Structure of SciW bound to the Rhs1 Transmembrane Domain from Salmonella typhimurium. Protein Data Bank: 6xrr

Sack; J.S. (2020). SUBSTITUTED BENZYLOXYTRICYCLIC COMPOUNDS AS RETINOIC ACID-RELATED ORPHAN RECEPTOR GAMMA T AGONISTS. Protein Data Bank: 6xae

Saridakis; V. (2020). Crystal Structure of Ubl123 with an EZH2 peptide. Protein Data Bank: 6p5l

Scally; S.W.; Bosch; A.; Castro et al. (2020). Crystal structure of 3246 Fab in complex with circumsporozoite protein NANA. Protein Data Bank: 6o26

Scally; S.W.; Bosch; A.; Prieto et al. (2020). Crystal structure of 2243 Fab in complex with circumsporozoite protein NANP5. Protein Data Bank: 6o23

Scott; W.; Lowrance; B.; Anderson et al. (2020). Crystal structure of the Clostridial cellulose synthase subunit Z (CcsZ) from Clostridioides difficile. Protein Data Bank: 6uje

Scott; W.; Lowrance; B.; Anderson et al. (2020). Crystal structure of the Clostridial cellulose synthase subunit Z (CcsZ) from Clostridioides difficile. Protein Data Bank: 6ujf

Seattle Structural Genomics Center for Infectious Disease (SSGCID) (2020). Crystal structure of dihydrofolate reductase from Mycobacterium ulcerans with SDDC-0001565 inhibitor. Protein Data Bank: 6uwq

Seattle Structural Genomics Center for Infectious Disease (SSGCID) (2020). Crystal structure of Acetyl-CoA synthetase 2 in complex with Adenosine-5'-propylphosphate from Candida albicans. Protein Data Bank: 7kds

Seattle Structural Genomics Center for Infectious Disease (SSGCID) (2020). CRYSTAL STRUCTURE OF SMT FUSION PEPTIDYL-PROLYL CIS-TRANS ISOMERASE FROM BURKHOLDERIA PSEUDOMALLEI COMPLEXED WITH SF355. Protein Data Bank: 6o4a

Seattle Structural Genomics Center for Infectious Disease (SSGCID) (2020). CRYSTAL STRUCTURE OF SMT FUSION PEPTIDYL-PROLYL CIS-TRANS ISOMERASE FROM BURKHOLDERIA PSEUDOMALLEI COMPLEXED WITH SF339. Protein Data Bank: 6o49

Seattle Structural Genomics Center for Infectious Disease (SSGCID) (2020). Crystal structure of ADP RIBOSYLATION FACTOR-LIKE GTP BINDING PROTEIN /Small COPII coat GTPase SAR1 from Encephalitozoon cuniculi in complex with GDP. Protein Data Bank: 6vs4

Shah; M.; Moraes; T.F.; Maxwell et al. (2020). Structure of a phage-encoded quorum sensing anti-activator, Aqs1. Protein Data Bank: 6v7u

Shah; M.; Moraes; T.F.; Maxwell et al. (2020). Structure of a phage-encoded quorum sensing anti-activator, Aqs1. Protein Data Bank: 6v7v

Shi; R.; Manenda; M. (2020). Crystal structure of the flavin-dependent monooxygenase PieE in complex with FAD and substrate. Protein Data Bank: 6u0s

Shi; R.; Manenda; M.; Picard et al. (2020). Crystal structure of PieE, the flavin-dependent monooxygenase involved in the biosynthesis of piericidin A1. Protein Data Bank: 6u0p

Thai; E.; Scally; S.W.; Julien et al. (2020). Crystal structure of antibody 5D5 in complex with PfCSP N-terminal peptide. Protein Data Bank: 6uud

Thai; E.; Scally; S.W.; Prieto et al. (2020). Crystal structure of 4498 Fab in complex with circumsporozoite protein NDN3 and anti-Kappa VHH domain. Protein Data Bank: 6ulf

The; J.; Hong; Z.; Dong et al. (2020). TUDOR DOMAIN OF TUMOR SUPPRESSOR P53BP1 WITH MFP-6008. Protein Data Bank: 6vip

Wallweber; H.; Mortara; K.; Ferri et al. (2020). Structure of apo unphosphorylated IRE1. Protein Data Bank: 6w3b

Wallweber; H.; Mortara; K.; Ferri et al. (2020). Structure of phosphorylated apo IRE1. Protein Data Bank: 6w3c

Wang; F.; Lin; D.; Cheng et al. (2020). The Crystal Structure of human LDHA from Wuxi Biortus. Protein Data Bank: 6zzr

Wang; F.; Lv; Z.; Cheng et al. (2020). The Crystal Structure of human PHGDH from Biortus. Protein Data Bank: 7cvp

Watanabe; N.; Hersch; S.J.; Dong et al. (2020). Crystal structure of Type VI secretion system effector, TseH (VCA0285). Protein Data Bank: 6v98

Wei; R.; Zhou; Y.F. (2020). NNAS Fc mutant. Protein Data Bank: 6x3i

Xu; S.; Grochulski; P.; Tanaka et al. (2020). X-ray crystallographic structure model of Lactococcus lactis prolidase mutant R293S. Protein Data Bank: 7k3u

Xu; S.; Grochulski; P.; Tanaka et al. (2020). X-ray crystallographic structure model of Lactococcus lactis prolidase mutant H38S. Protein Data Bank: 6xmr

Ye; Q.; Eves; R.; Campbell et al. (2020). Crystal structure of Rhagium Mordax antifreeze protein. Protein Data Bank: 6xnr

Ye; Q.; Vance; T.D.R.; Conroy et al. (2020). Crystal structure of tetra-tandem repeat in extending RTX adhesin from Aeromonas hydrophila. Protein Data Bank: 6xi1

Ye; Q.; Vance; T.D.R.; Davies et al. (2020). Crystal structure of tetra-tandem repeat in extending region of large adhesion protein. Protein Data Bank: 6xi3

Zeng; H.; Dong; A.; Headey et al. (2020). Tudor Domain of Tumor suppressor p53BP1 with MFP-4184. Protein Data Bank: 6va5

## DOCTORAL THESIS

Alana Ou Wang (2020). Application of Biochar to Stabilize Mercury in Riverbank Sediments and Floodplain Soils from South River, VA under Conditions Relevant to Riverine Environments. Supervisor: Ptacek, Carol. ON: University of Waterloo. http://hdl.handle.net/10012/15416

Alexander; John Andrew Nelson (2020). Understanding Staphylococcus aureus β-lactam resistance : a structural investigation. Supervisor: Strynadka, N.. British Columbia, Canada: University of British Columbia. http://hdl.handle.net/2429/75610

Blank; Matthew L. (2020). Exploiting Toxoplasma gondii MAF1 locus diversity to identify essential host proteins required for mitochondrial sequestration and manipulation. Supervisor: Boyle, Jon P.. Pennsylvania, USA: University of Pittsburgh. http://d-scholarship.pitt.edu/id/eprint/38223

Dan Luo (2020). Rational Structure Design of Transition Metal Chalcogenide Multifunctional Sulfur Immobilizer for Fast and Durable Li-S Performance. Supervisor: Zhongwei Chen. Ontario: University of waterloo. http://hdl.handle.net/10012/16117

Guobin Wen (2020). Nanostructured Materials and Electrodes Engineering for Efficient CO2 Conversion. Supervisor: Chen Zhongwei; Gostick Jeff.. ON, Canada: University of Waterloo. http://hdl.handle.net/10012/16283

Hao Weiduo (2020). Clay surface reactivity and its interaction with trace elements. Supervisor: Konhauser Kurt; Alessi, Daniel. Alberta, Canada: University of Alberta.

Jiatang Chen (2020). Electronic and local structures of Pt-based bimetallic alloy and core-shell systems. Supervisor: T. K. Sham. Ontario, Canda: The University of Western Ontario. https://ir.lib.uwo.ca/etd/7302/

Keonhag Lee (2020). Investigating Oxygen and Liquid Water Transport in Porous Transport Layers of Polymer Electrolyte Membrane Electrolyzers. Supervisor: Bazylak, Aimy. Ontario, Canada: University of Toronto. https://tspace.library.utoronto.ca/handle/1807/103292

Marta Zonno (2020). Correlated phenomena studied by ARPES : from 3d to 4f systems. Supervisor: Damascelli, Andrea. BC, Canada: University of British Columbia. http://hdl.handle.net/2429/74692

McLeod; Matthew (2020). Functional consequences of changing structure, dynamics, and free-energy landscapes of phosphoenolpyruvate carboxykinases. Supervisor: Holyoak, T.. Ontario, Canada: University of Waterloo. http://hdl.handle.net/10012/16332

Moss; Daniel Laurence (2020). Antigen Stability Influences Processing Efficiency Immunogenicity of Pseudomonas Exotoxin Domain III and Ovalbumin. Supervisor: Landry, Samuel J.. Louisiana, United States: Tulane University. https://search.proquest.com/docview/2404682104?accountid=14739

Mothersole; Robert Geoffrey (2020). Characterisation of three cofactor-containing proteins from the oral bacterium Fusobacterium nucleatum. Supervisor: Wolthers, K.. British Columbia, Canada: University of British Columbia. http://hdl.handle.net/2429/75294

Peng Qi (2020). Wide field x-ray spectral imaging using bent Laue monochromators. Supervisor: Chapman, Leroy D.; Pickering, Ingrid. Saskatchewan, Canada: University of Saskatchewan. https://harvest.usask.ca/handle/10388/12969

Sadegh Shokatian (2020). NEXAFS Spectroscopy of Condensed N-alkanes. Supervisor: Urquhart, S.G.. Saskatchewan Canada: University of Saskatchewan. https://harvest.usask.ca/handle/10388/13140

Samadi; Nazanin (2020). A REAL TIME PHASE SPACE BEAM SIZE AND DIVERGENCE MONITOR FOR SYNCHROTRON RADIATION. Supervisor: Chapman, Dean. Saskatchewan, Canada: University of Saskatchewan. https://harvest.usask.ca/handle/10388/12507

Seyedali Melli (2020). Compressed Sensing Based Reconstruction Algorithm for X-ray Dose Reduction in Synchrotron Source Micro Computed Tomography. Supervisor: Wahid, Khan; Babyn, Paul. Saskatchewan, Canada: University of Saskatchewan. https://harvest.usask.ca/handle/10388/12725

Tu; Kaiyang (2020). Developing Time-Resolved Synchrotron Infrared Spectroscopy for Spectroelectrochemical Measurements. Supervisor: Burgess, Ian J. Saskatchewan, Canada: University of Saskatchewan. https://harvest.usask.ca/handle/10388/12754

Ya-Ping Deng (2020). Material Design and Electrochemical Behavior Study on Metal-Based Electrocatalysts for Rechargeable Zn-Air Batteries. Supervisor: Zhongwei Chen. Ontario, Canada: University of Waterloo. http://hdl.handle.net/10012/16223

Zarabi; Sarah Farshchi (2020). Preclinical Evaluation of a Novel Anti-leukemic Mechanism. Supervisor: Schimmer, Aaron D.. Ontario, Canada: University of Toronto. <a http://hdl.handle.net/1807/101294

## CONF. PROCEEDINGS

Alexander, James; Banerjee, Neil; Van Loon, Lisa (2020). Application of Synchrotron Radiation X-Ray Diffraction (SR-XRD) and Electron Probe Microanalysis to Understanding Gold Mineralization at the Vertigo Target, White Gold District, West-Central Yukon Territory, Canada. Microscopy and Microanalysis, 1-4.10.1017/s1431927620016608

Fraund; Matthew; Bonanno; Daniel J.; China et al. (2020). Optical properties and composition of viscous organic particles found in the Southern Great Plains. Patent Number: 10.5194/acp-2020-255

Gossen; Bruce D.; Wang; Dongniu; McLean et al. (2020). Boron Sensitivity and Storage in Brassica Napus and Its Potential for Clubroot Management. Patent Number: 10.21203/rs.3.rs-41078/v1

Okbinoglu; Tulin; Kennepohl; Pierre (2020). The Nature of S-N Bonding in Sulfonamides and Related Compounds: Insights into π-Bonding Contributions from Sulfur K-Edge XAS. Patent Number: 10.26434/chemrxiv.13204985.v1

# Workshops

**331** — **ANNUAL USERS' MEETING**
A venue for synchrotron scientists from diverse disciplines to share their work and discuss future directions for their research.

**55** — **10th ANNUAL CLS MX DATA COLLECTION SCHOOL: VIRTUAL EDITION**
A special two-day virtual workshop comprised of specially curated lectures and tutorials to provide a basis in conducting remote crystallography experiments at the synchrotron.

**45** — **FAR-IR WEBINARS**
Short presentations and discussion sessions discussing the current state of Far-IR research and the future of the field.

**89** — **HXMA WEBINARS**
HXMA has focused on providing remote teaching approaches to HXMA XAS user community due to the pandemic's physical limitations, and delivered 4 webinars in 2020.

**89** — **MID-IR**
Data analysis workshop, including sessions on theory and preprocessing, data exploration and imaging, and classification and prediction.

**100** — **CANADIAN POWDER DIFFRACTION 13**
This workshop covered the basic theory of powder diffraction, experimental setups, sample preparation and data analysis. Other diffraction and scattering techniques were also presented.

**240** — **ADVANCED XAS DATA ANALYSIS AND MODELING VIRTUAL WORKSHOP 2020**
Included sessions on automated XAS data analysis, FEFF, FDMNES, and machine learning in the EXAFS context.

# STAFF 2020

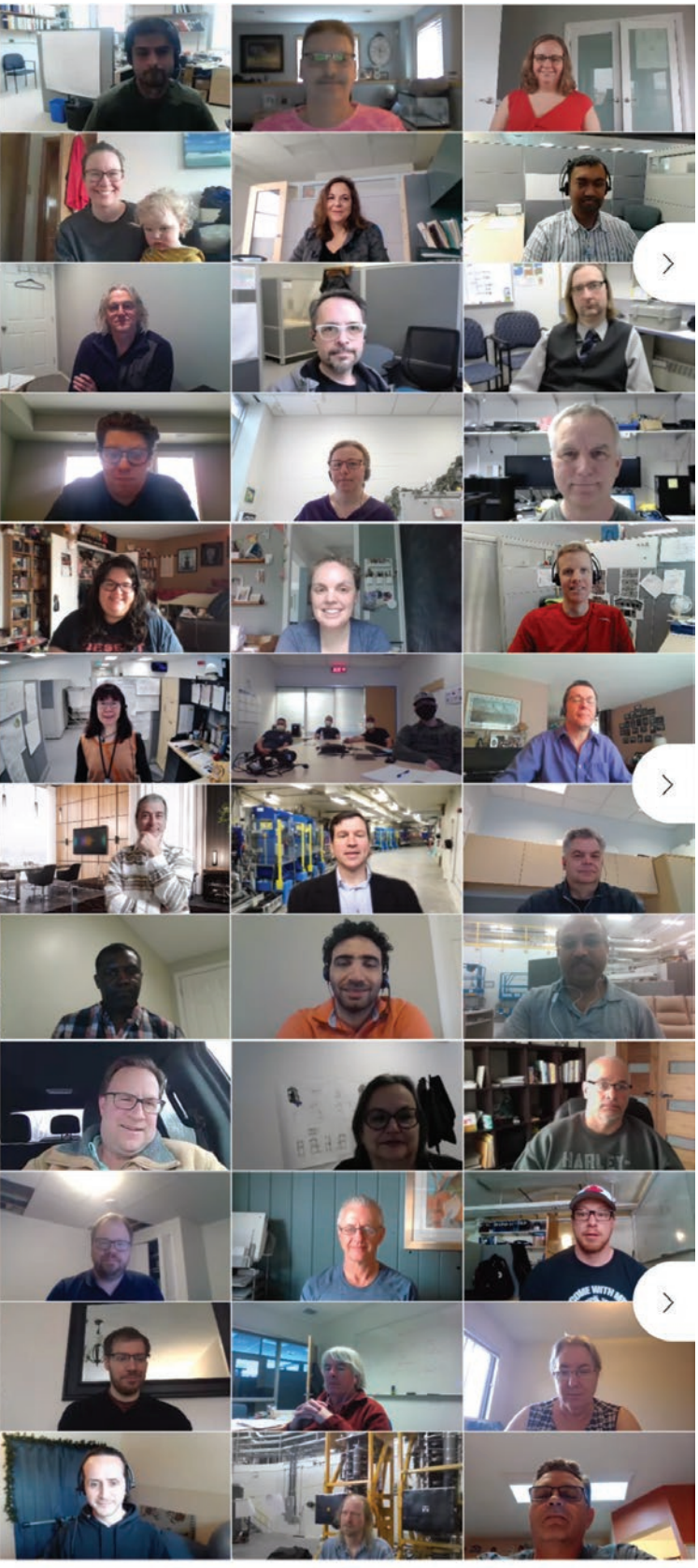

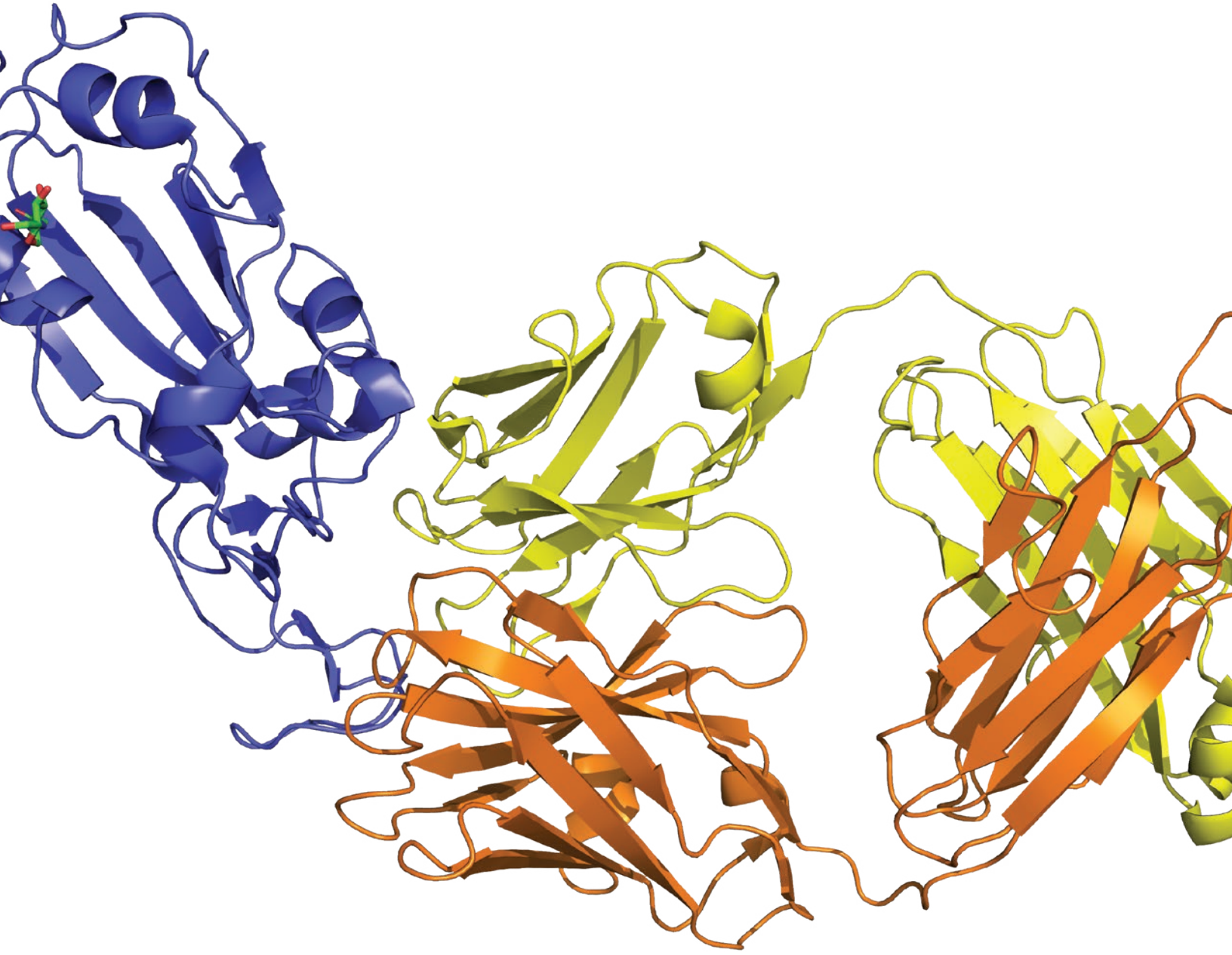

The Canadian Light Source is a national research facility of the University of Saskatchewan.

University of Saskatchewan

**Canadian Light Source Inc.**
44 Innovation Boulevard Saskatoon, SK, Canada S7N 2V3 | Phone: (306) 657-3500 Fax: (306) 657-3535

**www.lightsource.ca** **canlightsource**